

Electronic Scientific Notebook No. 274E:
Estimate Rock Fall in Emplacement Drifts
Induced by Earthquakes under Heated
Conditions to Provide Input for Performance
Assessment(06/09/1998 through 07/23/1998)

SCIENTIFIC NOTEBOOK

by

Rui Chen

SCIENTIFIC NOTEBOOK

by

Rui Chen

Southwest Research Institute
Center for Nuclear Waste Regulatory Analyses
San Antonio, Texas

July 23, 1998

Table of Contents

	Page
List of Figures	iii
List of Tables	iv
1. INITIAL ENTRIES	1
1.1 Objectives	1
1.2 Technical Approaches	1
1.3 Data Sources	3
1.4 Computers, Computer Codes, and Data Files	4
2. IN-PROGRESS ENTRIES	6
3. REFERENCES	10
Appendix A.	
Appendix B.	

List of Figures

RC

List of Tables

1. INITIAL ENTRIES

Scientific NoteBook: # 274

Issued to: Rui Chen

Issue Date: June 9, 1998

Printing Period: June 1998 to August 1998

Project Title: Seismic effect on drift stability under heated condition

By agreement with the CNWRA QA this NoteBook is to be printed at approximate quarterly intervals. This computerized Scientific NoteBook is intended to address the criteria of CNWRA QAP-001.

1.1. Objectives

The main objective of this project is to estimate rock fall in emplacement drifts induced by earthquakes under heated conditions to provide input for performance assessment. Such estimates should include: (i) range of rock block sizes (distribution of rock block sizes?), (ii) initiation of rock fall (thermally or seismically induced?), (iii) rate of rock fall, (iv) location of rock fall, and (iv) correlation of size, initiation, and rate of rock fall.

Other objectives may include to estimate: (i) seismic effect on drift stability in general by examining drift closure, joint displacement, yielding etc; (ii) effect of seismic load and rock fall on concrete lining; (iii) seismic effect on near field environment, including change in rock mass mechanical and hydrological properties which maybe important in post closure performance assessment.

1.2. Technical Approaches and Data Sources

The range and distribution of rock block sizes will be analyzed based on the range and distribution of joint spacing, joint sets, and orientation information developed for the Topopah Spring, the host rock of the repository at Yucca Mountain, through DOE site characterization activities and in situ measurements from the ESF. Sources for the measured joint information may be found in Fahy and Beason (1995), Brechtel et al. (1995), Lin et al. (1993).

UDEC computer code will be used to estimate seismic effect on emplacement drift, including size, initiation, and rate of rock fall; and correlation of these parameters.

Various reports and database developed by the DOE and its contractors and subcontractors for the Yucca Mountain project.

1.3. Computers, Computer Codes, and Data Files

Table 1-1 lists computer equipment and computer codes. Table 1-2 provides names, type, and content of computer files used in the seismic analysis project.

Table 1-1. Computing Equipment

Machine Name	Type	OS	Location	Computer Code	Language
Foxtrot	Ultra Sun Workstation	Solaris 2.5	Bldg. 189	UDEC	Fortran 77
Foxtrot	Ultra Sun Workstation	Solaris 2.5	Bldg. 189	XPLOT	N.A.

Table 1-2. Names, Type, and Content of Relative Files

File Name	Directory	Type	Content
Metra		executable	Executable of the TH part of Multiflo code
LBT-TH1.inp		text	Input data file for Multiflo analyses
		text	
		text	

2. IN-PROCESS ENTRIES

Analyses of rock fall should be able to establish technically sound criteria for determining the extent of rock fall around emplacement drifts and the size distribution of rock blocks that have the potential to fall onto the waste packages. Such analyses should explicitly account for three basic aspects:

- Analyses of size distribution of individual blocks
- Analyses of the possibility of simultaneous rock fall and vertical extent of rock fall
- Analyses of initiation, location, and rate of rock fall

The ultimate goal of these analyses is to yield technically sound estimation of the ranges of size of rock blocks that have the potential to fall onto the waste packages to provide input for the evaluation of impact of such rock fall on the integrity of the waste packages.

2.1 Measurement and Analyses of Joint Geometric Information and Distribution of Block Sizes

2.1.1 DOE Measurements and Analyses

Summary of Joint Orientation (Brechtel et al. (1995):

Existing data from previously reported oriented coring (Lin et al., 1993) and underground mapping data from the North Ramp Starter Tunnel (NRST) (Fahy and Beason, 1995) indicate that the predominant joint orientations consist of two relatively orthogonal joint sets with dips ranging generally from 70 deg to 90 deg:

- The predominant joints trend N17W to N-E with steep dips generally to the west. This set intersects the North Ramp alignment at angles of 44 to 60 deg which, combined with its steep dip, tends to reduce its structural impact.
- The other orthogonal set strikes N77E to due east, but occurs much less frequently.
- A N42 W set is more nearly parallel to the North Ramp alignment, but it occurs relatively infrequently which minimizes its structural impact.
- A subhorizontal joint set is also identified that may be associated with the horizontal foliation of the tuff beds. This set was observed in both the drilling data and tunnel mapping data. It was also observed to contribute to one localized roof instability in the NRST.

Summary of Fracture Frequency and Inclination (Brechtel et al. 1995):

The corrected linear fracture frequency (defined as the number of fractures that would exist for a unit length along a line perpendicular to the fracture plane) was calculated based on the NRG-series core hole data and shown in Table 2.1-1 for Tsw2 in 10-degree intervals. Four NRG-series core hole data were used in the calculations: USW G-1, USW G-4, UISW GU-3, and UE-25a #1.

Table 2.1-1 Corrected* fracture frequency by fracture inclination (m^{-1})

TM Unit	Fracture Dip Angle (Degree)								
	10	20	30	40	50	60	70	80	90
Tsw2	1.57	0.43	0.4	0.35	0.51	0.68	0.77	2.92	19
*Terzaghi's correction applied									

The volumetric fracture frequency, a nondirectional parameter without sampling bias, is estimated from the number of fractures in a sphere with a diameter of 1 m. It is linearly proportional to the total sum of the corrected fracture frequencies for all 10-degree intervals. The computed volumetric fracture frequencies for Tsw2 is $33.97 m^{-3}$.

Summary of Fracture Frequency(F_f) and Inclination Distributions (θ_f) (Schenker et al. 1995)

Fracture frequencies are determined from the down-hole fracture-count data for drillholes USW G-1, USW G-4, USW GU-3, and UE-25a #1. These data are reported as the number of fractures per 10-foot interval down the drillholes. They have been converted to number of fractures per 1-meter interval and grouped according to hydrogeologic unit. Table 2.1-2 shows basic statistics and the approximated beta-distribution exponents for fracture frequency for the TSw-2 unit. This table shows that the basic statistics have coefficients of variation (CV) of about 1.0. By definition, the exponential distribution has a CV of 1.0; therefore, it was assumed that the distribution can be represented by beta-function PDFs that approximate exponential distributions. For the exponential distribution, the minimum is zero and the maximum is infinity. To approximate an exponential PDF by a beta function requires that the maximum be set to a value less than infinity, so 30 times the mean value has been chosen. The resulting beta distribution is reasonably close to the desired exponential.

Table 2.1-2 Fracture frequency statistics and beta-distribution approximation of the exponential

Unit	Statistics					Approximated Exponential Distribution Parameters				
	n	E[x] (m^{-3})	CV	Min (m^{-1})	Max (m^{-1})	CV	Min (m^{-1})	Max (m^{-1})	Alpha	Beta
Tsw-2	323	3.0	1.0	0.2	23.3	1.0	0.0	90.0	-0.067	26.067

The orientations are compiled as numbers of fractures falling in each 10-degree increment between 0 and 90 degrees from vertical. Table 2.1-3 summarizes the statistics and the beta-PDF exponents for TSw-2. Fracture orientations in the YMP Reference Information Base (DOE, 1993) for welded tuffs have predominantly near-vertical dip angles, with a secondary grouping that is nearly horizontal. For Tsw-2, the fracture orientations also follow this trend, although the distributions generated are not as strongly bimodal. Because the fracture orientations are grouped at high and low angles, the probability distribution is "bathtub shaped". A typical PDF for TSw2 is shown in Figure 2.1-1.

Table 2.1-2 Fracture orientations/dip angle statistics and beta-distribution approximation of the exponential

Unit	Statistics					Beta-Distribution Parameters	
	n	E[x] (degree)	CV	Min (degree)	Max (degree)	Alpha	Beta
Tsw-2	399	58.183	0.478	0.000	90.000	-0.100	-0.508

Derivation of Joint Spacing and Other Parameters:

Fractures are modeled as a parallel array of planar fractures; this assumption permits the determination of fracture-model parameters that cannot be measured (I.e., spacing, hydraulic aperture, porosity, hydraulic conductivity, and air entry parameter) in terms of the ones that can be measured (bulk saturated hydraulic conductivity, fracture frequency, and fracture orientation) (Schenker et al. 1995).

The number of fracture per unit distance normal to the plane of the fractures is

$$N_p = F_f / \cos(\theta_f) \quad (2.1-1)$$

Parallel-plate fracture spacing (a_f):

$$a_f = 1/N_p = \cos(\theta_f)/F_f \quad (2.1-2)$$

To obtain distributions of the derived fracture parameters, a computer routine need to be developed that randomly samples certain numbers (say 100 values) of the measured variables from the probability distribution for these properties, and then calculates certain number (say 100 values) of the derived parameters based on the equations such as (2.1-1) and (2.1-2).

Fracture spacings for the TSw2 are calculated according to Equation (2.1-2) by Schenker et al. (1995). A set of 100 values is computed from randomly sampled inputs, and the basic statistics are then derived. The statistical data and the beta-distribution parameters are given in Table 2.1-4.

Table 2.1-4 Derived fracture spacing statistics and beta distribution parameters

Unit	Statistics					Beta-Distribution Parameters	
	n	E[x] (m)	CV	Min (m)	Max (m)	Alpha	Beta
Tsw-2	100	0.740	3.147	3.0×10^{-6}	19.878	-0.9400	0.5514

The distribution of fracture spacings is strongly skewed toward low values (close spacings). Figure 2.1-2 shows this for Tsw-2, showing that although most values are grouped near 0 m spacing, a few are very large.

2.1.2 Analyses of Size Distribution of Individual Blocks

The size distribution of individual rock blocks is determined by geometrical characteristics of in situ joints, including joint spacing, inclination, orientation, and trace length etc. Large amount of such data have been gathered by the DOE through various site characterization activities. These include data from NRC-series core holes (Lin et al., 1993), ESF mapping (Fahy and Beason, 1995; Brechtel et al. 1995), and surface mapping (Verbeek and Throckmorton, 1995; Sweetkind and Williams-Stroud, 1996). Schenker et al. (1995) performed statistical analyses for some of these individual parameters based on core hole and ESF data, including fracture frequency and inclination. They also derived some other basic parameters from measured parameters and certain assumptions, including joint spacing. Distribution of joint spacing derived by Schenker et al. (1995) assumed a parallel array of planar joints. In their rock fall analyses, Gauthier et al (1995) estimated size distribution of individual rock blocks using a modified (log-space) version of the Topopah Spring fracture spacing distribution developed by Schenker et al. (1995), assuming cubic and parallelepiped blocks.

Assumptions such as parallel array of planar joints and/or cubic and parallelepiped blocks may largely distort the actual size distribution. Key block studies need to be performed in three dimensional space to better estimate the distribution of rock block sizes based on field data, particularly the ESF data. Various tools exist for such studies. One example of such tools may be the fracture data analysis tool in commercial computer code FRACMAN (Dershowitz et al. 1995).

Size distribution of individual rock blocks, however, provides only a lower bound of sizes of available rocks that can fall. There is possibility of more than one individual blocks falling onto the waste packages at the same time, and therefore, increase the impact load under both thermal-mechanical load and seismic load. The extent of potential rock fall will provide an upper bound for the sizes of available rocks that can fall. To determine the possibility of multiple blocks falling at the same time and the extent of potential rock fall, thermal-mechanical and dynamic analyses need to be performed. Section 4.3.5.2 addresses such analyses.

(This part is to be completed after the on-going analysis is finished)

2.1.3 Summary of DOE Data

2.1.3.1 Core hole data: (these include USW G-1, USW G-4, USW GU-3, UE-25a#1, and four NRC drillholes)

Brechtel, C.E., M. Lin, E. Martin, and D. S. Kessel., 1995. *Geotechnical Characterization of the North Ramp of the Exploratory Studies Facility*. Vol. 1 - Data Summary and Vol. 2 - NRG Corehole Data Appendices. SAND95-0488/1. Albuquerque, NM: Sandia National Laboratories. (Eleven holes, the North Ramp Geotechnical (NRG) boreholes, drilled along the 2800-m route of the North Ramp).

Lin, M., M.P. Hardy, and S.J. Bauer. 1993. *Fracture Analysis and Rock Quality Designation Estimation for the Yucca Mountain Site Characterization Project*. SAND92-0449. Albuquerque, NM: Sandia National Laboratories. [A summary analysis of USW G-1 (Spengler et al., 1981), USW GU-3 (Scott and Castellanos, 1984), USW G-4 (Spengler and Chornack, 1984), and UE-25a#1 (Spengler et al., 1979)].



Spengler, R.W., M.P. Chornack, D.C. Muller, and J.E. Kibler. 1984. *Stratigraphic and Structural Characteristics of Volcanic Rocks in Core Hole USW G-4, Yucca Mountain, Nye County, Nevada*. USGS/OFR-84-789, U.S. Geological Survey, Denver, CO. (NNA.870519.0105) (USW G-4)

Spengler, R.W., F.M. Byers, Jr., and J.B. Warner. 1981. *Stratigraphy and Structure of Volcanic Rocks in Drill Hole USW-G1, Yucca Mountain, Nye County, Nevada*, USGS/OFR-81-1349, DOE/ET/44802/T4, U.S. Geological Survey, Denver, CO. (HQS.880517.1492) (USW G-1)

Spengler, R.W., and J.G. Rsenbaum. 1980. *Preliminary Interpretations of Geologic Results Obtained from Boreholes UE25a-4, -5, -6, and -7, Yucca Mountain, Nevada Test Site*, USGS/OFR-80-929, U.S. Geological Survey, Reston, VA. (NNA.890823.0106)

Spengler, R.W., D.C. Muller, and R.B. Livermore. 1979. *Preliminary Report on the Geology and Geophysics of Drill Hole UE-25a-1, Yucca Mountain Nevada Test Site*, USGS/OFR-79-1244. U.S. Geological Survey, Denver, CO. (HQS.880517.1491) (UE-25a #1)

Scott, R.B. and M. Castellanos. 1984. *Stratigraphic and Structural Relations of Volcanic Rocks in Drill Holes USW GU-3 and USW G-3, Yucca Mountain, Nye County, Nevada*, USGS/OFR-84-491, U.S. Geological Survey, Denver, CO. (NNA.890804.0017) (USW GU-3)

2.1.3.2 ESF Mapping Data

1. The reports that Larry provided
2. List of data available faxed by Chad Glenn
3. Handouts, DOE/NRC Appendix 7 meeting in Oct, 1997

According to Steven C. Beason, USBR (Principal Investigator, 1997, *Previous Mapping Efforts*, handout of Nuclear Regulatory Commission Appendix 7 Meetings, Oct. 16, 1997):

Surface geologic mapping (Day and others ?)
 Pavement and outcrop fracture studies (Sweetkind and others ?)
 Borehole studies (Rautman ?, Buesch ?, Brechtel)
 ESF geologic mapping (?)

SCP ESF Mpping Requirements:

- Full-periphery geologic mapping
- Detailed line surveys
- photography
- Sampling

ESF mapping techniques:

- full periphery geologic maps
- detailed line surveys
- stereophotography
- consolidated sampling (discontinued 9/95)

Surface geologic mapping (Day and others ?)
 Pavement and outcrop fracture studies (Sweetkind and others ?)
 Borehole studies (Rautman ?, Buesch ?, Brechtel)
 ESF geologic mapping (?)

SCP ESF Mpping Requirements:

- Full-periphery geologic mapping
- Detailed line surveys
- photography
- Sampling

ESF mapping techniques:

- full periphery geologic maps
- detailed line surveys
- stereophotography
- consolidated sampling (discontinued 9/95)

Anna, L.O. 1998. *Preliminary Three-Dimensional Discrete Fracture Model of Topopah Spring Tuff in the Exploratory Studies Facility, Yucca Mountain Area, Nye County, Nevada*. US Geological Survey Open-File Report 97-834.

Sweetkind, D.S. and S.C. Williams-Stroud. 1996. *Characteristics of Fractures at Yucca Mountain, Nevada: Synthesis Report*. Administrative Report, prepared for the Nevada Operations Office, U.S. Department of Energy, under Interagency Agreement DE-AI08NV10874.

2.1.3.3 Surface Mapping Data

Verbeek and Throckmorton, 1995;
 Sweetkind and Williams-Stroud, 1996

2.1.3.4 Summary

Considering the time constraint of the deliverable, it was decided that two options will be used for constructing a joint pattern for the preliminary case analyses (Case B):

1. A section of the full periphery mapping of fractures in the ESF main tunnel would be digitized and curvature-corrected to produce a sample repository drift cross section joint pattern. David Ferrill is assisting on this.
2. According to DOE determination of primary joint sets for Tsw2 from the ESF Main Drift (see notes of DOE/NRC Appendix 7 meeting on 10/16/97. All these have joint spacing that is a normal distribution. There are three primary joint sets: (a) strike 118 to 148 deg, dip ≥ 45 deg, and 60% spacing smaller than 0.4 m; (b) strike 220 to 250, dip ≥ 45 deg, and 50% spacing smaller than 2 m; © strike 323 to 353, dip < 45 , 50% spacing smaller than 4 m. UDEC command "JSET" will be used to generat these joints. However, it is an approximation, since UDEC use uniform distributions.

2.1.4 Summary of Literature on Analyses of *In Situ* Block Size Distribution

2.1.4.1 Yucca Mountain Literature

Some graphics results from Steven C. Beason, USBR (Principal Investigator, 1997, *Previous Mapping Efforts*, handout of Nuclear Regulatory Commission Appendix 7 Meetings, Oct. 16, 1997):

no actual methodology presented.

2.1.4.2 Others

Hadjigeorgiou, J., M. Grenon, and J.F. Lessard. 1998. Defining in-situ block size. *CIM Bulletin* 91 (1020)

2.2 Collection and Analyses of Earthquake Time Histories

Anderson, J.G., J.N. Brune, D.dePolo, J.Gomberg, S.C. Harmsen, M.K. Savage, A.F. Sheehan, and K.D. Smith. 1997. Preliminary report: the Little Skull Mountain Earthquake, June 29, 1992. *Seismic and Dynamic Analysis and Design Considerations for High Level Nuclear Waste Repositories*, J.C. Stepp edi., American Society of Civil Engineers, New York, NY.
Jga@seismo.unr.edu

Internet Sources:

- (1) SMDB: The Strong Motion DataBase of the Southern California Earthquake Center
<http://www.smdb.crustal.ucsb.edu>
Can download California earthquakes directly from the INTERNET, no membership or fee required.
Was able to down load Landers 1992 earthquake time histories.
- (2) SMCAT (Strong Motion Catalog) at NGDC (The National Geophysical Data Center)
<http://www.ngdc.noaa.gov/seg/hazard/strong.html>
The strong motion data need to be purchased on 3 volume CDROM or floppy discs for selected earthquakes.
Content of the catalog can be searched on-line.
Contains both structural and free-field data world-wide. The data include uncorrected (raw), corrected (filtered), and response spectra (includes Fourier spectra).
- (3) CIT-SMARTS version 2.0 (California Institute of Technology Strong Motion Accelerogram Transfer System)
<http://www.eerl.caltech.edu/smarts/smarts.html>
Specially processed near-field accelerograms
Fourier, response, and inter-story drift demand spectra
future data updates through the Internet from Caltech
The QuickBasic source code available
Fully compatible with data from the California Strong Motion Instrumentation Program (CSMIP) and the U.S. Geological Survey (USGS). CSMIP data may be downloaded into SMARTS directly from the Internet.
- (4) CSMIP (the California Strong Motion Instrumentation Program) at Mines & Geology, Department of Conservation.
<http://www.consrv.ca.gov/dmg/csmip/index.htm>
California data only, including Landers earthquake from more than 20 stations
Can download both time history and spectrum data

(5)

2.3 Summary of Results from Previous UDEC Parametric Analysis

Thermal-mechanical analyses at the drift scale up to 100 years (Ahola et al., 1996, Chen et al. 1998) show that thermal loading causes rather significant stress redistribution around the drift. The study was for a single drift in a rock mass that has a regular joint pattern with two joint sets (subhorizontal and subvertical). The analyses were conducted using computer code UDEC (Itasca Consulting Group, Inc.

1996). Figures 2.3-1 and 2.3-2 compares the distribution of principal stresses following drift excavation and after 100 years heating under 100 MTU/acre thermal load. Thermal load increased maximum compressive stress, rotated its direction from vertical to horizontal, and shifted its location from near drift side-walls to roof and floor areas. Spalling along side walls due to concentration of compressive stresses and lack of lateral support in underground mines and tunnels is a frequently observed phenomenon. When such compressive stress is rotated and shifted to the roof area, it could cause rock fall. Although such spalling may have limited vertical extent. They need to be further characterized. This study also reveals that thermal load could significantly increase yielding of intact rock blocks based on Mohr-Coulom failure

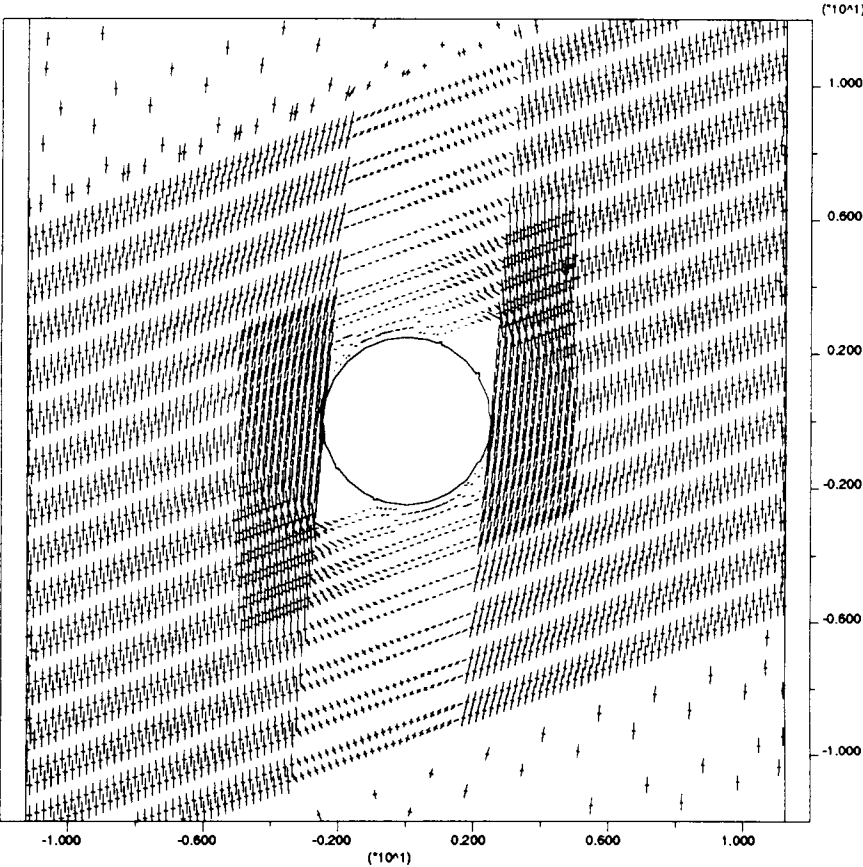


Figure 2.3-1 Distribution of principal stresses after drift excavation

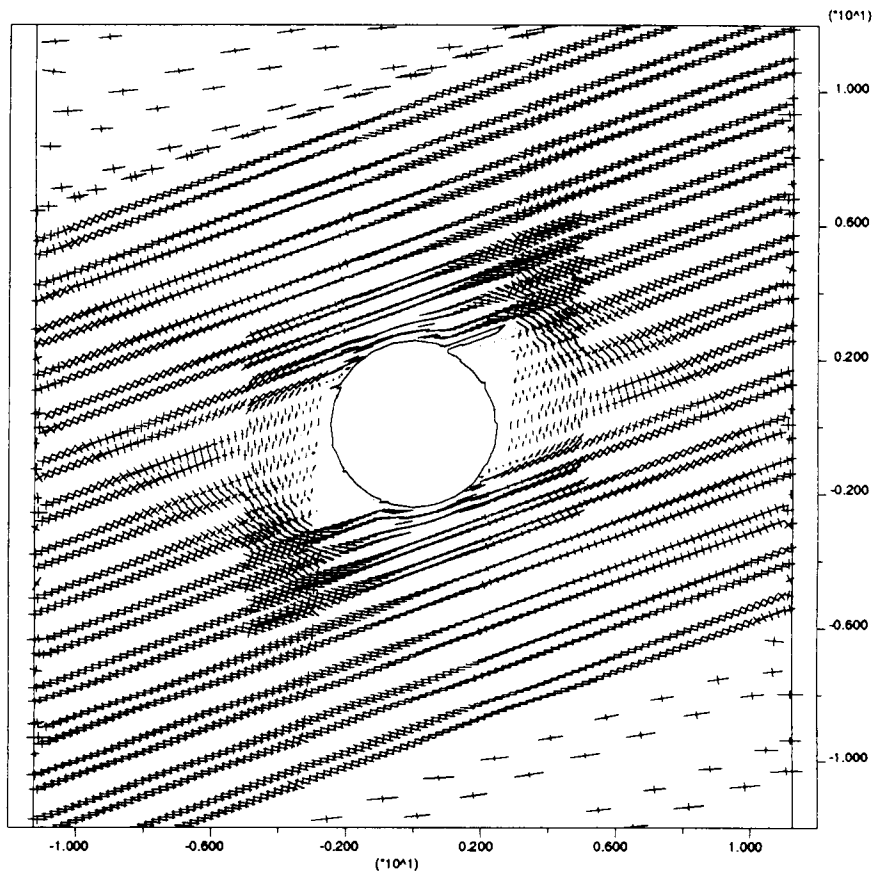


Figure 2.3-2 Distribution of principal stresses after 100 years of heating

model with a tensile cutoff. Although yield zones in most cases were localized to the immediate areas around the drift, they extended to the middle of the pillar in some cases for rock masses that are weaker and have high thermal expansion coefficient (figures 2.3-3 and 2.3-4). Although yielding of intact rock in discontinuum analyses may not be the direct evidences of explicit rock fall, it represents a failure or damage state and indicates the need to establish a criterion for mapping out the extent of potential rock fall area with appropriate modeling methodologies and input parameters (such as more realistic joint patterns).

2.4 Summary of Results from Previous UDEC Simulations on Seismic Effects

- Peak ground acceleration of 0.2 and 0.4 g were investigated on a model with regular joint pattern (Ahola, 1997) based on previous parametric studies (Ahola et al. 1996).
- Analyses indicate that slip along joints and closure of the drift take place with both single and repeated episodes of earthquake loading to a larger degree if the rock mass around the drift is in weakened or yielded state after the thermal loading and prior to the dynamic loading.
- If the rock remains in the elastic state after the thermal loading is applied, however, no measurable cumulative slip on joints or drift convergence is evident with repeated episodes of seismic loading up to 0.4 g, aside from that which occurs during the first sequence of seismic loading.
- No rock falls were explicitly simulated. Failure to simulate rock fall may be because of the regular joint pattern used in the model.

2.5 Additional UDEC Simulation Model (Case A)

The additional UDEC basecase model (case A) is a preliminary dynamic modeling study carried out at the CNWRA on a single drift in a rock mass that has irregular joint pattern and varying block sizes. It is a hypothetical case in that the joint patterns do not exactly represent the joint pattern observed at the proposed repository horizon. The model extended 50 meters above and below the repository level, where vertical displacement is assumed to be zero. The modeled region is a unit drift width (i.e., from one pillar center to an adjacent pillar center). The simulated region, therefore, includes an opening. Vertical boundaries were assumed to be no displacement boundary along the horizontal direction. The region is under in situ stress at the repository level of 7.0 MPa and 1.86 MPa in vertical and horizontal directions, respectively and stress gradient of 0.0225 MPa/m and 0.00599 MPa/m in vertical and horizontal directions, respectively. There is no thermal analyses in this preliminary case. Seismic ground motion was assumed to be a simple sigmoidal dynamic signal, corresponding to a maximum peak ground acceleration of approximately 0.4 g.

The preliminary modeling results show that it is possible for multiple rock blocks to fall simultaneously under seismic ground motion. Figures 2.4-1 and 2.4-2 compare falling blocks after subjecting to a sigmoidal dynamic signal for about 0.25 and 1.00 second, respectively. Although very preliminary, this modeling effort shows that the possibility of simultaneous rock fall could be explicitly simulated by dynamic analyses to some extent. It is also desirable (and possible) to establish a criterion that could be used to map out the maximum extent of areas of potential rock fall if enough dynamic analysis studies are carried out. Such criterion may be a function of joint shear and normal displacement, or joint shear and normal stresses and strength. The extent of rock fall will depend on factors such as level of ground motion, joint pattern, individual block sizes, and thermal and mechanical properties of the rock mass.

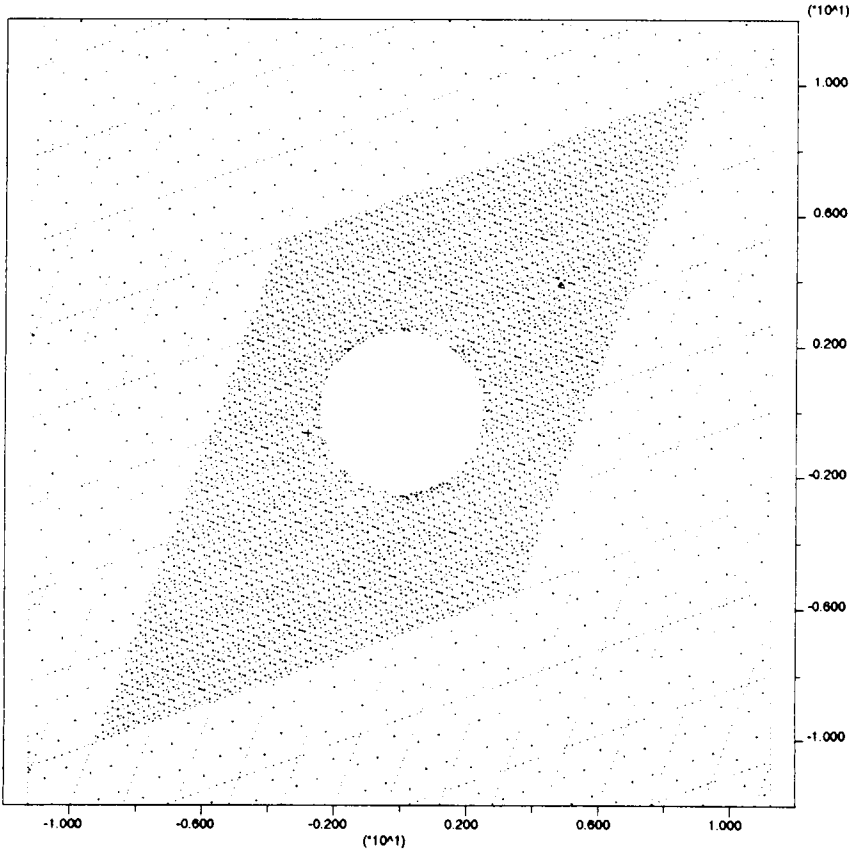


Figure 2.3-3 Distribution of yielding after drift excavation. Dots represent elastic state. Crosses represent yield. Dash lines represent joints

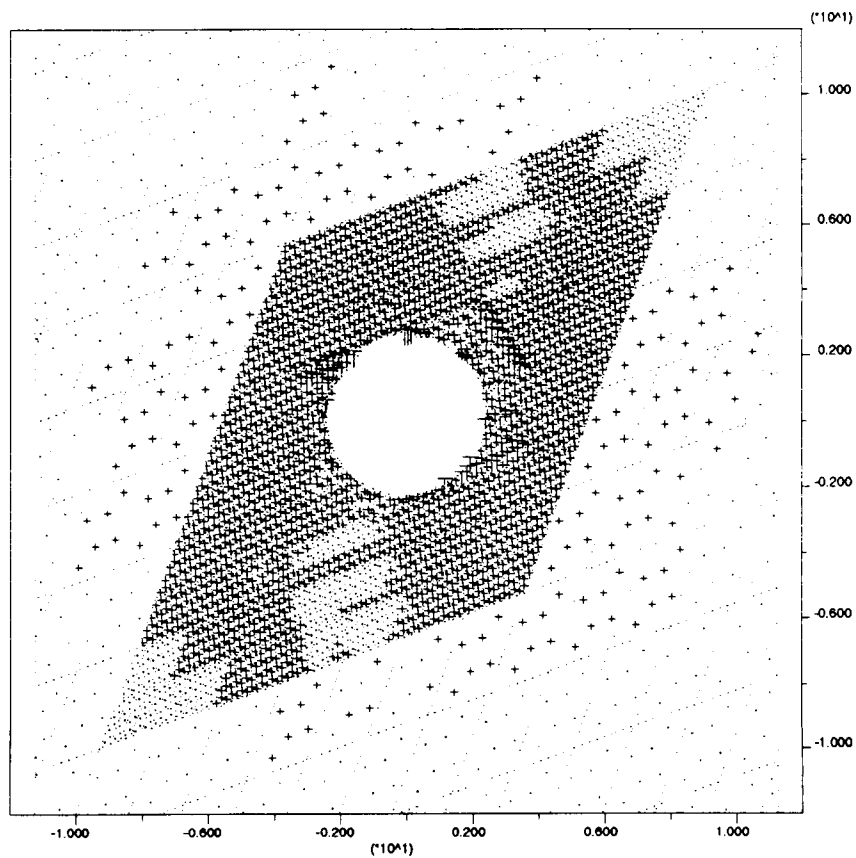


Figure 2.3-4 Distribution of yielding after 100 years of heating. Dots represent elastic state. Crosses represent yield. Dash lines represent joints

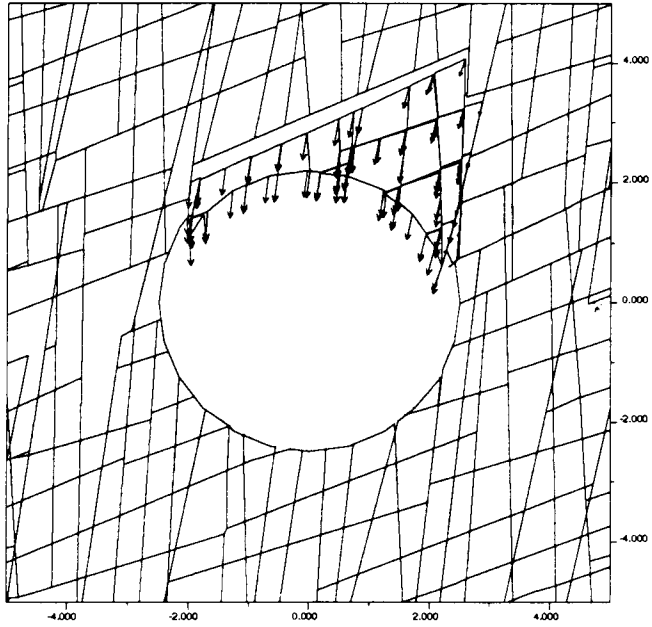


Figure 2.5-1 Rock fall simulated by dynamic analysis of a single drift in a rock mass with irregular joint pattern after subjecting to 0.25 sec of dynamic load

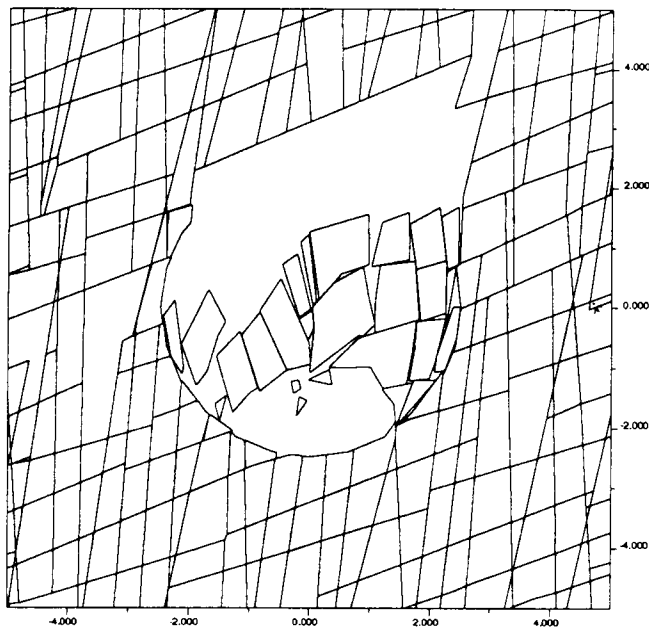


Figure 2.5-2 Rock fall simulated by dynamic analysis of a single drift in a rock mass with irregular joint pattern after subjecting to 1.0 sec of dynamic load.

2.6 Other parameters for additional UDEC dynamic analyses

Joint Patterns:

Set I: strick 118 to 148, dip ≥ 45 , spacing 80% smaller than 0.4

Set II: strick 220 to 250, dip ≥ 45 , spacing 80% smaller than 2

set III: strick 323 to 353, dip < 45 , spacing 50% smaller than 4

2.7 Additional UDEC Dynamic Analyses Model (Model B)

Model A described in section 2.5 was a very preliminary model in that: (1) joint pattern was not representative of the repository joint pattern, (2) thermal load was not considered, and (3) seismic load a simple sigmoidal form rather than a real seismic history from Yucca Mountain or its vicinity. Model B will use a joint pattern that is directly from the ESF full-periphery mapping data.

3. REFERENCES

Brechtel, C.E., M. Lin, E. Martin, and D. S. Kessel., 1995. *Geotechnical Characterization of the North Ramp of the Exploratory Studies Facility*. Vol. 1 - Data Summary. SAND95-0488/1. Albuquerque, NM: Sandia National Laboratories.

Dershowitz, et al. 1995. *Fracman - Discrete Feature Data Analysis, Geometric Modelling Exploration Simulation, and Flow and Transport Modelling*, Golder Associates, 1993.

Fahy, M.F. and F.C. Beason. 1995. *Geotechnical Analysis for the Exploratory Studies Facility North Ramp Boxcut and Starter Tunnel*. Preliminary report prepared for the Department of Energy of Management and Operating Contractor Architect/Engineer by the Bureau of Reclamation/U.S. Geological Survey, vol 1&2.

Lin, M., M.P. Hardy, and S.J. Bauer. 1993. *Fracture Analysis and Rock Quality Designation Estimation for the Yucca Mountain Site Characterization Project*. SAND92-0449. Albuquerque, NM: Sandia National Laboratories.

Schenker, A.R., D.C. Guerin, T.H. Robey, C.A. Rautman, and R.W. Barnard. 1995. *Stochastic Hydrogeologic Units and Hydrogeologic Properties Development for Total-System Performance Assessments*. SAND94-0244. Albuquerque, NM: Sandia National Laboratories.

Sweetkind and Williams-Stroud. 1996

Verbeek and Throckmorton, 1995

Appendix A
Input Data File for Case A

```

*****
* Part I:
*****
set log case12.log
set plot po
start
*****
* Title and block definition for AML100 with Lwp=18 m, Ldrift=22.5 m
*****
head
Thermal-Mechanical Analysis/Case12.dat
config thermal
*
* Properties
* ABCdEFgHi
* A = vertical joint orientation (85)
* B = horizontal joint orientation (20)
* c = vertical joint spacing (0.1)
* d = joint friction angle (28)
* E = thermal loading (100)
* F = intact rock cohesion (43)
* g = intact rock friction angle (20)
* H = intact rock Young's modulus (32)
* i = thermal expansion coefficient (6x10e-6)
*
**** Coarse Model ****
*** Joint orientations and spacing around the tunnel ***
* 1st joint set - 85 degrees from horizontal - 0.20 m spacing
* 2nd joint set - 20 degrees from horizontal - 1.25 m spacing
*
* Size of problem domain is -11.25<x<11.25 -225<y<225
* - Vertical boundaries are located along symmetry lines assuming
* 22.5 m drift spacings
* - Upper and lower horizontal boundaries set based on extent
* of thermal front at 100 years of heating.
*
round 0.02
set ovtol 1.0
block -13 -50 -13 50 13 50 13 -50
*
*****
* create jointing
*****
* -----
* outer problem domain
* -----

```

```

jregion -13 23 -13 50 13 50 13 23
jset 85.0 10.0 50.0 1.0 0.0 0.0 3.0 0.3 -13 23
jset 20.0 5.0 25.0 1.0 0.0 0.0 5.0 0.3 -13 23
*
jregion -13 23 -13 50 13 50 13 23 delete
*
jregion -13 -50 -13 -23 13 -23 13 -50
jset 85.0 10.0 50.0 1.0 0.0 0.0 3.0 0.3 -13 -50
jset 20.0 5.0 25.0 1.0 0.0 0.0 5.0 0.3 -13 -50
*
* -----
* inner problem domain
* -----
* angle,length,gap,spacing
*
jregion -13 -25 -13 -9 13 -9 13 -25 delete
jset 85.0 10.0 40.0 5.0 0.0 0.0 1.5 0.2 -13 -25
jset 20.0 5.0 20.0 2.5 0.0 0.0 3.0 0.2 -13 -25
*
jregion -13 9 -13 25 13 25 13 9
jset 85.0 10.0 40.0 5.0 0.0 0.0 1.5 0.2 -13 -25
jset 20.0 5.0 20.0 2.5 0.0 0.0 3.0 0.2 -13 -25
*
* -----
* more detailed inner domain
* -----
* angle,length,gap,spacing
*
jregion -13 -10 -13 10 -4.5 13 -4.5 -13
jset 85.0 10.0 17.5 1.0 -0.2 0.0 1.0 0.3
jset 20.0 5.0 15.0 1.0 -0.2 0.0 1.5 0.3
*
jregion 4.5 -10 4.5 10 13 10 13 -10
jset 85.0 15.0 17.5 1.0 -0.2 0.0 1.0 0.3
jset 20.0 5.0 15.0 1.0 -0.2 0.0 1.5 0.3
*
jregion -5 -10 -5 -5 5 -5 5 -10
jset 85.0 15.0 17.5 1.0 -0.2 0.0 1.0 0.3
jset 20.0 5.0 15.0 1.0 -0.2 0.0 1.5 0.3
*
jregion -5 5 -5 10 5 10 5 5
jset 85.0 15.0 17.5 1.0 -0.2 0.0 1.0 0.3
jset 20.0 5.0 15.0 1.0 -0.2 0.0 1.5 0.3
*
* -----
* detailed joint spacing around the tunnel
* -----
*
* angle,length,gap,spacing

```

```

*
jregion -6 -6 -6 6 6 6 6 -6 delete
jset 85.0 10.0 7.5 1.0 -0.2 0.0 0.4 0.1 -6 -6
jset 20.0 5.0 5.0 1.0 -0.2 0.0 0.75 0.1 -6 -6
*
jd
tunnel 0 0 2.5 24
del area 1.5e-2
return
*
* *****
* auto generation of zones
* *****
gen region -5 -5 -5 5 5 5 5 -5 edge 0.9
gen region -9 -9 -9 9 9 9 9 -9 edge 1.5
save t1_zone1.sav
gen region -13 -15 -13 15 13 15 13 -15 edge 3.0
gen region -13 -25 -13 25 13 25 13 -25 edge 3.0
gen region -13 -50 -13 50 13 50 13 -50 edge 5.5
save t1_zone2.sav
pr max
*
damp auto
*
*****
* apply mechanical boundary conditions (units, MPa)
*****
grav 0.0 -9.81
insitu stress -1.86 0.0 -7.0 ygrad 0.00599 0.0 0.0225 szz -1.86 &
zgrad 0.0 0.00599
bound -14 14 49 51 stress -1.86 0.0 -7.0 ygrad 0.00599 0.0 0.0225
bound -14 14 -51 -49 yvel=0.0
bound -14 -12 -51 51 xvel=0.0
bound 12 14 -51 51 xvel=0.0
*
*
*****
* define mechanical and thermal material properties for joints/intact blocks
*****
*
* material 1 = rock
*
change -14 14 -226 226 jcons=5
**
prop mat=1 k=18.3908e3 g=13.2231e3 d=0.002297
prop mat=1 cond=2.1 thexp=6.0e-06 spec=9.32e08
prop jmat=1 jks=1.0e5 jkn=1.0e5 jdil=0 jc=0.08 jfric=28.0 jtens=0.04 &
kn=1.0e5 ks=1.0e5
*

```

```

set jcondf 5
*
* mohr-coulomb failure parameters
*
prop mat=1 coh=43 fric=20 tens=5 dil=0
*
*****
* history records
*****
hist ncyc=10 unbal damp type 4
hist ydis 0 0 yvel 0 0 ydis 0 225 ydis 0 -225
hist ydis 0 15
hist sxx 0.0 0.0 syy 0.0 0.0
*
*****
* initial cycling equilibrium
*****
cycle 4000
save t1_ini.sav
*
*****
* remove tunnel blocks
*****
*
del ann 0 0 0 2.5
*
* reset displacements after applying in situ loading conditions
*
reset damp time hist dis rot
hist unbal damp
hist ydis 0.0 2.5 ydis 0 -2.5 ydis 0.0 50.0
hist xdis 0.0 2.5
hist sxx 0.0 3.0 syy 0.0 3.0 syy 3.0 0.0
*
* change material property to Mohr-Coulomb
change cons=3 mat=1
*
cycle 4000
*
sav t1_exc.sav
*
*****
* Part II: Seismic Load
*****
*
res t1_exc.sav
*
*****
* apply seismic load from bottom

```

```

* set up nonreflecting boundary
bound mat=1
bound xvisc range -14 -12 -51 51
bound xvisc range 12 14 -51 51
bound xvisc yvisc range -14 14 -51 -49
bound xvisc yvisc range -14 14 49 51
*
* apply sinusoidal stress wave from bottom (0.4 m/sec)
bound stress 0 0 -4.5 yhist=cos(2,1.0) range -14 14 -51 -49
reset time hist disp rot
hist unbal damp
hist ydis (-13,50) yvel (-13 50)
hist ydis (0,2.5) yvel (0,2.5)
hist ydis (2.5,0) yvel (2.5,0)
hist xdis (0,2.5) xvel (0,2.5)
hist xdis (2.5,0) xvel (2.5,0)
*
damp 0.1 1.0 mass
*
* -----
* cycle for 0.02 sec
* -----
cyc time=0.02
save t1_002.sav
*
res t1_002.sav
* -----
* cycle to 0.25 sec
* -----
cyc time=0.23
save t1_025.sav
*
* -----
* cycle to 0.5 sec
* -----
cyc time=0.25
save t1_050.sav
*
* -----
* cycle to 0.75 sec
* -----
cyc time=0.25
* save t1_075.sav
*
* -----
* cycle to 1.0 sec
* -----
cyc time=0.25

```

```

save t1_100.sav
*
* -----
* cycle to 2.0 sec
* -----
cyc time=1
save t1_200.sav
*
*****
return
*****
*****
* Part III: Thermal
*****
*
*****
* set thermal boundary and histories
*****
*
* set up thermal boundaries (default thermal b.c. are adiabatic)
*
* Initial temperature at repository horizon taken to be 29 C
* - temperature gradient taken to be 0.02 deg C/m
*
tfix 33.0 -13 13 -226.0 -224.0
tfix 25.0 -13 13 224.0 226.0
*
print bound
*
initem 29.0 -13 13 -226 226
thist ntcyc=10 tem 0 2.5 tem 0 5 tem 0 10 tem 0 25 tem 0 50 tem 0 100
thist tem 0 150 tem 0 200 tem 0 220 tem 2.5 0 tem 5 0 tem 10 0
thist tem 11.25 0
*
*****
* apply heat flux to tunnel wall
*****
thapp ann 0.0 0.0 2.4 2.56 flux 28.4701 -3.2197e-10
*
*
* run initial thermal time by explicit scheme for 100 steps
*
run age=3600 step=1000000 tol=0.05
reset damp
cycle 4000
pr max
*
* run thermal time to 3 months
*

```

```
run age=7.776e6 delt=3600.0 temp=10000 step=1000000 tol=0.05 impl
reset damp
cycle 4000
pr max
*
* run thermal time to 1 year
*
run age=3.1536e7 delt=7200.0 temp=10000 step=1000000 tol=0.05 impl
reset damp
cycle 4000
pr max
save c12_1y.sav
*
* run thermal time to 18 months
*
run age=4.7304e7 delt=7200.0 temp=10000 step=1000000 tol=0.05 impl
reset damp
cycle 4000
pr max
*
* run thermal time to 2 years
*
run age=6.3072e7 delt=7200.0 temp=10000 step=1000000 tol=0.05 impl
reset damp
cycle 4000
pr max
sav c12_2y.sav
*
* run thermal time to 3 years
*
run age=9.4608e7 delt=7200.0 temp=10000 step=1000000 tol=0.05 impl
reset damp
cycle 4000
sav c12_3y.sav
pr max
*
* run thermal time to 4 years
*
run age=1.26144e8 delt=7200.0 temp=10000 step=1000000 tol=0.05 impl
reset damp
cycle 4000
pr max
sav c12_4y.sav
*
* run thermal time to 5 years
*
run age=1.5768e8 delt=7200.0 temp=10000 step=1000000 tol=0.05 impl
reset damp
cycle 4000
```

```
pr max
sav c12_5y.sav
*
* run thermal time to 7.5 years
*
run age=2.3652e8 delt=7200.0 temp=10000 step=1000000 tol=0.05 impl
reset damp
cycle 4000
pr max
*
* run thermal time to 10 years
*
run age=3.1536e8 delt=7200.0 temp=10000 step=1000000 tol=0.05 impl
reset damp
cycle 4000
pr max
sav c12_10y.sav
*
* run thermal time to 20 years
*
run age=6.3072e8 delt=7200.0 temp=10000 step=1000000 tol=0.05 impl
reset damp
cycle 4000
pr max
save c12_20y.sav
*
* run thermal time to 30 years
*
run age=9.4608e8 delt=7200.0 temp=10000 step=1000000 tol=0.05 impl
reset damp
cycle 4000
pr max
sav c12_30y.sav
*
* run thermal time to 40 years
*
run age=12.6144e8 delt=7200.0 temp=10000 step=1000000 tol=0.05 impl
reset damp
cycle 4000
pr max
sav c12_40y.sav
*
* run thermal time to 50 years
*
run age=1.5768e9 delt=7200.0 temp=10000 step=1000000 tol=0.05 impl
reset damp
cycle 4000
pr max
sav c12_50y.sav
```

```
*
* run thermal time to 60 years
run age=1.89216e9 delt=7200.0 temp=10000 step=1000000 tol=0.05 impl
reset damp
cycle 4000
pr max
*sav c12_60y.sav
*
* run thermal time to 70 years
*
run age=2.20752e9 delt=7200.0 temp=10000 step=1000000 tol=0.05 impl
reset damp
cycle 5000
pr max
* sav c12_70y.sav
*
* run thermal time to 80 years
*
run age=2.52288e9 delt=7200.0 temp=10000 step=1000000 tol=0.05 impl
reset damp
cycle 4000
pr max
* sav c12_80y.sav
*
* run thermal time to 100 years
*
run age=3.1536e9 delt=7200.0 temp=10000 step=1000000 tol=0.05 impl
reset damp
cycle 4000
pr max
sav c12_100y.sav
return
```

Appendix B

RC

Electronic Scientific Notebook No. 274E:
Estimate Rock Fall in Emplacement Drifts
Induced by Earthquakes under Heated
Conditions to Provide Input for Performance
Assessment(06/09/1998 through 07/23/1998)

SCIENTIFIC NOTEBOOK

274E

by

Rui Chen

Printed: December 8, 1998

Rui Chen

SCIENTIFIC NOTEBOOK

INITIALS:

RC

SCIENTIFIC NOTEBOOK

274E

by

Rui Chen

Southwest Research Institute
Center for Nuclear Waste Regulatory Analyses
San Antonio, Texas

December 8, 1998

Table of Contents

	Page
List of Figures	iii
List of Tables	iv
1. INITIAL ENTRIES	1
1.1 Objectives	1
1.2 Technical Approaches	1
1.3 Computers, Computer Codes, and Data Files	2
2. IN-PROGRESS ENTRIES	3
3. REFERENCES	40

List of Figures

RC

List of Tables

1. INITIAL ENTRIES

Scientific NoteBook: # 274

Issued to: Rui Chen

Issue Date: June 9, 1998

Printing Period: June 1998 to December 1998

Project Title: Seismic effect on drift stability under heated condition

By agreement with the CNWRA QA this NoteBook is to be printed at approximate quarterly intervals. This computerized Scientific NoteBook is intended to address the criteria of CNWRA QAP-001.

1.1. Objectives

The main objective of this project is to estimate rock fall in emplacement drifts induced by earthquakes under heated conditions to provide input for performance assessment. Such estimates should include: (i) range of rock block sizes (distribution of rock block sizes?), (ii) initiation of rock fall (thermally or seismically induced?), (iii) rate of rock fall, (iv) location of rock fall, and (v) correlation of size, initiation, and rate of rock fall.

Other objectives may include to estimate: (i) seismic effect on drift stability in general by examining drift closure, joint displacement, yielding etc; (ii) effect of seismic load and rock fall on concrete lining; (iii) seismic effect on near field environment, including change in rock mass mechanical and hydrological properties which maybe important in post closure performance assessment.

(No new entries were make to section 1.1 during printing period ended September 30)

1.2. Technical Approaches and Data Sources

The range and distribution of rock block sizes will be analyzed based on the range and distribution of joint spacing, joint sets, and orientation information developed for the Topopah Spring, the host rock of the repository at Yucca Mountain, through DOE site characterization activities and in situ measurements from the ESF. Sources for the measured joint information may be found in Fahy and Beason (1995), Brechtel et al. (1995), Lin et al. (1993).

UDEC computer code will be used to estimate seismic effect on emplacement drift, including size, initiation, and rate of rock fall; and correlation of these parameters.

Various reports and database developed by the DOE and its contractors and subcontractors for the Yucca Mountain project.

(No new entries were made to section 1.2 during printing period ended September 30)

1.3. Computers, Computer Codes, and Data Files

Table 1-1 lists computer equipment and computer codes. Table 1-2 provides names, type, and content of computer files used in the seismic analysis project.

Table 1-1. Computing Equipment

Machine Name	Type	OS	Location	Computer Code	Language
Foxtrot	Ultra Sun Workstation	Solaris 2.5	Bldg. 189	UDEC	Fortran 77
Foxtrot	Ultra Sun Workstation	Solaris 2.5	Bldg. 189	XPLOT	N.A.

Table 1-2. Names, Type, and Content of Relative Files

File Name	Directory	Type	Content
Metra		executable	Executable of the TH part of Multiflo code
LBT-TH1.inp		text	Input data file for Multiflo analyses
		text	
		text	

(No new entries were made to section 1.3 during printing period ended September 30)

2. IN-PROCESS ENTRIES

Analyses of rock fall should be able to establish technically sound criteria for determining the extent of rock fall around emplacement drifts and the size distribution of rock blocks that have the potential to fall onto the waste packages. Such analyses should explicitly account for three basic aspects:

- Analyses of size distribution of individual blocks
- Analyses of the possibility of simultaneous rock fall and vertical extent of rock fall
- Analyses of initiation, location, and rate of rock fall

The ultimate goal of these analyses is to yield technically sound estimation of the ranges of size of rock blocks that have the potential to fall onto the waste packages to provide input for the evaluation of impact of such rock fall on the integrity of the waste packages.

2.1 Measurement and Analyses of Joint Geometric Information and Distribution of Block Sizes

2.1.1 DOE Measurements and Analyses

Summary of Joint Orientation (Brechtel et al. (1995):

Existing data from previously reported oriented coring (Lin et al., 1993) and underground mapping data from the North Ramp Starter Tunnel (NRST) (Fahy and Beason, 1995) indicate that the predominant joint orientations consist of two relatively orthogonal joint sets with dips ranging generally from 70 deg to 90 deg:

- The predominant joints trend N17W to N-E with steep dips generally to the west. This set intersects the North Ramp alignment at angles of 44 to 60 deg which, combined with its steep dip, tends to reduce its structural impact.
- The other orthogonal set strikes N77E to due east, but occurs much less frequently.
- A N42 W set is more nearly parallel to the North Ramp alignment, but it occurs relatively infrequently which minimizes its structural impact.
- A subhorizontal joint set is also identified that may be associated with the horizontal foliation of the tuff beds. This set was observed in both the drilling data and tunnel mapping data. It was also observed to contribute to one localized roof instability in the NRST.

Summary of Fracture Frequency and Inclination (Brechtel et al. 1995):

The corrected linear fracture frequency (defined as the number of fractures that would exist for a unit length along a line perpendicular to the fracture plane) was calculated based on the NRG-series core hole data and shown in Table 2.1-1 for Tsw2 in 10-degree intervals. Four NRG-series core hole data were used in the calculations: USW G-1, USW G-4, UISW GU-3, and UE-25a #1.

Table 2.1-1 Corrected* fracture frequency by fracture inclination (m^{-1})

TM Unit	Fracture Dip Angle (Degree)								
	10	20	30	40	50	60	70	80	90
Tsw2	1.57	0.43	0.4	0.35	0.51	0.68	0.77	2.92	19
*Terzaghi's correction applied									

The volumetric fracture frequency, a nondirectional parameter without sampling bias, is estimated from the number of fractures in a sphere with a diameter of 1 m. It is linearly proportional to the total sum of the corrected fracture frequencies for all 10-degree intervals. The computed volumetric fracture frequencies for Tsw2 is $33.97 m^{-3}$.

Summary of Fracture Frequency(F_v) and Inclination Distributions (θ_v) (Schenker et al. 1995)

Fracture frequencies are determined from the down-hole fracture-count data for drillholes USW G-1, USW G-4, USW GU-3, and UE-25a #1. These data are reported as the number of fractures per 10-foot interval down the drillholes. They have been converted to number of fractures per 1-meter interval and grouped according to hydrogeologic unit. Table 2.1-2 shows basic statistics and the approximated beta-distribution exponents for fracture frequency for the TSw-2 unit. This table shows that the basic statistics have coefficients of variation (CV) of about 1.0. By definition, the exponential distribution has a CV of 1.0; therefore, it was assumed that the distribution can be represented by beta-function PDFs that approximate exponential distributions. For the exponential distribution, the minimum is zero and the maximum is infinity. To approximate an exponential PDF by a beta function requires that the maximum be set to a value less than infinity, so 30 times the mean value has been chosen. The resulting beta distribution is reasonably close to the desired exponential.

Table 2.1-2 Fracture frequency statistics and beta-distribution approximation of the exponential

Unit	Statistics					Approximated Exponential Distribution Parameters				
	n	E[x] (m^{-3})	CV	Min (m^{-1})	Max (m^{-1})	CV	Min (m^{-1})	Max (m^{-1})	Alpha	Beta
Tsw-2	323	3.0	1.0	0.2	23.3	1.0	0.0	90.0	-0.067	26.067

The orientations are compiled as numbers of fractures falling in each 10-degree increment between 0 and 90 degrees from vertical. Table 2.1-3 summarizes the statistics and the beta-PDF exponents for TSw-2. Fracture orientations in the YMP Reference Information Base (DOE, 1993) for welded tuffs have predominantly near-vertical dip angles, with a secondary grouping that is nearly horizontal. For Tsw-2, the fracture orientations also follow this trend, although the distributions generated are not as strongly bimodal. Because the fracture orientations are grouped at high and low angles, the probability distribution is "bathtub shaped". A typical PDF for TSw2 is shown in Figure 2.1-1.

Table 2.1-2 Fracture orientations/dip angle statistics and beta-distribution approximation of the exponential

Unit	Statistics					Beta-Distribution Parameters	
	n	E[x] (degree)	CV	Min (degree)	Max (degree)	Alpha	Beta
TSw-2	399	58.183	0.478	0.000	90.000	-0.100	-0.508

Derivation of Joint Spacing and Other Parameters:

Fractures are modeled as a parallel array of planar fractures; this assumption permits the determination of fracture-model parameters that cannot be measured (I.e., spacing, hydraulic aperture, porosity, hydraulic conductivity, and air entry parameter) in terms of the ones that can be measured (bulk saturated hydraulic conductivity, fracture frequency, and fracture orientation) (Schenker et al. 1995).

The number of fracture per unit distance normal to the plane of the fractures is

$$N_p = F_f / \cos(\theta_p) \quad (2.1-1)$$

Parallel-plate fracture spacing (a_f):

$$a_f = 1/N_p = \cos(\theta_p)/F_f \quad (2.1-2)$$

To obtain distributions of the derived fracture parameters, a computer routine need to be developed that randomly samples certain numbers (say 100 values) of the measured variables from the probability distribution for these properties, and then calculates certain number (say 100 values) of the derived parameters based on the equations such as (2.1-1) and (2.1-2).

Fracture spacings for the TSw2 are calculated according to Equation (2.1-2) by Schenker et al. (1995). A set of 100 values is computed from randomly sampled inputs, and the basic statistics are then derived. The statistical data and the beta-distribution parameters are given in Table 2.1-4.

Table 2.1-4 Derived fracture spacing statistics and beta distribution parameters

Unit	Statistics					Beta-Distribution Parameters	
	n	E[x] (m)	CV	Min (m)	Max (m)	Alpha	Beta
TSw-2	100	0.740	3.147	3.0×10^{-6}	19.878	-0.9400	0.5514

The distribution of fracture spacings is strongly skewed toward low values (close spacings). Figure 2.1-2 shows this for Tsw-2, showing that although most values are grouped near 0 m spacing, a few are very large.

2.1.2 Analyses of Size Distribution of Individual Blocks

The size distribution of individual rock blocks is determined by geometrical characteristics of in situ joints, including joint spacing, inclination, orientation, and trace length etc. Large amount of such data have been gathered by the DOE through various site characterization activities. These include data from NRC-series core holes (Lin et al., 1993), ESF mapping (Fahy and Beason, 1995; Brechtel et al. 1995), and surface mapping (Verbeek and Throckmorton, 1995; Sweetkind and Williams-Stroud, 1996). Schenker et al. (1995) performed statistical analyses for some of these individual parameters based on core hole and ESF data, including fracture frequency and inclination. They also derived some other basic parameters from measured parameters and certain assumptions, including joint spacing. Distribution of joint spacing derived by Schenker et al. (1995) assumed a parallel array of planar joints. In their rock fall analyses, Gauthier et al (1995) estimated size distribution of individual rock blocks using a modified (log-space) version of the Topopah Spring fracture spacing distribution developed by Schenker et al. (1995), assuming cubic and parallelepiped blocks.

Assumptions such as parallel array of planar joints and/or cubic and parallelepiped blocks may largely distort the actual size distribution. Key block studies need to be performed in three dimensional space to better estimate the distribution of rock block sizes based on field data, particularly the ESF data. Various tools exist for such studies. One example of such tools may be the fracture data analysis tool in commercial computer code FRACMAN (Dershowitz et al. 1995).

Size distribution of individual rock blocks, however, provides only a lower bound of sizes of available rocks that can fall. There is possibility of more than one individual blocks falling onto the waste packages at the same time, and therefore, increase the impact load under both thermal-mechanical load and seismic load. The extent of potential rock fall will provide an upper bound for the sizes of available rocks that can fall. To determine the possibility of multiple blocks falling at the same time and the extent of potential rock fall, thermal-mechanical and dynamic analyses need to be performed. Section 4.3.5.2 addresses such analyses.

(This part is to be completed after the on-going analysis is finished)

2.1.3 Summary of DOE Data

2.1.3.1 Core hole data: (these include USW G-1, USW G-4, USW GU-3, UE-25a#1, and four NRC drillholes)

Brechtel, C.E., M. Lin, E. Martin, and D. S. Kessel., 1995. *Geotechnical Characterization of the North Ramp of the Exploratory Studies Facility*. Vol. 1 - Data Summary and Vol. 2 - NRG Corehole Data Appendices. SAND95-0488/1. Albuquerque, NM: Sandia National Laboratories. (Eleven holes, the North Ramp Geotechnical (NRG) boreholes, drilled along the 2800-m route of the North Ramp).

Lin, M., M.P. Hardy, and S.J. Bauer. 1993. *Fracture Analysis and Rock Quality Designation Estimation for the Yucca Mountain Site Characterization Project*. SAND92-0449. Albuquerque, NM: Sandia National Laboratories. [A summary analysis of USW G-1 (Spengler et al., 1981), USW GU-3 (Scott and Castellanos, 1984), USW G-4 (Spengler and Chornack, 1984), and UE-25a#1 (Spengler et al., 1979)].

Spengler, R.W., M.P. Chornack, D.C. Muller, and J.E. Kibler. 1984. *Stratigraphic and Structural Characteristics of Volcanic Rocks in Core Hole USW G-4, Yucca Mountain, Nye County, Nevada*. USGS/OFR-84-789, U.S. Geological Survey, Denver, CO. (NNA.870519.0105) (USW G-4)

Spengler, R.W., F.M. Byers, Jr., and J.B. Warner. 1981. *Stratigraphy and Structure of Volcanic Rocks in Drill Hole USW-G1, Yucca Mountain, Nye County, Nevada*, USGS/OFR-81-1349, DOE/ET/44802/T4, U.S. Geological Survey, Denver, CO. (HQS.880517.1492) (USW G-1)

Spengler, R.W., and J.G. Rsenbaum. 1980. *Preliminary Interpretations of Geologic Results Obtained from Boreholes UE25a-4, -5, -6, and -7, Yucca Mountain, Nevada Test Site*, USGS/OFR-80-929, U.S. Geological Survey, Reston, VA. (NNA.890823.0106)

Spengler, R.W., D.C. Muller, and R.B. Livermore. 1979. *Preliminary Report on the Geology and Geophysics of Drill Hole UE-25a-1, Yucca Mountain Nevada Test Site*, USGS/OFR-79-1244. U.S. Geological Survey, Denver, CO. (HQS.880517.1491) (UE-25a #1)

Scott, R.B. and M. Castellanos. 1984. *Stratigraphic and Structural Relations of Volcanic Rocks in Drill Holes USW GU-3 and USW G-3, Yucca Mountain, Nye County, Nevada*, USGS/OFR-84-491, U.S. Geological Survey, Denver, CO. (NNA.890804.0017) (USW GU-3)

2.1.3.2 ESF Mapping Data

1. The reports that Larry provided
2. List of data available faxed by Chad Glenn
3. Handouts, DOE/NRC Appendix 7 meeting in Oct, 1997

According to Steven C. Beason, USBR (Principal Investigator, 1997, *Previous Mapping Efforts*, handout of Nuclear Regulatory Commission Appendix 7 Meetings, Oct. 16, 1997):

Surface geologic mapping (Day and others ?)
 Pavement and outcrop fracture studies (Sweetkind and others ?)
 Borehole studies (Rautman ?, Buesch ?, Brechtel)
 ESF geologic mapping (?)

SCP ESF Mpping Requirements:

- Full-periphery geologic mapping
- Detailed line surveys
- photography
- Sampling

ESF mapping techniques:

- full periphery geologic maps
- detailed line surveys
- stereophotography
- consolidated sampling (discontinued 9/95)

Surface geologic mapping (Day and others ?)
 Pavement and outcrop fracture studies (Sweetkind and others ?)
 Borehole studies (Rautman ?, Buesch ?, Brechtel)
 ESF geologic mapping (?)

SCP ESF Mapping Requirements:

- Full-periphery geologic mapping
- Detailed line surveys
- photography
- Sampling

ESF mapping techniques:

- full periphery geologic maps
- detailed line surveys
- stereophotography
- consolidated sampling (discontinued 9/95)

Anna, L.O. 1998. *Preliminary Three-Dimensional Discrete Fracture Model of Topopah Spring Tuff in the Exploratory Studies Facility, Yucca Mountain Area, Nye County, Nevada*. US Geological Survey Open-File Report 97-834.

Sweetkind, D.S. and S.C. Williams-Stroud. 1996. *Characteristics of Fractures at Yucca Mountain, Nevada: Synthesis Report*. Administrative Report, prepared for the Nevada Operations Office, U.S. Department of Energy, under Interagency Agreement DE-AI08NV10874.

2.1.3.3 Surface Mapping Data

Verbeek and Throckmorton, 1995;
 Sweetkind and Williams-Stroud, 1996

2.1.3.4 Summary

Considering the time constraint of the deliverable, it was decided that two options will be used for constructing a joint pattern for the preliminary case analyses (Case B):

1. A section of the full periphery mapping of fractures in the ESF main tunnel would be digitized and curvature-corrected to produce a sample repository drift cross section joint pattern. David Ferrill is assisting on this.
2. According to DOE determination of primary joint sets for Tsw2 from the ESF Main Drift (see notes of DOE/NRC Appendix 7 meeting on 10/16/97. All these have joint spacing that is a normal distribution. There are three primary joint sets: (a) strike 118 to 148 deg, dip ≥ 45 deg, and 60% spacing smaller than 0.4 m; (b) strike 220 to 250, dip ≥ 45 deg, and 50% spacing smaller than 2 m; (c) strike 323 to 353, dip < 45 , 50% spacing smaller than 4 m. UDEC command "JSET" will be used to generate these joints. However, it is an approximation, since UDEC use uniform distributions.

2.1.4 Summary of Literature on Analyses of *In Situ* Block Size Distribution

2.1.4.1 Yucca Mountain Literature

Some graphics results from Steven C. Beason, USBR (Principal Investigator, 1997, *Previous Mapping*

Efforts, handout of Nuclear Regulatory Commission Appendix 7 Meetings, Oct. 16, 1997):
no actual methodology presented.

2.1.4.2 Others

Hadjigeorgiou, J., M. Grenon, and J.F. Lessard. 1998. Defining in-situ block size. *CIM Bulletin* 91 (1020)

(No new entries were made to section 2.1 during printing period ended September 30)

2.2 Collection and Analyses of Earthquake Time Histories

Anderson, J.G., J.N. Brune, D.dePolo, J.Gomberg, S.C. Harmsen, M.K. Savage, A.F. Sheehan, and K.D. Smith. 1997. Preliminary report: the Little Skull Mountain Earthquake, June 29, 1992. *Seismic and Dynamic Analysis and Design Considerations for High Level Nuclear Waste Repositories*, J.C. Stepp edi., American Society of Civil Engineers, New York, NY.
Jga@seismo.unr.edu

Internet Sources:

- (1) SMDB: The Strong Motion DataBase of the Southern California Earthquake Center
<http://www.smdb.crustal.ucsb.edu>
Can download California earthquakes directly from the INTERNET, no membership or fee required.
Was able to down load Landers 1992 earthquake time histories.
- (2) SMCAT (Strong Motion Catalog) at NGDC (The National Geophysical Data Center)
<http://www.ngdc.noaa.gov/seg/hazard/strong.html>
The strong motion data need to be purchased on 3 volume CDROM or floppy discs for selected earthquakes.
Content of the catalog can be searched on-line.
Contains both structural and free-field data world-wide. The data include uncorrected (raw), corrected (filtered), and response spectra (includes Fourier spectra).
- (3) CIT-SMARTS version 2.0 (California Institute of Technology Strong Motion Accelerogram Transfer System)
<http://www.eerl.caltech.edu/smarts/smarts.html>
Specially processed near-field accelerograms
Fourier, response, and inter-story drift demand spectra
future data updates through the Internet from Caltech
The QuickBaseic source code available
Fully compatible with data from the California Strong Motion Instrumentation Program (CSMIP) and the U.S. Geological Survey (USGS). CSMIP data may be downloaded into SMARTS directly from the Internet.
- (4) CSMIP (the California Strong Motion Instrumentation Program) at Mines & Geology, Department of Conservation.
<http://www.consrv.ca.gov/dmg/csmip/index.htm>
California data only, including Landers earthquake from more than 20 stations
Can download both time history and spectrum data

(5)

(No new entries were make to section 2.2 during printing period ended September 30)

2.3 Summary of Results from Previous UDEC Parametric Analysis

Thermal-mechanical analyses at the drift scale up to 100 years (Ahola et al., 1996, Chen et al. 1998)

show that thermal loading causes rather significant stress redistribution around the drift. The study was for a single drift in a rock mass that has a regular joint pattern with two joint sets (subhorizontal and subvertical). The analyses were conducted using computer code UDEC (Itasca Consulting Group, Inc. 1996). Figures 2.3-1 and 2.3-2 compares the distribution of principal stresses following drift excavation and after 100 years heating under 100 MTU/acre thermal load. Thermal load increased maximum compressive stress, rotated its direction from vertical to horizontal, and shifted its location from near drift side-walls to roof and floor areas. Spalling along side walls due to concentration of compressive stresses and lack of lateral support in underground mines and tunnels is a frequently observed phenomenon. When such compressive stress is rotated and shifted to the roof area, it could cause rock fall. Although such spalling may have limited vertical extent. They need to be further characterized. This study also reveals that thermal load could significantly increase yielding of intact rock blocks based on Mohr-Coulom failure

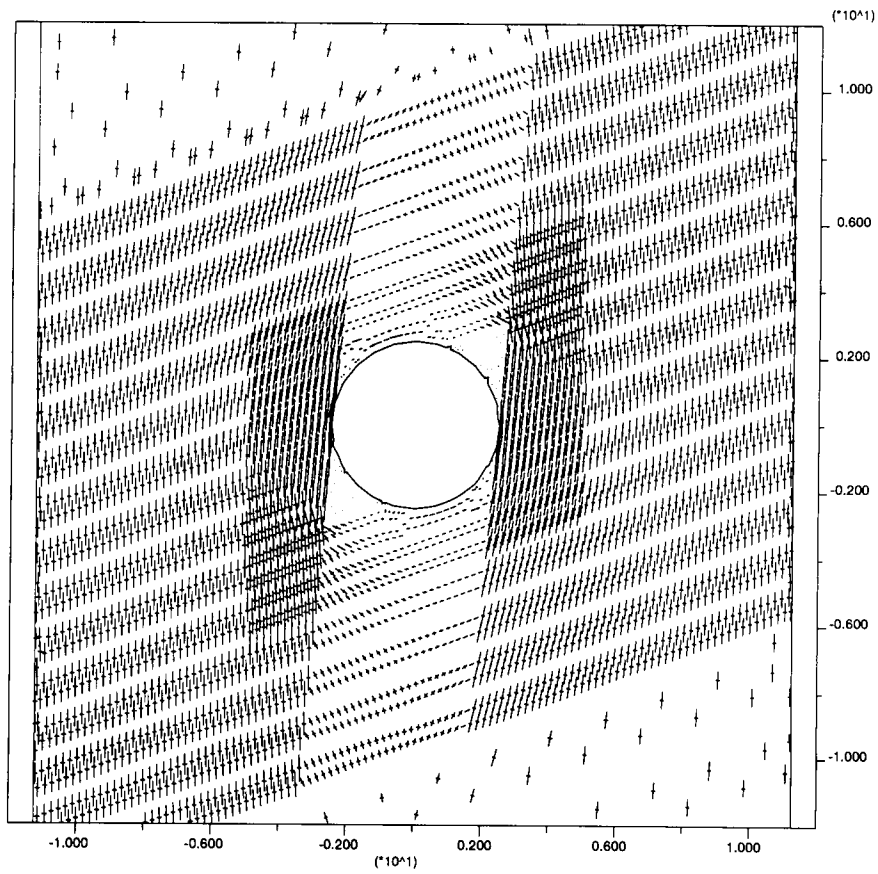


Figure 2.3-1 Distribution of principal stresses after drift excavation

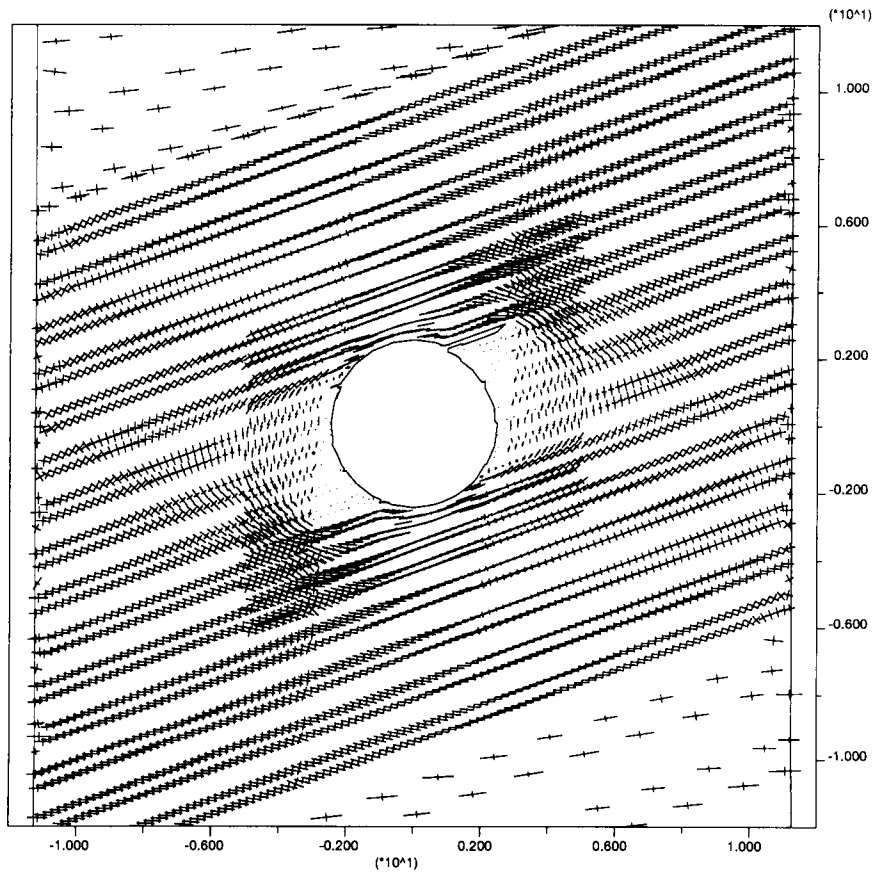


Figure 2.3-2 Distribution of principal stresses after 100 years of heating

model with a tensile cutoff. Although yield zones in most cases were localized to the immediate areas around the drift, they extended to the middle of the pillar in some cases for rock masses that are weaker and have high thermal expansion coefficient (figures 2.3-3 and 2.3-4). Although yielding of intact rock in discontinuum analyses may not be the direct evidences of explicit rock fall, it represents a failure or damage state and indicates the need to establish a criterion for mapping out the extent of potential rock fall area with appropriate modeling methodologies and input parameters (such as more realistic joint patterns).

(No new entries were make to section 2.3 during printing period ended September 30)

2.4 Summary of Results from Previous UDEC Simulations on Seismic Effects

- Peak ground acceleration of 0.2 and 0.4 g were investigated on a model with regular joint pattern (Ahola, 1997) based on previous parametric studies (Ahola et al. 1996).
- Analyses indicate that slip along joints and closure of the drift take place with both single and repeated episodes of earthquake loading to a larger degree if the rock mass around the drift is in weakened or yielded state after the thermal loading and prior to the dynamic loading.
- If the rock remains in the elastic state after the thermal loading is applied, however, no measurable cumulative slip on joints or drift convergence is evident with repeated episodes of seismic loading up to 0.4 g, aside from that which occurs during the first sequence of seismic loading.
- No rock falls were explicitly simulated. Failure to simulate rock fall may be because of the regular joint pattern used in the model.

(No new entries were make to section 2.4 during printing period ended September 30)

2.5 Additional UDEC Simulation Model (Case A)

The additional UDEC basecase model (case A) is a preliminary dynamic modeling study carried out at the CNWRA on a single drift in a rock mass that has irregular joint pattern and varying block sizes. It is a hypothetical case in that the joint patterns do not exactly represent the joint pattern observed at the proposed repository horizon. The model extended 50 meters above and below the repository level, where vertical displacement is assumed to be zero. The modeled region is a unit drift width (i.e., from one pillar center to an adjacent pillar center). The simulated region, therefore, includes on opening. Vertical boundaries were assumed to be no displacement boundary along the horizontal direction. The region is under in situ stress at the repository level of 7.0 MPa and 1.86 MPa in vertical and horizontal directions, respectively and stress gradient of 0.0225 MPa/m and 0.00599 MPa/m in vertical and horizontal directions, respectively. There is no thermal analyses in this preliminary case. Seismic ground motion was assumed to be a simple sigmoidal dynamic signal, corresponding to a maximum peak ground acceleration of approximately 0.4 g.

The preliminary modeling results show that it is possible for multiple rock blocks to fall simultaneously under seismic ground motion. Figures 2.4-1 and 2.4-2 compare falling blocks after subjecting to a sigmoidal dynamic signal for about 0.25 and 1.00 second, respectively. Although very preliminary, this modeling effort shows that the possibility of simultaneous rock fall could be explicitly simulated by dynamic analyses to some extent. It is also desirable (and possible) to establish a criterion that could be used to map out the maximum extent of areas of potential rock fall if enough dynamic analysis studies are carried out. Such criterion may be a function of joint shear and normal displacement, or joint shear and normal stresses and strength. The extent of rock fall will depend on factors such as level of ground motion, joint pattern, individual block sizes, and thermal and mechanical properties of the rock mass.

(No new entries were make to section 2.5 during printing period ended September 30)

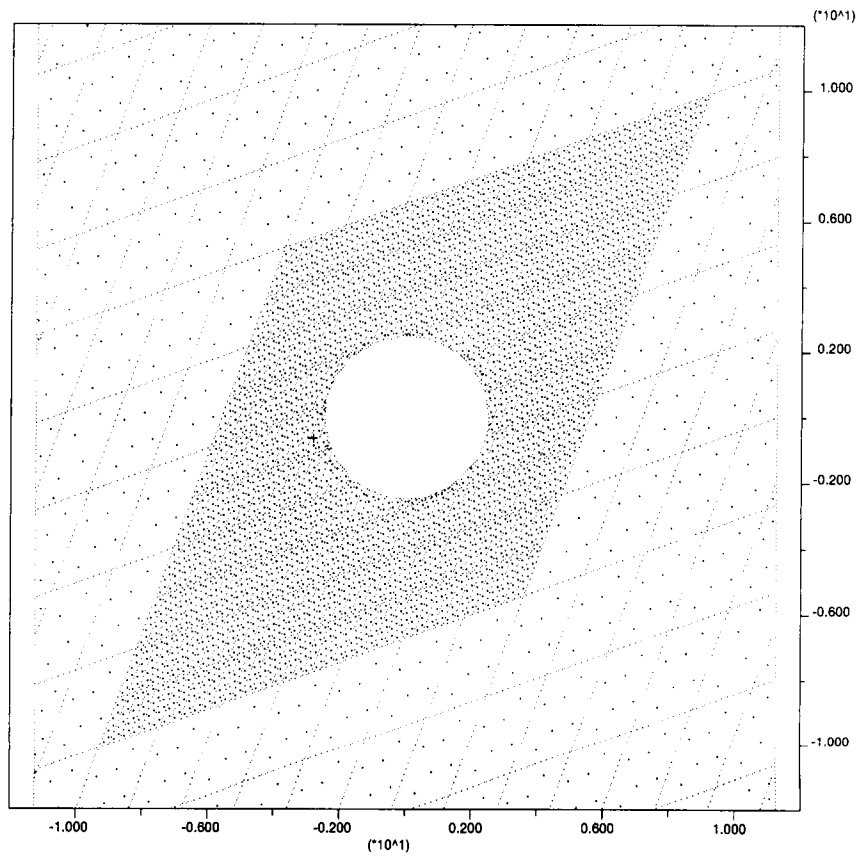


Figure 2.3-3 Distribution of yielding after drift excavation. Dots represent elastic state. Crosses represent yield. Dash lines represent joints

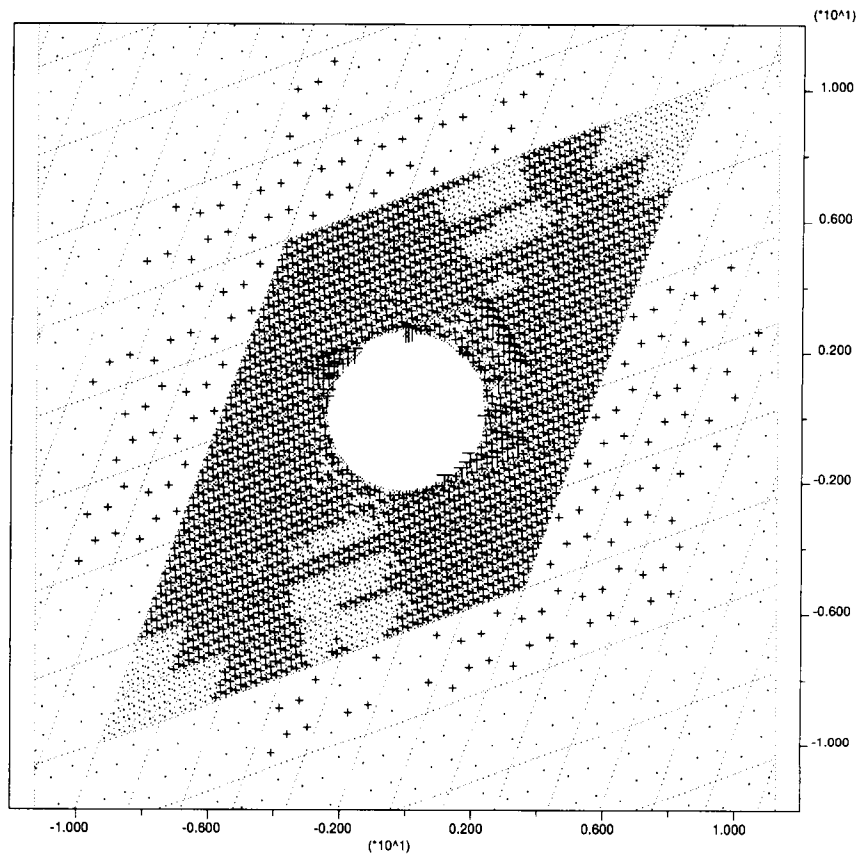


Figure 2.3-4 Distribution of yielding after 100 years of heating. Dots represent elastic state. Crosses represent yield. Dash lines represent joints

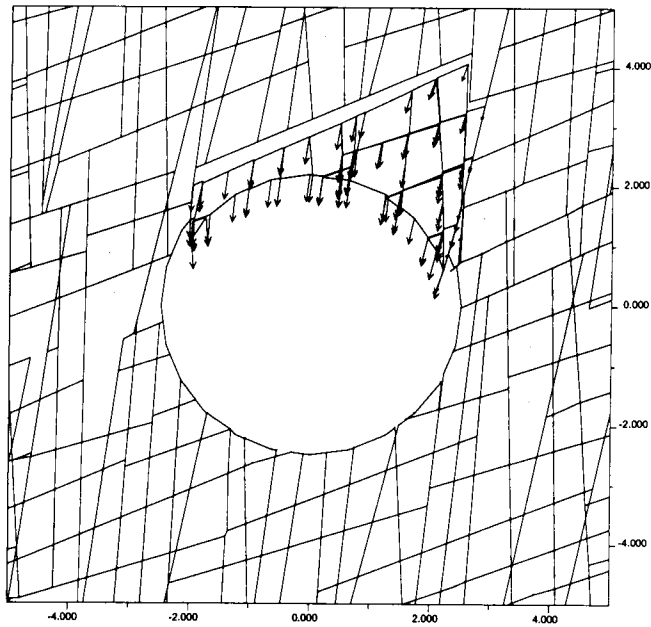


Figure 2.5-1 Rock fall simulated by dynamic analysis of a single drift in a rock mass with irregular joint pattern after subjecting to 0.25 sec of dynamic load

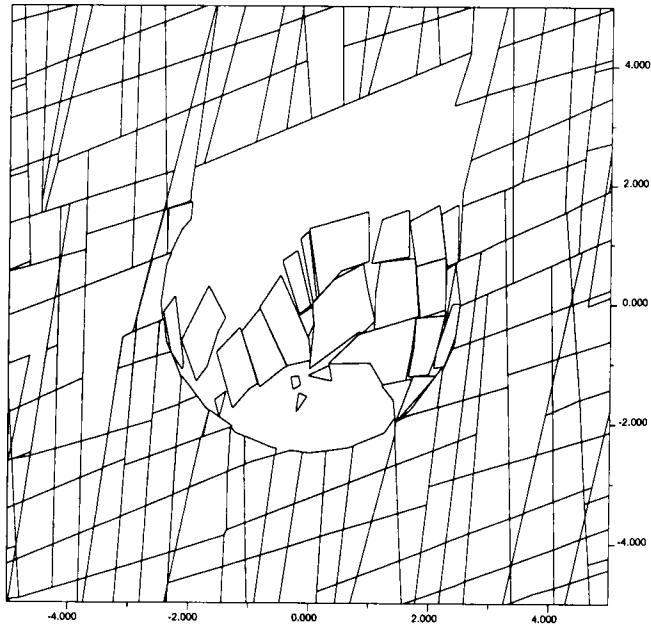


Figure 2.5-2 Rock fall simulated by dynamic analysis of a single drift in a rock mass with irregular joint pattern after subjecting to 1.0 sec of dynamic load.

2.6 Other parameters for additional UDEC dynamic analyses

Joint Patterns:

Set I: strick 118 to 148, dip ≥ 45 , spacing 80% smaller than 0.4

Set II: strick 220 to 250, dip ≥ 45 , spacing 80% smaller than 2

set III: strick 323 to 353, dip < 45 , spacing 50% smaller than 4

(No new entries were make to section 2.6 during printing period ended September 30)

2.7 Additional UDEC Dynamic Analyses Models

Model A described in section 2.5 was a very preliminary model in that: (1) joint pattern was not representative of the repository joint pattern, (2) thermal load was not considered, and (3) seismic load was a simple sigmoidal form rather that a real seismic history from Yucca Mountain or its vicinity. Model B will use a joint pattern that is directly from the ESF full-periphery mapping data.

New entries made during printing period ended September 30:

It was not yet practical to set model B with a joint pattern that is directly from the ESF full-periphery mapping data. Instead, for additional UDEC dynamic analyses, three cases were considered, each with a distinctive joint pattern.

2.7.1 Input Parameters

Fracture Characteristics

As discussed earlier, abundant information has been obtained on fracture characteristics at YM by the DOE through site characterization activities. Fracture data have been collected through core hole exploration (Brechtel et al., 1995; Lin et al., 1993; Spengler et al., 1984, 1981, 1980, and 1979; Scott and Castellanos, 1984), surface mapping (Sweetkind and Williams-Stroud, 1996), and full-periphery geological mapping and detailed line survey in the Exploratory Studies Facilities (ESF) (Beason, 1997; Anna, 1998). Detailed analyses of these fracture data are still in progress at the CNWRA, including analyses of *in situ* block size distributions and statistical summaries of fracture orientation, spacing, and persistence. For the current study, the DOE analyses (Pye et al., 1997) of fracture orientations, frequencies, and fracture sets for the TSw2 based on the detailed line survey data along the ESF main drift were used as the basis to generate fracture patterns for dynamic analyses.

Using stereo graphic projections (Schmidt equal area lower hemisphere projection), the DOE determined three primary fracture sets (Pye et al., 1997). It was also observed that fracture spacings follow log-normal distributions. For the current study, UDEC Version 3.0 command JSET was used to generate an approximation of these three fracture sets. It should be noted that there are a number of limitations in the UDEC Version 3.0 fracture generator including (i) it is limited to two dimensions (2D), (ii) fracture spacing, orientation, trace length, and persistence are assumed to have uniform distributions, and (iii) UDEC Version 3.0 is not capable of handling fractures that do not completely intersect a block. Ideally, a three-dimensional (3D) fracture generator that can account for a variety of distribution types should be used to generate fractures in 3D and obtain the required 2D cross section from the 3D model for mechanical analyses. Alternatively, fracture patterns on a typical cross section from the underground mapping data may be used to digitize the fractures and manually input them into the UDEC Version 3.0 model using UDEC Version

3.0 command CRACK. These options will be further explored in the future when more fracture analysis data become available.

Three fracture patterns were generated for thermal-dynamic analyses. All three cases were generated using as much DOE stereo graphic analysis results as possible under the limitations of UDEC Version 3.0 as described previously; that is, estimating a mean and a deviation value for fracture spacing and orientation based on information provided in DOE analyses (Pye et al., 1997) for each of the three primary fracture sets and using the estimated mean and deviation to generate a fracture pattern in UDEC Version 3.0. It is to be noted that individual judgment played an important role in selecting the mean and deviation for the three fracture sets in DOE data. The purpose of selecting three cases for analyses was to obtain a snap shot of the effect of fracture pattern on rockfall, not to systematically cover all the possible fracture patterns at the repository. Also, fracture trace length and persistence are mainly assumed data. These cases are referred to as cases A through C. Only two fracture sets were assumed for case A, whereas cases B and C had three fracture sets. Table 2.7-1 presents the UDEC Version 3.0 parameters used to generate these fracture patterns.

Table 2.7-1. UDEC Version 3.0 parameters used to generate fracture patterns

Case	Fracture Set	Angle From X Axis (degree)		Trace Length (m)		Gap Length (m)		Joint Spacing (m)	
		Mean	Deviation	Mean	Deviation	Mean	Deviation	Mean	Deviation
A	1st	85	10	7.5	1	0	0	0.4	0.1
	2nd	20	5	5	1	0	0	0.75	0.1
B	1st	85	10	12	4	0	0.1	0.3	0.05
	2nd	20	8	6	2	0	0.1	0.75	0.4
	3rd	110	10	12	4	0	0.1	1.8	0.5
C	1st	85	10	7.5	1	0	0	0.4	0.1
	2nd	20	5	5	1	0	0	0.75	0.1
	3rd	110	10	12	4	0	0.1	1.8	0.5

Thermal Load

The DOE current thermal loading strategy uses the concept of areal mass load (AML). AML refers to the mass of waste emplaced within a unit area occupied by WPs in the repository. Units are in metric tons of uranium per acre (MTU/acre). The Controlled Design Assumptions Document (Civilian Radioactive Waste Management System, Management and Operating Contractor, 1995) describes the assumptions for the thermal loading strategy for YM using the AML as a unit of measure. It states that surface, subsurface and WP designs will be based on a reference mass loading range of 80–100 MTU/acre, with 85 MTU/acre the highest AML that will result in rock temperatures below the geochemical thermal limit or the thermal goals [i.e., the temperature at the average top of the zeolite layer (170 m beneath the potential emplacement area) shall not exceed 90 °C (Civilian Radioactive Waste Management System, Management and Operating Contractor, 1996a)] (U.S. Department of Energy, 1998). Therefore, for the current modeling study,

85 MTU/acre AML was used. To maintain this mass density and consider the prescribed dimensions of the WPs to be disposed at YM, the DOE proposed six possible arrangements of WPs and calculated associated drift and WP spacings as shown in table 2-2, where there is an HLW package between every adjacent spent nuclear fuel (SNF) WPs [containing 21-Pressurized Water Reactor (PWR), 44-Boiling Water Reactor (BWR), or 12-PWR WPs]. The DOE analysis shows that to ensure every space between all SNF WPs can be arranged to accommodate an HLW package while the 85 MTU/acre is still maintained, a uniform drift spacing of 28 m needs to be planned for the entire repository. For 28 m drift spacing, the WP spacing is calculated to be 13.26 m. The heat mass content [$Q(t)$] is the sum of a 44-BWR package [$Q(t)_{44\text{ BWR}}$] and a HLW package [$Q(t)_{\text{HLW}}$] (table 2.7-2) for a single drift and a one-unit cell width (U.S. Department of Energy, 1998):

$$Q(t) = Q(t)_{44\text{BWR}} + Q(t)_{\text{HLW}} \quad (2.7-1)$$

Table 2.7-2. Six possible spent nuclear fuel waste package combinations and associated drift and waste package spacings (U.S. Department of Energy, 1998)

Sequence Number	Waste Package Arrangement	Maximum Drift Spacing (m)	Waste Package Spacing (m)
1	21-PWR HLW 44-BWR	30	13.28
2	21-PWR HLW 21-PWR	32	13.3
3	21-PWR HLW 12-PWR	25	13.67
4	44-BWR HLW 44-BWR	28	13.26
5	44-BWR HLW 12-PWR	23	13.68
6	12-PWR HLW 12-PWR	19	13.58

Note: PWR = Pressurized Water Reactor, HLW = High-Level Waste, and BWR = Boiling Water Reactor

The average thermal decay for a 44-BWR package and a n HLW package given in table V-1 of DOE (1998) was used in calculating $Q(t)$. These values are represented in table 2.7-3. Assuming that heat is uniformly distributed on the drift wall, the decay heat flux $q(t)$ is calculated as

$$q(t) = \frac{Q(t)}{\pi D L_{\text{wp}}} \quad (2.7-2)$$

where D is drift diameter (5 m) and L_{wp} is WP spacing (13.26 m). Version 3.0 of UDEC currently allows a thermal flux boundary condition to be input as a constant or simple exponentially decaying flux with a single decay coefficient of the form

$$q(t) = q_0 \exp(-\alpha t) \quad (2.7-3)$$

where q_0 is the initial surface heat flux (W/m^2) applied to the drift wall at time of emplacement and α is the decay constant ($1/\text{s}$). The initial heat flux was calculated to be $21.59 \text{ W}/\text{m}^2$ for $42.5 \text{ MTU}/\text{acre}$ (or $43.18 \text{ W}/\text{m}^2$ for $85 \text{ MTU}/\text{acre}$) thermal load according to Eq. (2.7-2) and the decay constant was determined to be $3.2197 \times 10^{-10}/\text{s}$ by a best-fitted curve using Microsoft Excel.

It is to be noted that this modeling approach is an approximation. First, in reality, heat transfer from the WP to surrounding rock in an unbackfilled drift would consist of a combination of radiative heat transfer to the wall of the emplacement drift as well as conductive heat transfer to the tunnel floor through the WP support system. Depending on if the unbackfilled drifts are ventilated, heat transfer could also take place in the form of forced convection. Because Version 3.0 of UDEC is incapable of modeling cavity radiation (i.e., currently it handles only boundary radiation to an infinite domain), it was decided to neglect modeling of the WP itself and apply the volumetric heat generated directly as a heat flux to the drift wall. In essence, the analysis neglects heat removal from ventilation. Second, as stated earlier, a best exponential fit using a single decay constant was used to approximate the heat generation rate (decay). In actuality, a number of exponentially decaying terms are usually required. For instance, a recent DOE TM analysis (TRW Environmental Safety Systems, Inc., 1995) used a decaying source term with four decay coefficients.

Table 2.7-3. Average heat flux at 42.5 MTU/acre thermal load for a unit cell (the sum of a 44-Boiling Water Reactor and a high-level waste package)

Time (y)	44 BWR (W/pkg)	HLW (W/pkg)	44 BWR+HLW (W/pkg)	Flux(W/m ²)
0	7493.21	1496.00	8989.21	21.59
5	6651.67	2350.00	8001.67	19.22
10	6051.52	1204.00	7255.52	17.43
20	5121.87	998.00	6119.87	14.70
30	4400.25	792.00	5192.25	12.47
40	3834.48	693.60	4528.08	10.88
50	3375.95	595.20	3971.15	9.54
60	3008.99	496.8	3505.79	8.42
70	2712.55	398.4	3110.95	7.47
80	2467.95	300.00	2767.95	6.65
90	2271.75	276.8	2548.55	6.12
100	2103.07	253.60	2356.67	5.66
150	1597.44	137.60	1735.04	4.17
200	1337.74	60.16	1397.9	3.36
300	1062.96	25.6	1088.56	2.61
400	895.55	16.13	911.68	2.19
500	776.30	10.54	786.84	1.89
600	679.93	9.26	689.19	1.66
700	604.73	7.98	612.71	1.47
800	539.66	6.70	546.36	1.31
900	487.87	5.42	493.29	1.18
1000	444.29	4.40	448.69	1.08
2000	230.59	2.88	233.47	0.56
3000	176.92	52.64	179.56	0.43
4000	157.32	2.40	1559.72	0.38
5000	146.55	2.16	148.71	0.36
6000	135.66	2.07	137.73	0.33
7000	127.07	1.98	129.05	0.31
8000	119.01	1.89	120.90	0.29
9000	112.33	1.81	114.14	0.27
10000	106.61	1.72	108.33	0.26

Note: PWR = Pressurized Water Reactor, HLW = High-Level Waste, and BWR = Boiling Water Reactor

Thermal-Mechanical Properties

TM properties for the current study were selected from a specific case of a previous parametric drift stability study (case 12 from Ahola et al., 1996). These parameter values are presented in table 2-4 for intact rock and fractures. This combination of intact and fracture TM properties caused relatively significant yielding and large shear displacement along fractures (Ahola et al., 1996). These parameter values represent an upper bound value for intact rock cohesion and intact rock Young's modulus; a lower bound value for fracture friction angle, thermal expansion coefficient, and intact rock friction angle; and an average value for the other parameters. As detailed in Ahola et al. (1996), the upper and lower bound and average values of various parameters were selected based on information available from a number of sources including the DOE YM Reference Information Base (U.S. Department of Energy, 1994), borehole drilling data from the YM region (Brechtel et al., 1995), as well as from the DOE thermal study reports (TRW Environmental Safety System, Inc., 1994a,b, 1995, 1996).

Table 2.7-4. Intact rock and fracture thermal-mechanical properties (Ahola et al., 1996)

Parameters	Parameter Values	Unit
Young's Modulus	32	GPa
Poisson's Ratio	0.21	-
Rock Friction Angle	20	Degrees
Rock Cohesion	43	MPa
Rock Tensile Strength	5	MPa
Rock compressive Strength	166	MPa
Rock Density	2297	kg/m ³
Fracture Friction Angle	38	degrees
Fracture Cohesion	0.08	MPa
Fracture Tensile Strength	0.04	MPa
Fracture Normal and Shear Stiffness	1.0×10^{-5}	MPa/m
Fracture Angle of Friction	0.04	-
Thermal Expansion Coefficient	6×10^{-6}	K ⁻¹
Thermal Conductivity	2.1	W/m-K
Specific Heat	932	J/Kg-K

Ground Motion

Since the main purpose of the current study is to establish a strategy to explicitly model rockfall, seismic ground motion input was kept simple. A simple sigmoidal dynamic signal was used, corresponding to a maximum peak ground acceleration of approximately 0.4 g. Potential effects of various characteristics of a more realistic earthquake time history will be investigated in the future. The dynamic signal was applied to the base of the model as a vertically propagating compressive stress wave.

2.7.2 MODEL GEOMETRY AND BOUNDARY CONDITIONS

Similar to previous studies (Ahola et al., 1996), selections of geometric models and boundary conditions were based on the assumption of multiple parallel emplacement drifts and a rock mass that is highly fractured. The study simulated a single emplacement drift placed in the middle of a group of similar emplacement drifts parallel to each other. The emplacement drifts were assumed to be long enough so the plane-strain condition applies. All the fractures were assumed to be 2D and had strikes parallel to the drift. Drift diameter was 5 m and drift spacing 28 m.

Figure 2.7-1 depicts the geometric model comprised of discrete element blocks for a particular fracture pattern analyzed (case C). The model extended vertically from ground surface (about 317 m above the repository horizon) to approximately the groundwater level (about 350 m below the repository level). At such extent, heat flux due to emplaced WPs is almost zero and the ambient temperatures applied along the upper and lower boundaries do not influence the results in the area around the drift for the selected simulation time of 100 yr. To maintain a reasonably small number of blocks and finite difference zones and therefore a workable problem size, only a region approximately one drift diameter in the rock mass was modeled as having the specified fracture spacings. Beyond this region, the size of the blocks was gradually scaled up, while maintaining a comparable fracture pattern. Zoning of the individual blocks was also scaled accordingly. Rock support around the emplacement drift was not modeled. Also, the emplacement drifts were assumed not ventilated.

The vertical boundaries represented lines of symmetry based on the assumption of multiple parallel emplacement drifts, and therefore, were assigned zero horizontal displacement and zero heat flux conditions. The top boundary representing the ground surface was stress free allowing for upward thermal expansion. The bottom boundary was fixed in the vertical direction. Temperature at the top boundary was fixed at 18.7 degrees and at the bottom boundary was fixed at 34.2 degrees. Geothermal gradient was ignored because it has a negligible effect on rockfall induced by either thermal or dynamic stresses. The *in situ* vertical stress at the repository horizon was set to be 7.0 MPa based on average measured values in the DOE advanced conceptual design (Civilian Radioactive Waste Management System, Management and Operating Contractor, 1996b). The vertical stress gradient with depth was assumed 0.0221 MPa/m based on a uniform rock density of 2257 kg/m³. The *in situ* horizontal stress was assumed related to the vertical stress by Poisson's ratio. The Poisson's ratio of 0.21 (see table 2-4) resulted in a horizontal stress gradient of 0.00587 MPa/m along the vertical and a 1.89 MPa horizontal stress at the repository level.

For dynamic analyses, a smaller submodel of the original problem domain was used to reduce the size of the problem and computational time required. This was achieved after the initial TM analyses. Solutions of stresses, temperature, and displacements from the TM analyses were used in the initial conditions for the subsequent dynamic analyses. The submodel extended 50 m above and below the repository horizon (figure 2.7-1). For this preliminary study, only a vertically propagating compressive wave was applied. Therefore, the vertical boundaries remained roller, as was the case for the TM analysis. After first solving for the new

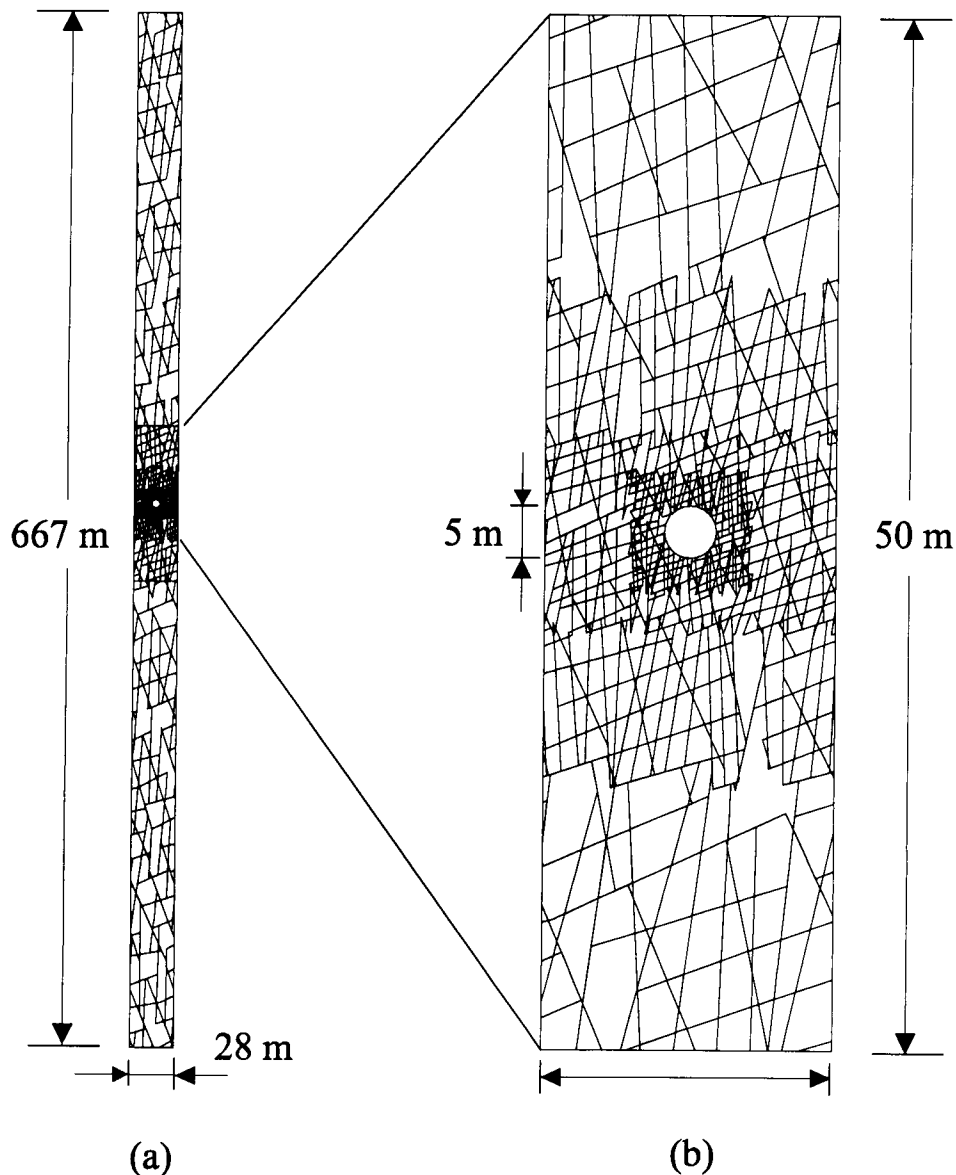


Figure 2.7-1. UDEC Version 3.0 model showing block geometry and a particular fracture pattern (case C). Fractures were assumed to be parallel in the third dimension and perpendicular to the cross section analyzed. (a) Full model for thermal-mechanical analyses. (b) Submodel for dynamic analyses.

boundary stresses (from the solution of the TM model) to be applied to these two boundaries of the submodel after deleting the upper and lower portions from the large TM model, viscous nonreflecting boundary conditions were applied to the top and base of the dynamic model. For the base of the model, this required imputing the earthquake signal as a stress wave rather than as a velocity time history since two velocity boundary conditions (i.e., viscous damping and earthquake velocity time history) cannot be applied at the same boundary. As a result, reflections from the drifts were allowed to pass through the base.

2.7.3 MODELING APPROACH

The modeling started by obtaining an initial model equilibrium under *in situ* stress. After the model reached the initial equilibrium, the tunnel was excavated and a new model equilibrium reached. After these initial analyses, the mechanical time was reset to zero for the TM analysis. UDEC Version 3.0 uses a sequential coupling approach in conducting a TM analyses. This approach consists of running the thermal analysis for a period of time during which the nodal or grid-point temperature is updated. The thermal time is then held fixed while mechanical cycling is conducted to update zone stresses, nodal displacements, and block rotations to reach a new mechanical equilibrium. In such analyses, thermal time is the actual simulation time while the mechanical time is a pseudo-time for the intermediate calculations. An implicit thermal solution scheme based on the Crank-Nicholson method (Itasca Consulting Group, Inc., 1996) was chosen to allow the user to specify a thermal time-step.

For each fracture pattern listed in table 2.7-1, two analyses were performed. The first (cases A, B, and C) assumes no thermal load and the models were subjected to only *in situ* stress and dynamic load. For the second set of analyses (cases A1, B1, and C1), the time-decay thermal load described in section 2.7.1 was applied to the emplacement drift for 100 yr. This corresponds to the repository preclosure time period. At 100 yr, dynamic analysis was conducted to model the effect of an earthquake. When desirable, the seismic load was repeated once to look at the effect of repetitive seismic load on rockfall.

2.7.4 MODELING RESULTS

Modeling results are discussed using explicit rockfall, fracture shear and normal displacements, yield of intact rock blocks, and the relationship among rockfall, fracture displacement, and yielding. A combination of these observations may provide indications of the maximum extent of the potential rockfall region. The observations may also be used as indices for establishing a rockfall criterion in future studies. Both thermal loading levels of 42.5 MTU/acre and 85 MTU/acre were analyzed, although only the latter case was presented in this chapter since these different thermal loading levels did not appear to affect explicit rockfall significantly. The effect of thermal loading level on stresses and displacements will be discussed in detail in the future.

EXPLICIT ROCKFALL

Explicit rockfall generated by dynamic simulation after subjecting to one episode of earthquake ground motion is shown for cases A (figure 2.7-2), B (figure 2.7-3), and C (figure 2.7-4). Rockfall in case A was limited to the upper-right corner of the drift. The drift appeared to be in a rather stable state after the first rockfall because a second episode of earthquake ground motion did not induce further rockfall. Case C had the most extensive rockfall. Rock blocks within a wide region extending 3–3.5 m into the roof area fell into the drift simultaneously after one episode of seismic load, causing the entire opening to collapse. Comparison of the cross sectional area of the opening with the area of the simulated rockfall region indicated this particular rockfall event could fill most of the drift with falling blocks and completely bury the WP. The drift appeared to be unstable after the first episode of seismic load and rock blocks continued to fall off. In case B, the upper-right corner and the first layer of blocks fell off after the first episode of seismic load. The extension of the region of rockfall on the upper-right corner was much greater than that of case A. Continuing analysis showed the upper-right corner was rather unstable, causing collapse of the drift wall on the right-hand side.

As indicated by fracture patterns shown in figures 2.7-2 through 2.7-4 and fracture parameters shown in table 2.7-1, among the three cases, the fracture pattern was the simplest in case A, which included two fracture sets. The first two fracture sets in case B were essentially the same as those in case A, except case B included a third fracture set oriented about 110 degrees from the x-axis. Although this third fracture set had large spacings, its inclusion in the model increased the amount of simulated rockfall significantly. The fracture pattern in case C was similar to that in case B, however, block size was smaller and more irregular in the roof region. These comparisons indicate that the more irregular the fracture pattern, the more extensive the rockfall. Rockfall also shows dependence on block size: the smaller the block size, the more extensive the rockfall. Further analyses are necessary to confirm these observations.

In the case of heated drifts (i.e., conducting TM analyses for 100 yr prior to dynamic analyses), some rock blocks fell during thermal loading stage. For example, the blocks on the upper-right corner in case A1 fell off during the thermal loading and then the opening appeared to be stable with no further falling blocks during seismic load. In case B1, blocks on the upper-right corner loosened during thermal loading and eventually fell off at the early stage of seismic loading (figure 2.7-5 a,b). It is interesting to note that the region involving rockfall for the case of heated drift is actually smaller than that in the case of unheated drift. Repetitive seismic load did not cause further rockfall. A similar phenomenon was also observed in case C1. Blocks in the roof region in case C1 loosened during thermal loading and gradually fell off during the early stage of seismic loading (figures 2.7-6a,b). Similar to case B1, the region involving rockfall in the case of heated drift is somewhat smaller than that of an unheated drift during the first episode of seismic loading. Rockfall continued during the subsequent modeling, however, and the opening appeared to be unstable as was the case in the unheated drift.

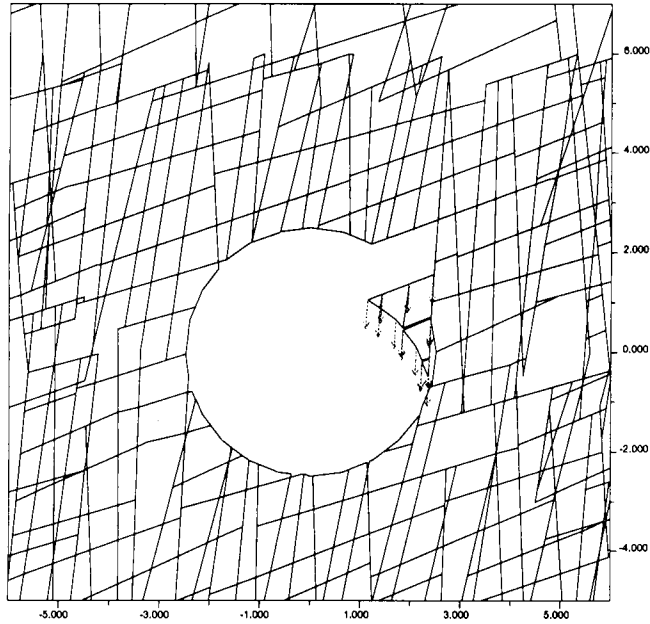


Figure 2.7-2. Explicit rockfall generated by dynamic simulation after subjecting to one episode of earthquake ground motion for case A (unheated drift)

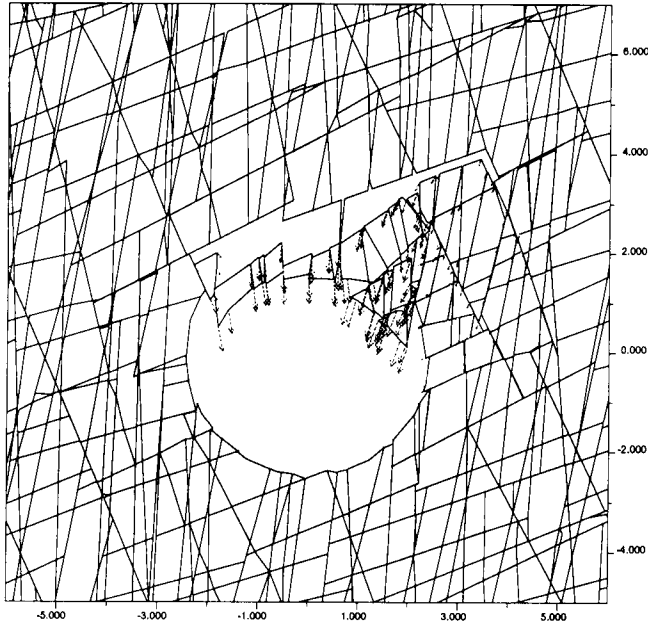


Figure 2.7-3. Explicit rockfall generated by dynamic simulation after subjecting to one episode of earthquake ground motion for case B (unheated drift)

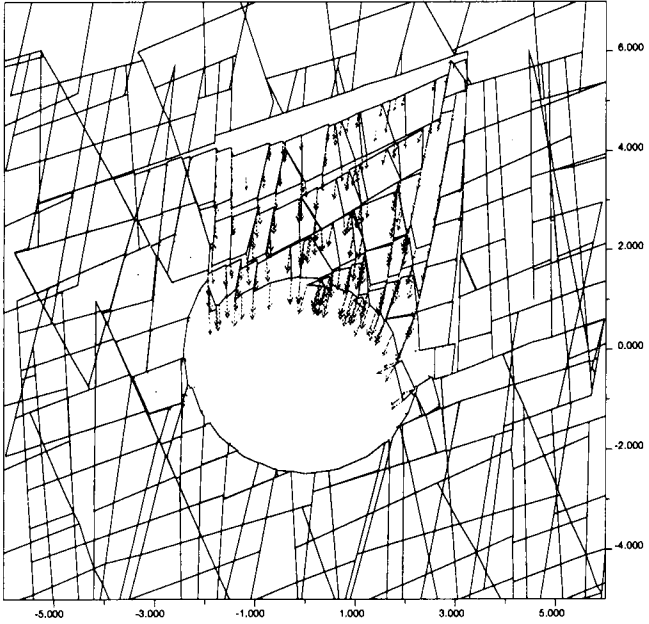


Figure 2.7-4. Explicit rockfall generated by dynamic simulation after subjecting to one episode of earthquake ground motion for case C (unheated drift)

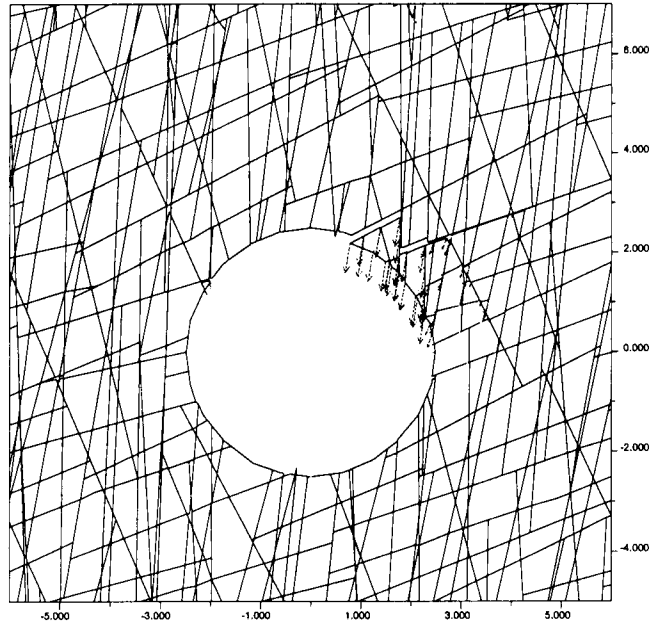


Figure 2.7-5a. Explicit rockfall generated by thermal and dynamic simulation for case B1 (heated drift) after 100 yr of thermal loading

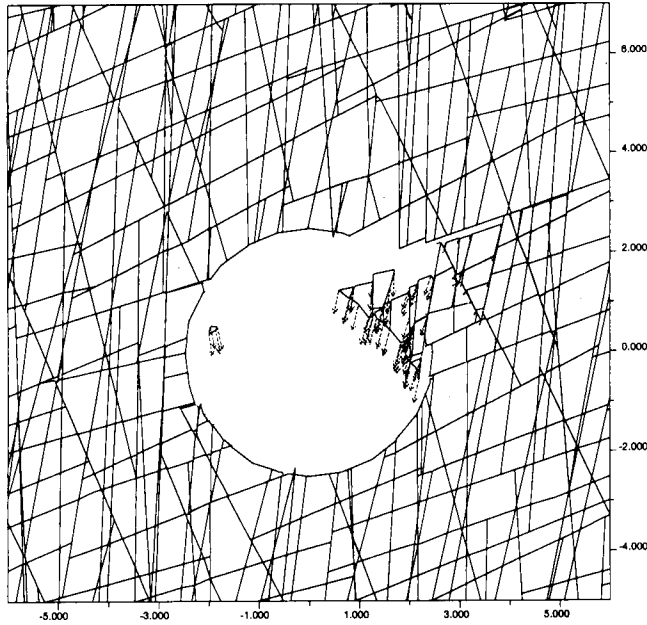


Figure 2.7-5b. Explicit rockfall generated by thermal and dynamic simulation for case B1 (heated drift) after 100 yr of thermal loading and one episode of earthquake ground motion

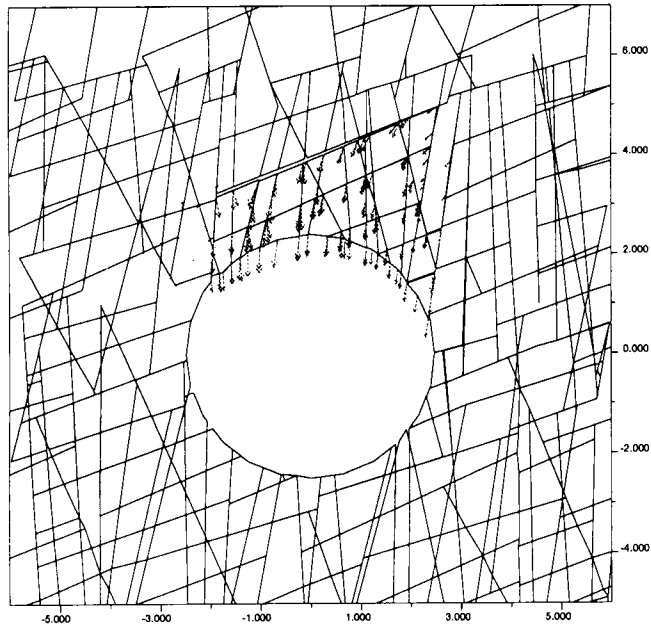


Figure 2.7-6a. Explicit rockfall generated by thermal and dynamic simulation for case C1 (heated drift) after 100 yr of thermal loading

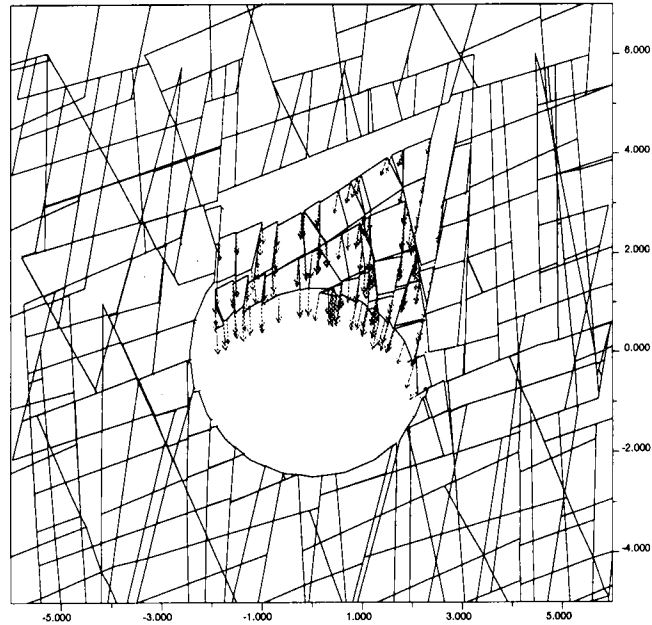


Figure 2.7-6b. Explicit rockfall generated by thermal and dynamic simulation for case C1 (heated drift) after 100 yr of thermal loading and one episode of earthquake ground motion

FRACTURE DISPLACEMENT

Thermal loading has been observed to generally increase fracture shear displacement and fracture opening (Ahola et al., 1996). A similar phenomenon was observed in the current modeling analyses. Furthermore, seismic load appears to increase both fracture shear displacement and fracture opening significantly. An increase in fracture displacement was observed in all three cases for both heated and unheated drifts. It is not practical, however, to quantify these changes in fracture displacements at the current stage. Further modeling effort is necessary, especially since fracture displacements also depend on *in situ* fracture patterns.

YIELD OF INTACT ROCK BLOCKS

The yield of intact rock blocks was observed previously to increase with thermal load (Ahola et al., 1996) and if extensive yield had already occurred during thermal loading, seismic load will further increase the yield (Ahola, 1997). Not much yield of intact rock blocks was observed during the current study; this may be because of the relatively lower thermal load. Since the yield of intact rock depends largely on rock TM properties, conclusions with regard to the yield cannot be drawn at this stage. Future studies will consider the effect of fracture and intact rock TM properties.

7.2.5 DISCUSSIONS

EFFECT OF FRACTURE PATTERN ON ROCKFALL

As discussed earlier, fracture pattern appears to have the controlling effects on the amount of simulated rockfall. With increasing complexity of fracture patterns, especially significantly varying orientations, and decreasing block sizes (or fracture spacings), it appears the number of rock blocks falling on a WP increases. Even with the same set of fracture parameters (i.e., statistical data summarized based on field mapping and other measuring results), the generated fracture pattern could be slightly different. The slight difference in fracture pattern, especially near roof area, could result in a different amount of rockfall during each seismic ground motion episode. The controlling effect of fracture patterns, particularly those of irregular nature, on underground opening stability has been observed in the literature (e.g., Bhasin and Hoeg, 1998; Makurat et al., 1990; Leung and Quek, 1995). It is, therefore, important to be able to characterize fracture distribution and generate fracture patterns representative of the *in situ* fracture pattern at the repository. The fracture generator in Version 3.0 of UDEC is limited to uniform distribution. As mentioned previously, most fracture parameters (e.g., fracture spacing and inclination angle), show a log-normal distribution at YM. Controlling the generated intact block size in the current version of UDEC Version 3.0 is achieved by adjusting the fracture spacing and is not straight forward. Additional external calculations are necessary to estimate the generated block size distribution. Therefore, it is not easy to isolate the effect of block size with similar fracture patterns on rockfall.

Also, fracture patterns may have significant spatial variations within the repository, depending on the nearby stratigraphic and faulting characteristics. It is, therefore, necessary in future studies to consider an array of fracture patterns. To accomplish this, the results of a detailed study of fractures is necessary. Two approaches have been considered: use a more applicable fracture generator and generate fracture patterns based on statistical fracture parameter data from detailed fracture studies and digitize selected fracture mapping results, such as the full-periphery mapping at the ESF main drift with tunnel curvature corrected. The second approach is rather straight forward and relatively easy to interpret. The representiveness of the selected mapped sections may be limited, however. The first approach should be more representative statistically, however, it needs significant effort in identifying and utilizing a practical fracture generator and

detailed fracture study using commercial software, such as FRACMAN (Dershowitz et al., 1993). A recently developed technical approach for defining *in situ* block size proposed by Hadjigeorgiou and Grenon (1998) may also be modified and used as a fracture generator.

Another important aspect of the *in situ* fracture geometric characteristic is block size distribution. *In situ* block size distribution is also important in assessing the potential impact of rockfall on WPs—it provides a lower bound for the potential impact force on the WPs by falling blocks. Some research has been done on *in situ* block size at YM. For example, Gauthier et al. (1995) estimated size distribution of individual rock blocks using a modified (log-space) version of the Topopah Spring fracture spacing distribution developed by Schenker et al. (1995), assuming cubic and parallel-piped blocks. It should be noted that assumptions of cubic or parallel-piped block shape may distort the estimation of size distribution of *in situ* blocks through various assumptions with regard to the extent of fractures in the 3D. In published literature in recent years, several models have been developed capable of simulating the 3D nature of a rock mass (e.g., Dershowitz and Einstein, 1988). These models differ in degree of complexity and sophistication and basic theoretical background (e.g., finite/infinite fracture size and block shape). Examples of these models include the Simblock model developed by Peaker (1990), the Blocks model developed by Maerz and Germain (1992), and the Stereoblock model developed by Hadjigeorgiou et al. (1995) and Hadjigeorgiou and Grenon (1998). These models will be further examined and applied to analyzing block size distributions at YM.

EFFECT OF SEISMIC TIME HISTORY ON ROCKFALL

As indicated in section 2.7.1, seismic ground motion input in the current modeling study was a sigmoidal dynamic signal to simplify the problem. In an actual earthquake time history, the acceleration pulses are of varying amplitudes and frequencies. Since ground motion at a particular site is influenced by source, travel path characteristics, and local site conditions, it is important in dynamic response analyses to use ground motion input that is site specific. Historically recorded ground motion time histories at YM are currently being selected and analyzed to generate representative site-specific ground motion time histories for continuing dynamic analyses. These three basic steps should be performed in the following order:

- (1) Collection and selection of recorded ground motion time histories
- (2) Spectrum analyses for source and path characteristics
- (3) Generation of a range of site-specific ground motion time histories depicting source and path characteristics

EFFECT OF INTACT ROCK AND FRACTURE THERMAL-MECHANICAL PROPERTIES

It is recognized that current information and the level of understanding regarding long-term degradation of the rock mass within the near-field repository environment is limited. As a result, the previous parametric study of stability of drift under static load employed ranges of TM parameters measured in the laboratory or field to account for the variation of parameters at the YM site as well as how they may change or degrade with temperature, time, stress, and moisture content (Ahola et al., 1996). The effect of rock and fracture TM properties on stability of drift under dynamic load will be considered and studied in more detail in the future.

EFFECT OF MODEL SETUP ON ROCKFALL

For block dynamic analysis of a discontinuum system, a few modeling considerations may actually

affect modeling results significantly and such effects need to be understood in future modeling exercises. These considerations may include mechanical damping, wave transmission in a discontinuum system, boundary effects, and loading approach. Currently, the performance of the UDEC Version 3.0 code with regard to how these modeling considerations may have affected modeling results is not yet well understood.

EXPLICIT MODELING OF ROCKFALL AND ROCKFALL CRITERIA

Since the number of computer simulations that can model rockfall explicitly is limited, it is desirable to establish a rock fall criterion to define the vertical extent of the potential rockfall region using indices such as the amount of explicitly simulated rockfall, fracture shear and normal displacements, and yielding of intact rock blocks. Such a rockfall criterion may be a function of fracture pattern, size of *in situ* rock blocks, and level of earthquake ground motion for a specific combination of rock mass TM properties. Future analyses may also explore the dependence of this rockfall criterion on rock mass TM properties.

Section 2.8 through 2.10 are new entries made during printing period ended September 30

2.8 Check of UDEC Version 3.0 Thermal Scheme and Modeling Strategies

Further analyses of UDEC trial cases reveal that there is a bug in udec30. UDEC Version 3.0 formal release as received from Itasca resulted in incorrect thermal calculations. The problem was reported to Itasca. After a couple of weeks of debugging, Itasca found out that the code mistakenly takes single zone blocks as heat sinks. Therefore, if a specific model has many small blocks that are zoned as single zone blocks, the calculated temperature will be very wrong. Consequently, thermal stresses are incorrect. This indicates that the more single zone blocks a specific model has, the further off the thermal results are from the correct solution. The only case that this bug does not appear to affect the results is for models that do not have any single zone blocks.

The problem appears to be a memory allocation problem and is fixed by making the following change in the source code per e-mail message from Branko dated 11/3/98:

```
In file udecom.inc
change:
      .          kbtm=25, kbdt1=26, kbthm=27, kbfix=28, kbdtm=29)
to:
      .          kbtm=25, kbdt1=26, kbthm=27, kbfix=27, kbdtm=29)
```

After making this correction, the thermal results appear to be correct. Cases A through C discussed in section 2.7 were recalculated with the UDEC Version 3.0 fixed. The results shown that the bug did not appear to have significantly affected the qualitative results of rockfall, fracture shear displacement, or yielding.

2.9 Wave Transmission in UDEC Version 3.0 and Dynamic Modeling

Entries into Scientific Notebook No. 274 for the period July through September, 1998 have been made by Rui Chen on 12/08/98.

No original text entered into this Scientific Notebook has been removed.


 12/08/98

3.0 REFERENCES

- Ahola, M.P., R. Chen, H. Karimi, S.M. Hsiung, and A.H. Chowdhury. 1996. *A Parametric Study of Drift Stability in Jointed Rock Mass, Phase I: Discrete Element Thermal-Mechanical Analysis of Unbackfilled Drifts*. CNWRA 96-009. San Antonio, TX: Center for Nuclear Waste Regulatory Analyses.
- Ahola, M.P. 1997. *A Parametric Study of Drift Stability in Jointed Rock Mass—Phase II: Discrete Element Dynamic Analysis of Unbackfilled Drifts*. CNWRA 97-007. San Antonio, TX: Center for Nuclear Waste Regulatory Analyses.
- Anna, L.O. 1998. *Preliminary Three-Dimensional Discrete Fracture Model of Topopah Spring Tuff in the Exploratory Studies Facility, Yucca Mountain Area, Nye County, Nevada*. USGS Open-File Report 97-834. Washington, DC: U.S. Geological Survey.
- Beason, S.C. 1997. Previous mapping efforts. *Handout and presentation at U.S. Department of Energy/Nuclear Regulatory Commission Appendix 7 Meetings, October 16, 1997*. Washington, DC.
- Bhasin, R., and K. Hoeg, 1998. Parametric study for a large cavern in jointed rock using a distinct element model (UDECB-BB). *International Journal of Rock Mechanics and Mining Sciences* 35(1): 17–29.
- Brechtel, C.E., M. Lin, E. Martin, and D. S. Kessel., 1995. *Geotechnical Characterization of the North Ramp of the Exploratory Studies Facility*. Vol. 1 - Data Summary. SAND95-0488/1. Albuquerque, NM: Sandia National Laboratories.
- Civilian Radioactive Waste Management System, Management and Operating Contractor. 1995. *Controlled Design Assumptions Document*. B00000000–01717–4600–00032. Rev. 02, ICN 01. Las Vegas, NV: Civilian Radioactive Waste Management System.
- Civilian Radioactive Waste management System, Management and Operating Contractor. 1996a. *Thermal Loading Study for FY1996*. B00000000–01717–5705–00044. Rev. 1. Las Vegas, NV: Civilian Radioactive Waste Management System.
- Civilian Radioactive Waste Management System, Management and Operating Contractor. 1996b. *Mined Geologic Disposal System Advanced Conceptual Design Report*. Volume II. B00000000–01717–5705–00015. Rev. 00. Las Vegas, NV: Civilian Radioactive Waste Management System.
- Dershowitz, W.S., and H.H. Einstein. 1988. Characterizing rock joint geometry with joint system models. *Rock Mechanics* 21: 21–51.
- Dershowitz, W., G. Lee, J. Geier, S. Hitchcock, and P. LaPointe. 1993. *FRACMAN-Interactive Discrete Feature Data Analysis, Geometric Modeling, Exploration Simulation*. Redmond, WA: Golder Associates Inc.
- Fahy, M.F. and F.C. Beason. 1995. *Geotechnical Analysis for the Exploratory Studies Facility North Ramp Boxcut and Starter Tunnel*. Preliminary report prepared for the Department of Energy of Management and Operating Contractor Architect/Engineer by the Bureau of Reclamation/U.S. Geological Survey, vol 1&2.
- Gauthier, J.H., M.L. Wilson, D.J. Borns, and B.W. Arnold. 1995. Impacts of seismic activity on long-term repository performance at Yucca Mountain. *Focus '95: Proceedings of the Methods of Seismic Hazards Evaluation*. La Grange Park, IL: American Nuclear Society: 159–168.

- Hadjigeorgiou, J., and M. Grenon. 1998. Defining in-situ block size. *The Canadian Mining and Metallurgical Bulletin* 91(1020): 72–75.
- Hadjigeorgiou, J., J.F. Lessard, and F. Flament. 1995. Characterizing in-situ block distribution using a stereological model. *Canadian Tunneling Journal*: 201–211
- Itasca Consulting Group, Inc. 1996. *UDEC—Universal Distinct Element Code. Version 3.0, Volume I: User's Manual*. Minneapolis, MN: Itasca Consulting Group, Inc.
- Leung, C.F., and S.T. Quek. 1995. Probabilistic stability analysis of excavations in jointed rock. *Canadian Geotechnical Journal* 32: 397–407.
- Lin, M., M.P. Hardy, and S.J. Bauer. 1993. *Fracture Analysis and Rock Quality Designation Estimation for the Yucca Mountain Site Characterization Project*. SAND92-0449. Albuquerque, NM: Sandia National Laboratories.
- Maerz, N.H., and P. Germain. 1992. Block size determination around underground openings using simulations based on scanline mapping. *Preprints of the International Society for Rock Mechanics Conference on Fractured and Jointed Rock Masses, Lake Tahoe, Nevada*. Berkeley, CA: Lawrence Berkeley National Laboratory.
- Makurat, A., N. Barton, G. Vik, P. Chryssanthakis, and K. Monsen. 1990. *Rock Joints*. Barton and Stephansson, eds. ISBN 90 61901 1095. Balkema, Rotterdam.
- Peaker, S.M. 1990. *Development of a simple block size distribution model for the classification of rock masses*. Master's thesis, University of Toronto.
- Pye, J.H., D.C. Kicker, and G.H. Nieder-Westermann. 1997. Plans for mapping of subsurface Facilities. *Notes from U.S. Department of Energy/Nuclear Regulatory Commission Appendix 7 Discussions, October 16, 1997*. Washington, DC.
- Schenker, A.R., D.C. Guerin, T.H. Robey, C.A. Rautman, and R.W. Barnard. 1995. *Stochastic Hydrogeologic Units and Hydrogeologic Properties Development for Total-System Performance Assessments*. SAND94-0244. Albuquerque, NM: Sandia National Laboratories.
- Scott, R.B., and M. Castellanos. 1984. *Stratigraphic and Structural Relations of Volcanic Rocks in Drill Holes USW GU-3 and USW G-3, Yucca Mountain, Nye County, Nevada*. USGS/OFR-84-491 (NNA.890804.0017, USW GU-3) Denver, CO: U.S. Geological Survey.
- Spengler, R.W., D.C. Muller, and R.B. Livermore. 1979. *Preliminary Report on the Geology and Geophysics of Drill Hole UE-25a-1, Yucca Mountain Nevada Test Site*. USGS/OFR-79-1244 (HQS.880517.1491) (UE-25a #1). Denver, CO: U.S. Geological Survey.
- Spengler, R.W., and J.G. Rsenbaum. 1980. *Preliminary Interpretations of Geologic Results Obtained from Boreholes UE25a-4, -5, -6, and -7, Yucca Mountain, Nevada Test Site*. USGS/OFR-80-929 (NNA.890823.0106). Reston, VA: U.S. Geological Survey.
- Spengler, R.W., F.M. Byers, Jr., and J.B. Warner. 1981. *Stratigraphy and Structure of Volcanic Rocks in Drill Hole USW-G1, Yucca Mountain, Nye County, Nevada*. USGS/OFR-81-1349, DOE/ET/44802/T4

(HQS.880517.1492) (USW G-1). Denver, CO: U.S. Geological Survey.

Spengler, R.W., M.P. Chornack, D.C. Muller, and J.E. Kibler. 1984. *Stratigraphic and Structural Characteristics of Volcanic Rocks in Core Hole USW G-4, Yucca Mountain, Nye County, Nevada*. USGS/OFR-84-789 (NNA.870519.0105) (USW G-4). Denver, CO: U.S. Geological Survey.

Sweetkind, D.S., and S.C. Williams-Stroud. 1996. *Characteristics of Fractures at Yucca Mountain, Nevada: Synthesis Report*. Administrative Report. Denver CO: U.S. Geological Survey.

TRW Environmental Safety Systems, Inc. 1994a. *Initial Summary Report for Repository/Waste Package Advanced Conceptual Design*. B00000000-01717-5705-00015. Volume I, Rev. 00. Las Vegas, NV: TRW Environmental Safety Systems, Inc.

TRW Environmental Safety Systems, Inc. 1994b. *FY93 Thermal Loading Systems Study Final Report*. Volumes I and II, Rev. 1. Las Vegas, NV: TRW Environmental Safety Systems, Inc.

TRW Environmental Safety Systems, Inc. 1995. *Thermomechanical Analyses*. Prepared for the U.S. Department of Energy. BC0000000-0717-5705-00013. Rev. 00. Las Vegas, NV: TRW Environmental Safety Systems, Inc.

TRW Environmental Safety Systems, Inc. 1996. *Thermal Loading Study for FY1995*. Las Vegas, NV: TRW Environmental Safety Systems, Inc.

U.S. Department of Energy. 1994. *Reference Information Base (RIB), Yucca Mountain Site Characterization Project*. Washington, DC: U.S. Department of Energy.

U.S. Department of Energy. 1998. *Repository Thermal Loading Management Analysis*. B00000000-01717-0200-00135. Rev. 00. Washington, DC: U.S. Department of Energy.

Wernicke, B.P. 1992. Cenozoic extensional tectonics of the Western Cordillera. The Cordilleran Orogen: Conterminous U.S. B.C. Burchfiel, P.W. Lipman, and M.C. Zoback, eds. *The Geology of North America*. Boulder, CO: Geological Society of America G-3: 553-581.

Wong, I.G., and J.C. Stepp. 1998. *Probabilistic Seismic Hazard Analyses for Fault Displacement and Vibratory Ground Motion at Yucca Mountain, Nevada*. Final report. Oakland, CA: Civilian Radioactive Waste Management System.

Sweetkind and Williams-Stroud. 1996

Verbeek and Throckmorton, 1995

Electronic Scientific Notebook No. 274E:
Estimate Rock Fall in Emplacement Drifts
Induced by Earthquakes under Heated
Conditions to Provide Input for Performance
Assessment(06/09/1998 through 07/23/1998)

SCIENTIFIC NOTEBOOK

by

Rui Chen

SCIENTIFIC NOTEBOOK

by

Rui Chen

Southwest Research Institute
Center for Nuclear Waste Regulatory Analyses
San Antonio, Texas

August 23, 1999

RC

1. INITIAL ENTRIES

Scientific Notebook: # 274 (Part 2)
Issued to: Rui Chen
Issue Date: June 9, 1998
Printing Period: April 1999 to June 1999
Project Title: Seismic effect on drift stability under heated condition

By agreement with the CNWRA QA this Notebook is to be printed at approximate quarterly intervals. This computerized Scientific Notebook is intended to address the criteria of CNWRA QAP-001.

1.1. Objectives

The main objective of this project is to estimate rock fall in emplacement drifts induced by earthquakes under heated conditions to provide input for performance assessment. Such estimates should include: (i) range of rock block sizes (distribution of rock block sizes?), (ii) initiation of rock fall (thermally or seismically induced?), (iii) rate of rock fall, (iv) location of rock fall, and (iv) correlation of size, initiation, and rate of rock fall.

Other objectives may include to estimate: (i) seismic effect on drift stability in general by examining drift closure, joint displacement, yielding etc; (ii) effect of seismic load and rock fall on concrete lining; (iii) seismic effect on near field environment, including change in rock mass mechanical and hydrological properties which maybe important in post closure performance assessment.

(No new entries were make to section 1.1 during printing period ended September 30)

1.2. Technical Approaches and Data Sources

The range and distribution of rock block sizes will be analyzed based on the range and distribution of joint spacing, joint sets, and orientation information developed for the Topopah Spring, the host rock of the repository at Yucca Mountain, through DOE site characterization activities and in situ measurements from the ESF. Sources for the measured joint information may be found in Fahy and Beason (1995), Brechtel et al. (1995), Lin et al. (1993).

UDEC computer code will be used to estimate seismic effect on emplacement drift, including size, initiation, and rate of rock fall; and correlation of these parameters.

Various reports and database developed by the DOE and its contractors and subcontractors for the Yucca Mountain project.

(No new entries were made to section 1.2 during printing period ended June 30, 1999)

RC

1.3. Computers, Computer Codes, and Data Files

Table 1-1 lists computer equipment and computer codes. Table 1-2 provides names, type, and content of computer files used in the seismic analysis project.

Table 1-1. Computing Equipment

Machine Name	Type	OS	Location	Computer Code	Language
Foxtrot	Ultra Sun Workstation	Solaris 2.5	Bldg. 189	UDEC	Fortran 77
Foxtrot	Ultra Sun Workstation	Solaris 2.5	Bldg. 189	XPLOT	N.A.

Table 1-2. Names, Type, and Content of Relative Files

File Name	Directory	Type	Content
udec30		executable	Executable of udec software version 3.0
*.dat		text	Input data file for udec analyses
*.sav		binary	Result file from udec analyses
		text	

(No new entries were made to section 1.3 during printing period ended June 30, 1999)

2. IN-PROCESS ENTRIES

Analyses of rock fall should be able to establish technically sound criteria for determining the extent of rock fall around emplacement drifts and the size distribution of rock blocks that have the potential to fall onto the waste packages. Such analyses should explicitly account for three basic aspects:

- Analyses of size distribution of individual blocks
- Analyses of the possibility of simultaneous rock fall and vertical extent of rock fall
- Analyses of initiation, location, and rate of rock fall

The ultimate goal of these analyses is to yield technically sound estimation of the ranges of size of rock blocks that have the potential to fall onto the waste packages to provide input for the evaluation of impact of such rock fall on the integrity of the waste packages.

2.9 Check Wave Transmission in UDEC Version 3.0 and Dynamic Modeling in General

Checking of wave transmission was performed using a simple model of 100 m high and 28 m wide with no joints or opening. A simple cosine wave history was used, starting with only compressive wave applied as stress wave to the bottom of the model. The desired velocity amplitude of 0.0625 m/s was calculated from the desired acceleration amplitude of 0.4g and the desired input signal frequency of 10 hz. Velocity wave history was converted to stress wave history according to equations k.5 and k.6 on page K-5 of UDEC manual. The input data is attach as appendix A (wave.dat). Calculated velocity and displacement were monitored at a few points in the model. The following observations were made:

1. The magnitude of input and simulated velocity: Calculated velocity was about 28 percent less than the input velocity due to one-dimensional approximation in converting velocity history to stress history. After a couple of trial runs, it was determined that a scaling factor of 1.4 is necessary to bring the modeled velocity to the input velocity level.
2. Distortion of wave shape and the effect of zone size: No distortion of input wave shape occur with or without joints and opening. Changing zone edge size from 10 to 2 did not seem to make any difference.
3. Modeling of shear wave: Modeling of shear wave need to use free-field boundary conditions. The process is very tricky in UDEC.. See detailed notes in the input file, i.e., file wave.dat. It seems that only the normal stress boundary need to be scaled for the free-field boundary element. However, the compressive component always need to be scaled.
4. Model complexity:
 - 4-1 Effect of joint spacing around the opening
Compare wave.dat vs. wave1.dat. No significant difference found.
 - 4-2 Effect of jointing other than those around the opening

RC

Compare wave.dat vs wave2.dat. No significant difference found.

4-3 Effect of boundary extent

5. Effect of input wave frequency

6. Damping issues

2.10 Design Earthquake Time Histories at YM

Design basis ground motion time histories from DOE (Risk Engineering, Inc., 1999) were digitized and used as input for a test run with the data file named Design.dat. Distortion occurred.
Need to investigate why!

2.11 Development of Fracture Pattern and UDEC Interpretation

Development of fracture pattern initiated during April 1 - June 30. John Hadjigeorgiou of Georock is conducting the analyses and work will be reported in his scientific notebook.

3. REFERENCES

Risk Engineering, Inc., 1999. *Seismic Design Basis Inputs for a High-Level Waste Repository at Yucca Mountain, Nevada*. A report by the seismic design team. Document No. B00000000-01727-5700-0018 Rev 0.

Entries into Scientific Notebook # 274 for the period June 9, 1998 to August 2000 have been made by Rui Chen / *[Signature]* / 8/18/2000.

Entries into Scientific Notebook # 274 have been made by Rui Chen / *[Signature]* / 8/18/2000. No original text entered into this S/N has been removed. *[Signature]*, 8/18/2000

Date: 4/20/99
Sender: Rui Chen
To: Bruce Mabrito
cc: Asadul Chowdhury
Priority: Normal
Subject: Scientific Notebook #
Bruce,

There are not entries made to Scientific Notebook No. 274 during the period ended on March 31, 1999.

Rui

Date: 10/29/99
Sender: Rui Chen
To: Bruce Mabrito
cc: Asadul Chowdhury
Priority: Normal
Subject: Re:AP-3-1 Forms/Scientific Notebooks

No entries were made to scientific notebook # 274 during the last reporting period (July-September). Also, no new entries will be made to the same scientific notebook. Please close this scientific notebook. The continuation of the work (a completely new phase) will be documented by a manual scientific notebook with a different number.

Rui Chen

Reply Separator

Subject: AP-3-1 Forms/Scientific Notebooks
Author: Bruce Mabrito
Date: 10/29/99 12:45 AM

The following message is being sent to individuals who have not returned the CNWRA Acknowledgement Page from documents sent to them over 30 days ago.

We request you return the respective CNWRA Acknowledgement Page to QA at this time.

**A separate follow up call will be made for Electronic Scientific Notebooks.
Bruce Mabrito**

Forward Header

Subject: Ap-3-1 Forms/Scientific Notebooks
Author: Maria Padilla
Date: 10/28/99 12:51 PM

Update on AP-3-1 forms.

The following individuals have not returned the AP-3-1 (Acknowledgement form) for the following:

TOP-018, Development & Control of Scientific and Engineering Software,
distributed on 5/01/98
R. Martin - reprinted and reissued on 10/28/99 (2nd time)

QAP-002 Review of CNWRA Documents, Reports, Papers and Presentation Materials,
distributed on 8/12/98
R. Martin -reprinted and reissued on 10/28/99 (2nd time)

QAP-001 SCIENTIFIC NOTEBOOK CONTROL distributed on 9/14/98
R. Martin - reprinted and reissued on 10/28/99 (2nd time)

QAP-006 Acceptance & Identification on Procured Items, Samples, and Software,
distributed 11/16/98
R. Martin reprinted and reissued on 10/28/99 (2nd time)

QAP-003 Standard Procurement Document Quality Requirements for Scientific Investigations, Interpretations and Analysis Service Suppliers, Rev 0/Chg. 0,
distributed 5/14/99
B. Meehan - reprinted and resent on 10/26/99

Operations Plan for Technical Assistance on Department of Energy Aluminum Based Spent Nuclear Fuels Disposition Program, Rev 1/Chg. 1, distributed 5/28/99
B. Meehan - reprinted and resent on 10/26/99



CENTER FOR NUCLEAR WASTE REGULATORY ANALYSES

SCIENTIFIC NOTEBOOK REVIEW CHECKLIST RECORD

Scientific Notebook No.: 274 E

Accomplished

- 1. Initial entries per QAP-001
- 2. Dating of entries
- 3. Corrections (crossed out, one line through w/initials/date)
- 4. White out not used
- 5. Page number visible on original notebook
- 6. In process entries per QAP-001
- 7. Figure numbers present
- 8. Text visible
- 9. Electronic Scientific Notebook changes initialed and dated
- 10. Permanent ink or type only
- 11. Signing of entries (not required on each page)
- 12. Statement at the end of electronic Scientific Notebook print outs—"No original text removed"
- 13. Electronic media in the scientific notebook properly labeled

Discrepancies have been identified. Yes No

Checker: *Sharon Williams*

Date: 8/18/00

The discrepancies identified in this Scientific Notebook Review Checklist have been addressed by:

[Signature]
Signature

8/18/2000
Date

Electronic Scientific Notebook No. 274E:
Estimate Rock Fall in Emplacement Drifts
Induced by Earthquakes under Heated
Conditions to Provide Input for Performance
Assessment(06/09/1998 through 07/23/1998)

SCIENTIFIC NOTEBOOK

#274E

by

Rui Chen

SCIENTIFIC NOTEBOOK

#274E

by

Rui Chen

Southwest Research Institute
Center for Nuclear Waste Regulatory Analyses
San Antonio, Texas

August 9, 2000

ARC

Table of Contents

	Page
1. INITIAL ENTRIES	3
1.1 Objectives	3
1.2 Technical Approaches	4
1.3 Computers, Computer Codes, and Data Files	4
2. IN-PROGRESS ENTRIES	7
3. REFERENCES	20
APPENDIX A	23
APPENDIX B	27
APPENDIX C	31
APPENDIX D	32
APPENDIX E	47
APPENDIX F	73

1. INITIAL ENTRIES

Scientific Notebook: # 274 (Part 2)

Issued to: Rui Chen

Issue Date: June 9, 1998

Printing Period: December 1999 to August 2000

Project Title: Seismic effect on drift stability under heated condition

By agreement with the CNWRA QA this Notebook is to be printed at approximate quarterly intervals. This computerized Scientific Notebook is intended to address the criteria of CNWRA QAP-001.

1.1. Objectives

The main objective of this project is to estimate rock fall in emplacement drifts induced by earthquakes under heated conditions to provide input for performance assessment. Such estimates should include: (i) range of rock block sizes (distribution of rock block sizes?), (ii) initiation of rock fall (thermally or seismically induced?), (iii) rate of rock fall, (iv) location of rock fall, and (iv) correlation of size, initiation, and rate of rock fall.

Other objectives may include to estimate: (i) seismic effect on drift stability in general by examining drift closure, joint displacement, yielding etc; (ii) effect of seismic load and rock fall on concrete lining; (iii) seismic effect on near field environment, including change in rock mass mechanical and hydrological properties which may be important in post closure performance assessment.

(No new entries were make to section 1.1 during printing period ended September 30, 1999)

(No new entries were make to section 1.1 during printing period ended December 31, 1999)

New for 2000:

A paper was prepared and submitted to the 4th North American Rock Mechanics Symposium. The paper summarized dynamic analyses and concluded that UDEC is not a good tool for modeling rockfall. Original objectives, therefore, need to be modified. Also, based on the current status of repository design and design analyses at YM. Analyses for ground support was added.

Objectives modified as of March 2000:

The modified objective of this study is to understand rock mass behavior, drift stability, and ground support performance under heated conditions. The emphasis of modeling exercise is on those aspects of rock mass deformation that distinguish a thermal-stress controlled problem from conventional mining and tunneling problems under ambient conditions. Ground support was assumed to be fully grouted rock bolts and steel sets. The study also examined the effect of rock mass properties, fracture network characteristics, and input ground motion parameters on drift stability and ground support performance

1.2. Technical Approaches and Data Sources

The range and distribution of rock block sizes will be analyzed based on the range and distribution of joint spacing, joint sets, and orientation information developed for the Topopah Spring, the host rock of the repository at Yucca Mountain, through DOE site characterization activities and in situ measurements from the ESF. Sources for the measured joint information may be found in Fahy and Beason (1995), Brechtel et al. (1995), Lin et al. (1993).

UDEC computer code will be used to estimate seismic effect on emplacement drift, including size, initiation, and rate of rock fall; and correlation of these parameters.

Various reports and database developed by the DOE and its contractors and subcontractors for the Yucca Mountain project.

(No new entries were made to section 1.2 during printing period ended June 30, 1999)

New as of March, 2000:

The new UDEC model will use the Enhanced Design Alternative II (EDA-II) design (TRW Environmental Safety Systems, Inc., 1999). This design has a drift spacing of 81 meters. Such a model, however, represents a drift in the central portion of the repository emplacement drift panel. The effect of repository edges is not considered.

Vertically, the model extends from the ground surface (approximately 320 m above the waste emplacement level) to the ground water table (about 350 m below the waste emplacement level). For dynamic analyses, a submodel extending 50 m above and 50 m below the emplacement horizon is used to reduce the size of the problem. To further reduce the size of the problem, a detailed fracture pattern will be modeled only in close vicinity of the drift. Beyond this region, fracture spacings were scaled up, whereas a comparable fracture pattern was maintained.

1.3. Computers, Computer Codes, and Data Files

Table 1-1 lists computer equipment and computer codes. Table 1-2 provides names, type, and content of computer files used in the seismic analysis project.

Table 1-1. Computing Equipment

Machine Name	Type	OS	Location	Computer Code	Language
Foxtrot	Ultra Sun Workstation	Solaris 2.5	Bldg. 189	UDEC	Fortran 77
Foxtrot	Ultra Sun Workstation	Solaris 2.5	Bldg. 189	XPLOT	N.A.
TYANA	PC	Windows NT	Bldg. 189	UDEC 3.1	Fortran 77

Table 1-2. Names, Type, and Content of Relative Files

File Name	Directory	Type	Content
udec30		executable	Executable of udec software version 3.0
*.dat		text	Input data file for udec analyses
*.sav		binary	Result file from udec analysis
		text	

(No new entries were made to section 1.3 during printing period ended June 30, 1999)

Rui Chen

SCIENTIFIC NOTEBOOK

INITIALS:

AHC

New starting from March 2000:

Summary of cases for sensitivity analyses. Input and output files are located in D:\NRC Project\EDA2\

Table 1-3. Summary of analysis cases

Fracture Pattern	PatternC		PatternE		PatterF	
	RMQ5	RMQ1	RMQ5	RMQ1	RMQ5	RMQ1
TM (no support)	C17	C19	E2	E4	F6	F7
TM (bolt)	C27	C29	E22	E24	F26	F27
TM (steel sets)			E32	E34		
TM (steel sets/bolt)						
TM/dynamics (no support, 0.4g, cosin, 1 sec)	f=10	PC17aF10	PC19aF10	PE2aF10	PE4aF10	
	f=5	PC17aF5	PC19aF5	PE2aF5	PE4aF5	
	f=1	PC17aF1	PC19aF1	PE2aF1	PE4aF1	
TM/dynamics [bolt, 0.4g, cosin, 1sec)	f=10	PC27aF10	PC29aF10	PE22aF10	PE24aF10	
	f=5	PC27aF5	PC29aF5	PE22aF5	PE24aF5	
	f=1	PC27aF1	PC29aF1	PE22aF1	PE24aF1	
TM/dynamics (bolt, f=5, cosin, 1 sec)	PGA= 0.8g			PE22bF5	PE24bF5	
TM/dynamics (bolt, f=5, cosin, 0.4g)	t=4 sec			PE22cF5	PE24cF5	
TM/dynamics (bolt)	design motion			PE22dF5	PE24dF5	
TM/dynamics (bolt, f=5, 0.4g, cosin, 1 sec)	repeated motion			PE22eF5	PE24eF5	
TM/dyanmics (steel sets)						
TM/dynamics (steel sets/rock bolt)						

2. IN-PROCESS ENTRIES

Analyses of rock fall should be able to establish technically sound criteria for determining the extent of rock fall around emplacement drifts and the size distribution of rock blocks that have the potential to fall onto the waste packages. Such analyses should explicitly account for three basic aspects:

- Analyses of size distribution of individual blocks
- Analyses of the possibility of simultaneous rock fall and vertical extent of rock fall
- Analyses of initiation, location, and rate of rock fall

The ultimate goal of these analyses is to yield technically sound estimation of the ranges of size of rock blocks that have the potential to fall onto the waste packages to provide input for the evaluation of impact of such rock fall on the integrity of the waste packages.

2.9 Check Wave Transmission in UDEC Version 3.0 and Dynamic Modeling in General

Checking of wave transmission was performed using a simple model of 100 m high and 28 m wide with no joints or opening. A simple cosine wave history was used, starting with only compressive wave applied as stress wave to the bottom of the model. The desired velocity amplitude of 0.0625 m/s was calculated from the desired acceleration amplitude of 0.4g and the desired input signal frequency of 10 hz. Velocity wave history was converted to stress wave history according to equations k.5 and k.6 on page K-5 of UDEC manual. The input data is attach as appendix A (wave.dat). Calculated velocity and displacement were monitored at a few points in the model. The following observations were made:

1. The magnitude of input and simulated velocity: Calculated velocity was about 28 percent less than the input velocity due to one-dimensional approximation in converting velocity history to stress history. After a couple of trial runs, it was determined that a scaling factor of 1.4 is necessary to bring the modeled velocity to the input velocity level.
2. Distortion of wave shape and the effect of zone size: No distortion of input wave shape occur with or without joints and opening. Changing zone edge size from 10 to 2 did not seem to make any difference.
3. Modeling of shear wave: Modeling of shear wave need to use free-field boundary conditions. The process is very tricky in UDEC.. See detailed notes in the input file, i.e., file wave.dat. It seems that only the normal stress boundary need to be scaled for the free-field boundary element. However, the compressive component always need to be scaled.
4. Model complexity:
 - 4-1 Effect of joint spacing around the opening
Compare wave.dat vs. wave1.dat. No significant difference found.
 - 4-2 Effect of jointing other than those around the opening
Compare wave.dat vs wave2.dat. No significant difference found.
 - 4-3 Effect of boundary extent
5. Effect of input wave frequency
6. Damping issues

2.10 Design Earthquake Time Histories at YM

Design basis ground motion time histories from DOE (Risk Engineering, Inc., 1999) were digitized and used as input for a test run with the data file named Design.dat. Distortion occurred. Need to investigate why!

2.11 Development of Fracture Pattern and UDEC Interpretation

Development of fracture pattern initiated during April 1 - June 30. John Hadjigeorgiou of Georock is conducting the analyses and work will be reported in his scientific notebook.

New of March 2000:

2.12 Trial UDEC Analysis Cases

Trial runs included six different fracture patterns (PatternA through PatternF). Differences among these different patterns are detailed at the beginning of each input file also in attached hand-written pages attached as Appendix A and pages are numbered as A1 through A11.

Based on these analyses, PatternC, PatternE, and PatternF were chosen for further analyses. Specifically, the input files for the chosen cases for further sensitivity analyses are in table 2-1, all with extension .dat. The variation cases and associated inputs are given in table 1-3.

Table 2-1 Cases of Three Fracture Patterns for Further Analyses

PatternC17	PatternC19	PatternE2	PatternE4	PatternF6	PatternF7
PatternC27	PatternC29	PatternE22	PatternE24	PatternF26	PatternF27

2.13 Initial Conditions

Stresses:

The initial vertical stress (σ_v) was defined using a vertical stress gradient of 0.022 MPa/m, equivalent to an average overburden rock mass density of 2,210 kg/m³ and gravitational acceleration of 9.81 m/s². The initial horizontal stress (σ_h) was estimated from vertical stress using a horizontal to vertical stress ratio of approximately 0.266 [based on a Poisson's ratio (ν) of 0.21 and $\sigma_h = \sigma_v \nu / (1 - \nu)$]. The resultant stresses at the repository horizon were approximately 7 MPa and 1.9 MPa in vertical and horizontal directions, respectively.

In UDEC input, calculation of the in situ stress is done using a FISH function. The hand-confirmatory calculation and the FISH function are included in Appendix B (page B1 and B2).

Temperature

Initial temperature was set to be 18.7° C at the ground surface and interpolated using the geothermal gradient for the YM site given in table 2-2 (Civilian Radioactive Waste Management System Management and Operating Contractor, 1997c). These data gave a temperature of 34.3° C at the base of the model and 24.7° C at the repository horizon.

Table 2-2. Geothermal gradient at YM (Civilian Radioactive Waste Management System Management and Operating Contractor, 1997c)

Depth (m)	Geothermal Gradient (°C/m)
0-150	0.020
150-400	0.018
400-700	0.030
>700	0.008

The temperature gradient is calculated using a fish function called from UDEC input file. The confirmatory hand calculation and the fish function are included in Appendix B (page B3 and B4).

2.14 Loads

Thermal load

In EDA-II, thermal load is designed to be an areal mass loading of 60 MTU/acre. Using the inventory data (i.e., 70,011 MTU total mass and 71,499 kW total heat output, see 1998b) presented in Civilian Radioactive Waste Management System Management and Operating Contractor (CRWMS M&O) (1997c) this translates to about 71 W/m² initial heat flux on drift walls.

The 71 W/m² initial heat flux was modeled to decrease with time exponentially with a single decay constant (exponent) of -0.0104 (W/m²)/yr. This decay constant was obtained using a curve-fitting procedure following the decay characteristics defined in table V-1 of Civilian Radioactive Waste Management System Management and Operating Contractor (CRWMS M&O) (1997c) as described in detail in Chen (1998). The

decay constant from curve-filling was further modified (calibrated) through a trial-and-error process. The trial-and-error process compared temperature history at the drift wall from the UDEC model for the first 150 yr following waste emplacement with temperatures from a parallel study using a continuum modeling approach (Ofoegbu, 2000).

The calculation of thermal loading and supporting materials are included in Appendix C.

Dynamic load

Design ground motion parameters for the proposed repository are yet to be finalized by DOE. Consequently, this study considered a range of ground motion parameters. The basecase used a simple cosine wave with frequency of 5 Hz and acceleration amplitude of 0.4 g in both vertical and horizontal directions, assuming a single ground motion event. In the basecase, the model was subjected to the ground motion for a 1 s simulation time followed by a 2 s simulation period for the model to return to equilibrium. Both shear wave and compressive waves were applied to the model assuming that the two components have the same amplitude. The effect of frequency content was examined by varying frequency to 1 Hz and 10 Hz from the basecase model (5 Hz). For the 1 Hz cases, the duration of the ground motion was increased to 5 s to allow a reasonable number of loading cycles, followed by a 5 s recovery time if no significant rockfall is simulated and numerical stability is maintained. If significant rockfall is simulated, however, UDEC would have difficulty maintaining numerical stability and would drop the time step significantly and make it impractical to regain model equilibrium within a reasonable computational time. The effect of ground motion amplitude was studied by doubling the basecase ground motion level (i.e., to 0.8 g). The effect of duration was evaluated by increasing the duration of strong motion from 1 s to 4 s. The effect of repeated ground motion events was analyzed by subjecting the model to the basecase ground motion twice. Finally, the effect of wave form was studied by subjecting the model to the preliminary design ground motion time histories (velocity histories) for YM at the repository level (figure 2-2). This design ground motion was developed by Risk Engineering, Inc. (1998) based on site specific probabilistic seismic hazard analyses (Wong and Stepp, 1998). Velocity history was used because UDEC Version 3.1 does not account for acceleration or displacement histories. Also, because UDEC Version 3.1 does not perform frequency-domain analyses, only time-domain analyses were conducted.

As mentioned previously, it is necessary to use viscous boundaries at the base of the model for nonrigid boundaries to minimize seismic reflection. In UDEC, the use of viscous boundaries at the base restricts the input ground motion waves to be stress waves rather than velocity waves. Also, UDEC does not take acceleration or displacement as dynamic input. Therefore, acceleration was converted to velocity and, then, to stresses as seismic input for simple cosine waves. For a cosine wave of angular frequency ω and amplitude A , the displacement time history is:

$$x(t)=A \cos (\omega t) \quad (2-1)$$

where t is time. Angular frequency ω is equal to $2\pi f$, where f is frequency. The velocity and acceleration are simply:

$$\begin{aligned} V(t) &= \frac{dx}{dt} = -A\omega \sin(\omega t) \\ a(t) &= \frac{d^2x}{dt^2} = -A\omega^2 \cos(\omega t) \end{aligned} \quad (2-2)$$

Consequently, the amplitude of the input ground acceleration, a in g , can be converted to ground velocity, V , as

$$V = \frac{g}{2\pi f} a \quad (2-3)$$

where g is gravitational acceleration and is equal to 9.81 m/s^2 . Equation (2-3) was used to convert acceleration to velocity. The converted velocity for a $0.4g$ cosine wave is given in Table 2-2 for the three frequencies considered in this study.

To convert a velocity history to a stress history for UDEC Version 3.1 modeling, the procedure recommended by Itasca Consulting Group, Inc. (2000) was followed:

$$\begin{aligned} \sigma_n &= 2(\rho C_p) V_n \\ \sigma_s &= 2(\rho C_s) V_s \end{aligned} \quad (2-4)$$

where σ_n and σ_s are applied normal and shear stresses, respectively; C_p and C_s are rock mass p- and s-wave velocities, respectively; V_n and V_s are input normal and shear ground motion velocities; and ρ is rock mass density. C_p and C_s can be estimated from rock mass density and elastic properties as

$$\begin{aligned} C_p &= \sqrt{\frac{k + 4G/3}{\rho}} \\ C_s &= \sqrt{G/\rho} \end{aligned} \quad (2-5)$$

where K and G are rock mass bulk and shear moduli, respectively. These parameters for the proposed YM repository host rock masses are given later in Section 2.4 for rock mass quality category 5 (RMQ5), and rock mass quality category 1 (RMQ1), respectively. Using the rock mass bulk and shear moduli and equations 2-4 and 2-5, the input ground motion velocity histories were converted to stress histories. Table 2-2 gives the converted stress wave amplitudes for a $0.4g$ cosine wave and for RMQ5 and RMQ1 rock masses. For the cases that used design ground motion as seismic input, the stress histories were calculated using equations 2-4 and 2-5 directly from velocity histories given in figure 2-2.

Table 2-2. Converted velocity and stress wave amplitudes for a 0.4 g cosin wave

Frequency (Hz)	Velocity (m/s ²)	Stress (MPa)			
		RMQ5		RMQ1	
		Normal	Shear	Normal	Shear
10	0.0625	1.13	0.68	0.55	0.33
5	0.125	2.25	1.37	1.10	0.67
1	0.625	11.26	6.83	5.49	3.33

The conversion of seismic ground motion was conducted by Fish functions called in directly from UDEC input file. The hand-verification calculation and the fish function are included in Appendix D.

2.15 Rock Block Thermal-Mechanical and Fracture Mechanical Properties

Rock block properties include rock mass density, thermal properties (thermal expansion coefficient, thermal conductivity, and specific heat capacity), elastic properties (Young's modulus and Poisson's ratio), strength properties (cohesion and friction angle), and post-failure properties (dilation angle).

The property data used in this study were consistent with a parallel modeling effort using a continuum approach conducted by Ofoegbu.

The bulk density of 2210 kg/m³ for the TSw2 lower lithophysal unit was used (see table 4-3 in Civilian Radioactive Waste Management System Management and Operating Contractor, 1998). Thermal expansion coefficient was chosen to be 7.5×10^{-6} per °C. This is within the range measured by DOE (Civilian Radioactive Waste Management System Management and Operating Contractor, 1997a). Thermal conductivity and specific heat capacity were chosen to be 2.13 W/m-K and 968.96 J/kg-K, respectively (Civilian Radioactive Waste Management System Management and Operating Contractor, 1998).

Two groups of rock mass mechanical property data were considered (table 2-3). These two sets of properties represent a strong (RMQ5) rock mass, and a weak (RMQ1) rock mass. The elastic properties for RMQ5 and RMQ1 rock masses were selected based on property values proposed by the DOE for VA (Civilian Radioactive Waste Management System Management and Operating Contractor, 1998). The strength properties, particularly friction angles used in this modeling, were lower than those proposed by the DOE. As detailed in Chen et al. (2000) and Ofoegbu (2000), the lower friction angles were chosen for three primary reasons: (i) DOE strength property values are inconsistent with empirical procedures used to determine these values, nor are they consistent with measured laboratory or field data; (ii) strength property values much lower than those estimated by DOE were obtained based on DOE rock mass quality data (Ofoegbu, 2000); (iii) strength properties are likely to degrade under sustained thermal load (Ofoegbu, 2000). Dilation for rock blocks was chosen as one half of friction angle. Unconfined compressive strength and uniaxial tensile strength were calculated from cohesion and friction angle based on Mohr-Coulomb failure criterion. For comparison, both rock mass mechanical property values used in this study and those used in DOE VA analyses (Civilian Radioactive Waste Management System Management and Operating Contractor, 1998) are presented in table 2-3. Fracture normal and shear stiffness were assumed to be 500 GPa/m.

Fracture cohesion was chosen to be 0.07 MPa (Civilian Radioactive Waste Management System Management and Operating Contractor, 1997b) with no dilation. Fracture friction angle of 35° was used rather than the 56° used in most analyses conducted by DOE (e.g., Civilian Radioactive Waste Management System Management and Operating Contractor, 1998, 1997b). This lower fracture friction angle was a median value from independent laboratory testing at Center for Nuclear Waste Regulatory Analyses (Hsiung et al., 1993). Fracture mechanical property data are also given in table 2-3.

Table 2-3. Rock Block and Fracture Mechanical Properties

Rock Mass Elastic Properties	RMQ5	RMQ1	VA_RMQ5	VA_RMQ1
Mass density (kg/m ³)	2210	2210	2235	2235
Young's modulus (GPa)	32.61	7.76	32.61	7.76
Poisson's ratio	0.21	0.21	0.21	0.21
Bulk modulus (GPa)	18.74	4.46	18.74	4.46
Shear modulus (GPa)	13.48	3.21	13.48	3.21
Rock Mass Strength Properties	RMQ5	RMQ1	VA_RMQ5	VA_RMQ1
Cohesion (MPa)	5.08	2.82	5.2	1.5
Friction angle (degrees)	34.42	27.50	46.0	43.0
Unconf comp strength (MPa)	19.28	9.29	26.09	7.08
Dilation angle	17.21	13.75	0.0	0.0
Tensile strength (MPa)	5.35	4.42	4.21	1.32
Joint Properties	RMQ5	RMQ1	VA_RMQ5	VA_RMQ1
Cohesion (MPa)	0.07	0.07	0.07	0.07
Friction angle (degrees)	35	35	56	56
Dilation angle (degrees)	0	0	0	0
Tensile strength (MPa)	0	0	0	0
Normal strength (MPa)	500	500	50	50
Shear stiffness (GPa/m)	500	500	50	50

As examples, UDEC input files for PatternE2 (RMQ5) and PatternE4(RMQ1) are included in Appendix E.

2.16 Fracture Network Characteristics

Three fracture patterns were selected for analyses in this study to further explore the effects of fracture pattern on ground support and drift stability (table 2-4). PatternC and PatternF are regular fracture patterns. Fracture spacing in PatternF is about twice that in PatternC. PatternE is an irregular fracture pattern, with

parameters selected based on previous studies (Chen, 1999, 1998) and DOE preliminary statistical analyses of site-specific fracture data.

Table 2-4. UDEC version 3.1 parameters used to generate fracture patterns

Pattern	Fractur Set	Angle ¹		Trace Length		Gap Length		Fracture Spacing	
		Mea	Deviation ²	Mean	Deviation ²	Mea	Deviation ²	Mea	Deviation ²
C	1st	85	0	Infinite	NA	NA	NA	1.0	0.0
	2nd	15	0	Infinite	NA	NA	NA	2.0	0.0
E	1st	85	10	7.5	1	-0.2	0	0.4	0.1
	2nd	20	5	5.0	1	-0.2	0	0.75	0.1
	3rd	110	10	12.0	4	-0.3	0	1.8	0.5
F	1st	85	0	Infinite	NA	NA	NA	0.5	0.0
	2nd	15	0	Infinite	NA	NA	NA	1.0	0.0

¹ The angle is measured counter-clockwise from the horizontal axis. ² Deviation is the standard deviation from the mean, assuming a uniform probability distribution.

2.17 Ground Support

Rock Bolts:

UDEC rock bolt logic is used.

Three groups of input parameters are necessary in modeling rock bolts. These include geometric parameters, parameters of the reinforcing steel bar or cable (bolt parameters), and grout parameters. Geometric parameters include length of the rock bolt, bolt diameter (D), and thickness of the grout (t) or hole diameter ($D+2t$). In UDEC, bolt length needs to be specified and D and t are used to estimate grout mechanical and strength parameters.

Grout parameters include grout shear modulus (G) and ground compressive strength (F). However, these parameters are not directly used in UDEC. Instead, grout shear stiffness (cb_Kbond) and the maximum bond force per unit length (cb_Sbond) are used. cb_Kbond is estimated from G , t , and D (Itasca Consulting Group, Inc., 2000):

$$K_{bond} = \frac{2\pi G}{10 \ln \left(1 + \frac{2t}{D} \right)} \quad (2-6)$$

cb_Sbond is either directly measured by pull-out tests conducted at different confining pressures or estimated from (Itasca Consulting Group, Inc., 2000):

$$S_{bond} = \pi(D + 2t)\tau_{peak} \quad (2-7)$$

$$\tau_{peak} = \tau_l Q_B$$

where τ_i is approximately one-half of the uniaxial compressive strength of the weaker of the rock and grout (usually rock), Q_B is the quality of the bond between the grout and rock ($Q_B = 1$ for perfect bonding).

Bolt parameters include bolt Young's modulus (cb_ymod), bolt tensile yield force (cb_yield), bolt density ($cb_density$), bolt thermal expansion coefficient (cb_thexp), bolt compressive yield force (cb_ycomp , 1.0e4MN is UDEC default), and bolt extensional failure strain ($cb_fstrain$, optional, can be unlimited). These parameters are direct input in UDEC.

In this study, length of the rock bolts was assumed to be the same as the radius (2.75 m) of the emplacement drifts. Barton et al. (1974) recommended that the length of rock bolts be estimated as:

$$L = 2 + 0.15 \frac{B}{ESR} \quad (2-8)$$

where L is length in meters, B is span in meters, and ESR is excavation support ratio. For emplacement drifts, B=5.5 m and assuming ESR=1, the recommended rock bolt length is 2.825 m. This number is close to the 2.75 m bolt length used in this modeling. Twelve rock bolts were installed with a uniform spacing in upper spring-line and roof areas (figure 2-3). The rock bolts are numbered sequentially from left to right.

Parameters used in this study are listed in table 2-5. The study initiated with the first set of parameters. This set of parameters was chosen from the rock bolt design parameters selected by the DOE for the ESF (Civilian Radioactive Waste Management System Management and Operating Contractor, 1995), assuming bolting pattern is based on 1.0 m row spacing in the out-of-plane direction. The bolt type represented by this set of parameters is Williams' hollow continuous threaded steel bar (Williams Form Engineering Corp., 1992). As stated in equation (2-7), τ_i is approximately one-half of the uniaxial compressive strength of the weaker of rock and grout. According to CRWMS and M&O (1995), grout compressive strength is 20.685 GPa, much greater than the rock compressive strength. The rock compressive strength equation (q_u) can be evaluated based on Mohr-Coulomb yield criterion as:

$$q_u = 2c \tan(\alpha) \quad (2-9)$$

where c and α are cohesion and friction angle, respectively. Based on c and α used in this study for RMQ5 and RMQ1 rock masses (Table 2-3) and equation (2-7), cb_Sbond is calculated to be 1.513 MN/m and 0.744 MN/m, respectively, for RMQ5 and RMQ1 rock masses. These calculations are recorded in Appendix F.

Using this set of parameters, however, rock bolts experienced both extensive element axial failure and grout failure under thermal load. In order better examine the performance of rock bolts in terms of load built up in the cable element and between cable nodes and host rock mass, the second set of parameters was chosen to increase tensile yielding force for the cable element, because most axial failure was tensile failure when the first set of parameters was used. In the model using the second set of parameters, maximum bond force per unit length was also increased to avoid grout failure. Physically, increasing tensile yielding force for the cable reinforcement can be achieved by selecting stronger steels. Increasing maximum bond force per unit length can be achieved by increasing grout thickness [or hole diameter, see equation (2-7)]. When grout thickness or hole diameter is increased, Cb_kbond will also change (see equation 2-6) which may alter shear force on the grout/rock interface and consequently, failure status. Alternatively, different grout shear modulus may need to be selected to determine a proper value for Cb_kbond . These design details are beyond the scope of this study. The second set of parameters for grout in table 2-5 is hypothetical and is not directly calculated from the geometrical data of rock bolts. Thermal expansion coefficient for rock bolts is assumed to be the

same as rock mass thermal expansion coefficient to avoid differential expansion between rock mass and reinforcement or bolts. Future studies need to consider differential thermal expansion because it is not likely that the two thermal expansion coefficients are the same and the difference could be big. Differential expansion may cause more extensive failure of both the reinforcing and grout elements.

Table 2-5. Parameters for rock bolts

	Parameters	Unit	First Set ¹	Second Set
Geometric	Bolt Diameter (D)	cm	0.3	-
	Grout Thickness (t)	m	0.105	-
	Hole Diameter (D+2t)	m	0.53	-
Bolt	Young's Modulus (E) (<i>cb_ymod</i>),	MPa	2.0×10^5	2.0×10^5
	Tensile Yield Force (<i>cb_yield</i>)	MN	0.267	0.534
	Density (<i>cb_density</i>)	kg/m ³	7875	7875
	Thermal Expansion Coefficient (<i>cb_thexp</i>)	/°C	7.5×10^{-6}	7.5×10^{-6}
	Compressive Yield Force (<i>cb_ycomp</i>)	MN	1.0×10^4	1.0×10^4
	Extensional Failure Strain (<i>cb_fstrain</i>)	-	no limit	no limit
Grout	Shear Modulus (G)	MPa	8.97×10^3	8.97×10^3
	Compressive Strength	MN	20.685	20.685
	Grout Shear Stiffness (<i>cb_kbond</i>)	MN/m/m	16.34×10^3	16.34×10^3
	Maximum Bond Force Per Length (<i>cb_sbond</i>)	MN/m	RMQ5: 1.513 RMQ1: 0.744	RMQ5: 3.088 RMQ1: 1.488

Steel Sets

Steel sets can be simulated using the 2-dimensional structural (beam) elements in UDEC (Itasca Consulting Group, Inc., 2000). Steel sets, like surface linings for tunnels and exposed slopes are typically thin, and their characteristic response to bending usually cannot be neglected. Beam elements usually provide an effective method to include bending effects. In UDEC, the beam elements are attached to a rock surface via spring connections oriented both radially and tangentially with respect to the support structure. Also in

UDEC, the structural element formulation is a plane-stress formulation. Therefore, it can be directly applied in modeling steel sets so long as the elastic modulus of the beam element is scaled to account for the spacing of the steel sets. Therefore, the force and moments in the beam structural element, which are calculated by UDEC, are scaled forces and moments. To simplify the interpretation of the UDEC results, this study assumes that the steel sets have unit spacing (i.e., 1 m). Also, it assumes that the steel sets have rectangular cross section and cross sectional area and moment of inertia are taken as those for the W8×30 steel sets described in CRWMS M&O (1995). These data are given in table 2-6. Steel sets thickness in radial direction is assumed to be 0.1 m, Young's modulus was taken from CRWMS M&O (1995). Other parameters are assumed lacking actual property values. Cohesion, friction angle, dilation angle, and tensile strength for the rock/steel sets interface were assumed the same as host rock mass properties to be conservative. Interface normal stiffness and shear stiffness were taken as rock fracture normal and shear stiffness, respectively.

Table 2-6. Parameters for steel sets

	Parameters	Unit	Values
Geometric	Thickness	m	0.1
	Cross Sectional Area	m ³	5.9×10 ⁻³
	Moment of Inertia	m ⁴	4.578×10 ⁻⁵
Steel Sets	Young's Modulus	MPa	2.0×10 ⁵
	Tensile Yield Strength	MN	4.0
	Density	kg/m ³	7875
	Thermal Expansion Coefficient	/°C	7.5×10 ⁻⁶
	Compressive Yield Force	MN	1.0×10 ⁴
	Poisson's Ratio	-	0.2

2.18 Results Presented in Final Report and Output Files**Chapter 3: Performance of Drift Without Ground Support**Table 3-1

Input: PatternC17.dat, PatternC19.dat, PatternF6.dat, PatternF7.dat, PatternE2.dat PatternE4.dat
 output: C17_exc.sav, C17_150y.sav, C19_exc.sav, C19_150y.sav, F6_exc.sav, F6_150y.sav, F7_exc.sav,
 F7_150y.sav, E2_exc.sav, E2_150y.sav, E4_exc.sav, E4_150y.sav

Figure 3-1

Input: PatternC17.dat, PatternC19.dat, PatternF6.dat, PatternF7.dat, PatternE2.dat PatternE4.dat
 output: C17_exc.sav, C19_exc.sav, F6_exc.sav, F7_exc.sav,, E2_exc.sav, E4_exc.sav

Figures 3-2 & 3-3

Input PatternF6.dat, PatternF7.dat
 Output F6_exc.sav, F7_exc.sav, F6_150y.sav, F7_150y.sav

Figure 3-4

Input PatternE4.dat
 output E4_exc.sav, E4_150y.sav

Figure 3-5

Input PE2aF10.dat, PE4aF10.dat
 Output E2aF10_225.sav E4aF10_100.sav

Figures 4-1 through 4-5

Input PatternE22.dat, PatternE24.dat
 Output E22_exc.sav, E24_exc.sav, E22_150.sav, E24_150y.sav

Figures 4-6 through 4-10

Input PatternE32.dat, PatternE34.dat
 Ouput E32_exc.sav, E34_exc.sav, E32_150.sav, E34_150.sav

Figures 4-11 through 4-13

Input PatternE22.dat, PatternF26.dat, PatternC27.dat
 Output E22_150y.sav, F26_150y.sav, C27_150y.sav

Figures 4-14 through 4-16

Input PE22aF10.dat, PE22aF5.dat, PE22aF1.dat
Output E22aF10_300.sav, E22aF5_300.sav, E22aF1_200.sav

Figures 4-17 through 4-19

Input PE24aF10.dat, PE24aF5.dat, PE24aF1.dat
Output E22aF10_300.sav, E22aF5_300.sav, E22aF1_300.sav

Figures 4-20 through 4-22

Input PE22aF5.dat, PE22bF5.dat, PE22cF5.dat, PE22eF5.dat
Output E22aF5_300.sav, E22bF5_200.sav, E22cF5_491.sav, E22eF5_500.sav

These input and output files are located on Tyana, DNRC Project\EDA2\QA. This directory also include the WP80 file of the final report and graphics files (.ai). All the graphics files were done with Adobe Illustrator.

3. REFERENCES

Ahola, M.P., R. Chen, H. Karimi, S.M. Hsiung & A.H. Chowdhury. *A Parametric Study of Drift Stability in Jointed Rock Mass, Phase I: Discrete Element Thermal-Mechanical Analysis of Unbackfilled Drifts*. CNWRA 96-009. San Antonio, TX. 1996.

Ahola, M.P. *A Parametric Study of Drift Stability in Jointed Rock Mass—Phase II: Discrete Element Dynamic Analysis of Unbackfilled Drifts*. CNWRA 97-007. San Antonio, TX. 1997.

Anna, L.O. *Preliminary Three-Dimensional Discrete Fracture Model of Topopah Spring Tuff in the Exploratory Studies Facility, Yucca Mountain Area, Nye County, Nevada*. USGS Open-File Report 97-834. 1998.

Barton, N., R. Lien, and J. Lunde. Engineering classification of rock masses for design of tunnel support. *Rock Mechanics* 6(4):189-236. 1974.

Barton, N., S. Bandis, and K. Bakhtzer. *Strength, Deformation and Conductivity Coupling of Rock Joints*. International Journal of Rock Mechanics and Mining Sciences and Geomechanics Abstracts. 22(3): 121-140. 1985. 1985.

Barrett, L.H. Letter to Jared L. Cohon and Enclosure: *Basis for Department of Energy Design Selection*. September 10. DOE (1998b). 1999.

Brechtel, C.E., M. Lin, E. Martin & D. S. Kessel. *Geotechnical Characterization of the North Ramp of the Exploratory Studies Facility*. SAND95-0488/1. Albuquerque, NM. 1995.

Chen, R. *Analyses of Drift Instability and Rockfall due to Earthquake Ground Motion at Yucca Mountain, Nevada: Progress Report*. San Antonio: TX: Center for Nuclear Waste Regulatory Analyses. 1998.

Chen, R. Analyses of drift stability and rockfall due to earthquake ground motion at Yucca Mountain, Nevada. *Proceedings of the 37th U.S. Rock Mechanics Symposium, Rock Mechanics for Industry*, B. Amadei, R.L. Kranz, G.A. Scott, and P.H. Smeallie, eds., 759-766. 1999.

Chen, R., M.P. Ahola, S.M. Hsiung, and A.H. Chowdhury. Thermal-mechanical stability of emplacement drifts for a proposed nuclear waste repository at Yucca Mountain. *Environmental Geotechnology 1&2: Proceedings, 4th International Symposium on Environmental Geotechnology and Global Sustainable Development*, In press. 1999.

Chen, R., G.I. Ofoegbu, and S. Hsiung. Modeling drift stability in fractured rock mass at Yucca Mountain, Nevada-discontinuum approach. *Proceedings, 4th North American Rock Mechanics Symposium*, Seattle, Washington, July 30th -August 2nd. In press. 2000.

CRWMS M&O. *ESF Ground Support Design Analysis*, BABEE0000-01717-0200-00002 Rev 00. 1995.

CRWMS M&O. *Yucca Mountain Site Geotechnical Report*, DI: B00000000-01717-5705-00043 Rev 01. Las Vegas, NV: CRWMS M&O. 1997a.

CRWMS M&O. *Confirmation of Empirical Design Methodologies*:DI: BABEE0000-01717-5705-00002 Rev 00. Las Vegas, NV: CRWMS M&O. 1997b.

CRWMS M&O. *Repository Thermal Loading Management Analysis*. B00000000-01717-0200-00135. Revision 00. Las Vegas NV: Civilian Radioactive Waste Management Systems Management and Operating Contractor. 1997c.

CRWMS M&O. *Repository Ground Support Analysis for Viability Assessment*. DI: BCAA00000-01717-0200-00004 Rev 01. Las Vegas, NV: CRWMS M&O. 1998.

CRWMS M&O. *Fracture Data from the Exploratory Studies Facility*. Design Input Transmittal EBS-SSR-993001. T. Las Vegas, NV: CRWMS M&O. ACC.: MOL. 19991011.0070. 1999a.

CRWMS M&O. *Drift Degradation Analysis*. ANL-EBS-MD-000027 Rev 00. Las Vegas, NV: CRWMS M&O. 1999b.

Goodman, R.E. and G. Shi. *Block theory and Its Application to Rock Engineering*, Englewood Cliffs, New Jersey: Prentice-Hall, Inc. 1985.

Hsiung, S.M., D.D. Kana, M.P. Ahola, A.H. Chowdhury, and A. Ghosh. *Laboratory Characterization of Rock Joints*, NUREG/CR-6178, CNWRA 93-013, San Antonio, TX: Center for Nuclear Waste Regulatory Analyses. 1993.

Hoek, E. and E.T. Brown. *Underground Excavations in Rock*, The Institute of Mine and Metallurgy, London, England. 1980.

Itasca Consulting Group, Inc. *UDEC—Universal Distinct Element Code, Version 3.1*. Minneapolis, MN. 2000.

Lin, M., M.P. Hardy & S.J. Bauer. *Fracture Analysis and Rock Quality Designation Estimation for the Yucca Mountain Site Characterization Project*. SAND92-0449. Albuquerque, NM. 1993.

Ofoegbu, G.I. *Thermal-Mechanical Effects on Long-Term Hydrological Properties at the Proposed Yucca Mountain Nuclear Waste Repository*. CNWRA2000-San Antonio, TX: Center for Nuclear Waste Regulatory Analyses. In press. 2000.

Ofoegbu, G. I., S. Painter, R. Chen, R.W. Fedors, and D.H. Ferrill. *Geomechanical and Thermal Effects on Moisture Flow at the Proposed Yucca Mountain Nuclear Waste Repository*. Nuclear Technology. In Review. 2000.

Risk Engineering, Inc. *Seismic Design Basis Inputs for a High-Level Waste Repository at Yucca Mountain, Nevada*. B00000000-01727-5700-0018, Rev. 0. 1998.

Sweetkind, D.S. and S.C. Williams-Stroud. *Characteristics of Fractures at Yucca Mountain, Nevada: Synthesis Report*, Administrative Report, Denver, CO: U.S. Geological Survey. 1996.

U.S. Department of Energy. *Repository Thermal Loading Management Analysis*. B00000000-01717-0200-00135. Rev. 0. 1998b.

U.S. Department of Energy. *Preclosure Seismic Design Methodology for a Geologic Repository at Yucca Mountain*. Topical Report YMP/TR-003-NP. Las Vegas, NV: U.S. Department of Energy, Office of Civilian Radioactive Waste Management. 1997.

U.S. Nuclear Regulatory Commission. *Issue Resolution Status Report, Key Technical Issue: Structural Deformation and Seismicity*. Revision 2. Washington DC: Division of Waste Management, Office of Nuclear Material Safety and Safeguards, U.S. Nuclear Regulatory Commission. 1999a.

U.S. Nuclear Regulatory Commission. *Issue Resolution Status Report, Key Technical Issue: Repository Design and Thermal-Mechanical Effects*. Revision 2. Washington DC: Division of Waste Management, Office of Nuclear Material Safety and Safeguards, U.S. Nuclear Regulatory Commission. 1999b.

TRW Environmental Safety Systems, Inc. License Application Design Selection Report. B00000000-01717-4600-00123, Rev. 01. 1999.

Wernicke, B.P. Cenozoic extensional tectonics of the Western Cordillera. The Cordilleran Orogen: Conterminous U.S. B.C. Burchfiel, P.W. Lipman and M.C. Zoback (eds), *The Geology of North America*. Boulder, CO: Geological Society of America G-3: 553-581. 1992.

Wong, I.G. and J.C. Stepp. *Probabilistic Seismic Hazard Analyses for Fault Displacement and Vibratory Ground Motion at Yucca Mountain, Nevada*. Final report. Oakland, CA. 1998.

Williams Form Engineering Corp. *Rock Anchor Systems No. 392*, Los Angeles CA. 1992.

APPENDIX A Initial Trial Runs to Select Cases for Final AnalysisPattern A (minimum number of fractures to create opening)

Pattern A1.dat	Cosine P-wave only
Pattern A2.dat	Cosine S-wave only
Pattern A3.dat	Cosine P- and S- waves
Pattern A4.dat	P and S waves from design ground motion, RMQ5 (replaced by PatternA5.dat)
Pattern A5.dat	Same as PatternA 4.dat, added history monitoring points, VA-RMQ5
Pattern A6.dat	Same as PatternA5.dat, rock mass friction angle is 28° instead of 46° , RMQ5. Other changes include: (1) surface y-coord to 320 from 317m, (2) change of in situ temperature with depth (geothermal gradient)
Pattern A7.dat	Similar to PatternA5.dat, using RMQ1 properties instead of RMQ5 properties
Pattern A8.dat	Similar to PatternA7, rock mass friction angle is 28° instead of 43°
Pattern A9.dat	New parameters for RMQ5 produced an extensive failure zone (over the entire pillar)
Pattern A10.dat	changed the cohesion back to zero to see if the extensive failure is due to cohesion (half of function instead of zero) still shows a lot of failure. Case deleted for no further use.
PatternA11.dat	changed the time history of the thermal loading. The extensive failure is not due to change in temperature time history. Case deleted for no further use.
PatternA12.dat	change "prop" back to that of PatternA6.dat from PatterA9.dat to see if the extensive failure is due to property change. This case verified that the extensive failure is due to material properties. Which properties? Most likely thermal-expansion coefficient. PatternA13 will test it. Case deleted for no further use.
PatternA13.dat	change strength and joint parameters back to those desired. Keep thermal properties as previous. It seems like thermal properties is driving the extensive fail, particularly thermal expansion coefficient
PatternA14.dat	use new properties as agreed upon with Goodluck Ofoegbu. However, thermal expansion coefficient 1×10^{-5} led to excessive failure. 6×10^{-6} is used instead. Computed wall temperature from ABAQUS is used to scale the initial heat thermal for UDEC.
PatternA15.dat:	same as PatternA14. RMQ1, $\alpha = 6 \times 10^{-6}$
PatternA16.dat:	same as PatternA14. RMQ5 $\alpha = 7.5 \times 10^{-6}$
PatternA17.dat:	similar to PatternA16 RMQ1

AHc

PatternB joint spacing 2m and 4m regular

Pattern B1: joint spacing (2m, 4m) RMQ5. Design ground motion

PatternC: Regular joint spacing 1m and 2m

- PatternC1.dat RMQ5, cosine wave
 PatternC2.dat RMQ1, cosine wave
 PatternC3.dat: similar to PatternC1.dat, except rock block friction angle is 28° instead of 46°
 PatternC4.dat: similar to PatternC3.dat, except fracture friction angle is reduced to 35 from 56
 PatternC5.dat: similar to PatternC2 except rock mass friction angle is 28° instead of 43°
 RMQ1
 PatternC6.dat: similar to PatternC5 except fracture friction angle is 35° instead of 56° , cosine wave
 PatternC7.dat: similar to PatternC4.dat, except detailed jointing area is extended to see the effect (-50, +50)
 PatternC8.dat: similar to PatternC7.dat, except jointing area is extended throughout the whole model to see the effect.
 PatternC9.dat: RMQ5, $\alpha = 7.5 \times 10^{-6}$
 PatternC10.dat: RMQ1, $\alpha = 7.5 \times 10^{-6}$
 PatternC11.dat: RMQ5, $\alpha = 10 \times 10^{-6}$
 PatternC12.dat: added joints in pillar. RMQ5, $\alpha = 10 \times 10^{-6}$
 to compare with PatternC11-still got failure controlled by joints. didn't seem to help much. <Seismic Run on this Case>
 PatternC13.dat: Adjusted the domain to be parallel to joint orientations otherwise similar to PatternC12
 PatternC14.dat: add joints to domain sides as the DOE VA, do not seem to have effects
 PatternC15.dat: larger jointed zone (throughout the pillar) extend 27.5 m above and below the opening.
PatternC16.dat RMQ5 $\alpha = 10 \times 10^{-6}$. Joint of the entire model extended based on PatternC13.
PatternC17.dat RMQ5 $\alpha = 7.5 \times 10^{-6}$
PatternC18.dat RMQ1 $\alpha = 10 \times 10^{-6}$
PatternC19.dat RMQ1 $\alpha = 7.5 \times 10^{-6}$

Numer 2- represent rock bolts

- PatternC26.dat: based on PatternC16. RMQ5, $\alpha = 10 \times 10^{-6}$ with rock bolt. First try.
 PatternC27.dat: Same as PatternC17, with rock bolts
 PatternC28.dat: based on PatternC18 with rock bolts, RMQ1 $\alpha = 1.0 \times 10^{-6}$.
 PatternC28-1.dat: same as PatternC28.dat, except $jks = jkn = 5 \times 10^4$ instead of 5×10^5 , Did not see much effects.

PatternD Similar to Pattern 3, irregular {jset 85 10 7.5 1.0 0 0 1 0.1}
{jset 15 5 5 1.0 0 0 2 0.2}

PatternD1.dat RMQ5, rock mass friction angle=48, fracture friction angle = 56
 PatternD2.dat RMQ5, rock mass friction angle=28, fracture friction angle = 35
 PatternD4.dat fracture entire model. Simpler irregular joints. RMQ5, $\alpha = 10e-6$
 PatternD5.dat RMQ1, $\alpha = 10e-6$
 PatternD6.dat MR05, $\alpha = 7.5e-6$
 PatternD7.dat RMQ1 $\alpha = 7.5e-6$

PatternE (time joint pattern as in Case C before)

PattenE1.dat rock mass friction angle = 28, joint friction angle=35, Partially fractured model
PatternE2.dat entire model fractured, RMQ5, $\alpha = 7.5e-6$
 PatternE3.dat same as PatternE2.dat. Seismic only, without thermal.
PatternE4.dat same as PatternE2.dat. RMQ1
PatternE22.dat same as PatternE2.dat. with bolt. RMQ5, $\alpha = 7.5 \times 10^{-6}$, jks jkn = 5×10^4
 PatternE23.dat: same as PatterE22.dat, except RMQ1 instead of RMQ5
 RMQ1 $\alpha = 7.5 \times 10^{-6}$ jks jkn = 5×10^4
 PatternE5.dat: RMQ5 $\alpha = 10 \times 10^{-6}$
 PatternE6.dat: RMQ1 $\alpha = 10 \times 10^{-6}$

PatternF (doubled fracture population as PatternC)

PatternF1.dat: <Seismic Run on this Case> RMQ5, $\alpha = 7.5 \times 10^{-6}$
 PatternF2.dat: similar to PatternF1.dat, RMQ1, $\alpha = .5 \times 10^{-6}$
 PatternF3.dat: failure all over. No increase in rock fall RMQ5, $\alpha = 10 \times 10^{-6}$
 PatternF4.dat: limited failure, nice distribution of close & open
 RMQ1, $\alpha = 10 \times 10^{-6}$
 PatternF5.dat: fracture entire model, interesting large rock fall
 RMQ5 $\alpha = 10 \times 10^{-6}$,
PatternF6.dat: fracture entire model RMQ5 $\alpha = 7.5 \times 10^{-6}$
PatternF26.dat: same as PatterF5.dat RMQ5 $\alpha = 7.5 \times 10^{-6}$, jks jkn = 5×10^4 ,
 rock bolts
PatternF7.dat: fracture entire model RMQ1 $\alpha = 7.5 \times 10^{-6}$
PatternF27.dat Bolts
 PatternF8.dat: fracture entire model RMQ1 $\alpha = 10 \times 10^{-6}$
 PatternF8a.dat

APPENDIX B Initial ConditionsIn Site StressRock mass Density (TSW2 - Tptpl) (kg/m^3)

$$\begin{aligned}\rho &= 2210 \text{ kg/m}^3 \\ &= 0.00221 \times 10^6 \text{ kg/m}^3\end{aligned}$$

Gravitational Acceleration

$$g = -9.81 \text{ m/sec}^2$$

$$\sigma_v = \rho gh$$

$$= -0.00221 \times 10^6 \text{ kg/m}^3 \times 9.81 \text{ m/sec}^2 \times h$$

$$\sigma_v / h = -0.02168 [10^6 \text{ kg/(m sec}^2)]/\text{m}$$

$$= -0.02168 \text{ MPa/m}$$

$$\sigma_h = \frac{\nu}{1 - \nu} \sigma_v$$

$$\sigma_h / h = \frac{\nu}{1 - \nu} \sigma_v / h$$

$$= \frac{0.21}{1 - 0.21} \times (-0.02168) \text{ MPa/m}$$

$$= -0.005763 \text{ MPa/m}$$

At the repository (320 m below ground surface):

$$\sigma_v = -0.02168 \text{ MPa/m} \times 320 \text{ m} = -6.9376 \text{ MPa}$$

$$\sigma^h = -0.005763 \text{ MPa/m} \times 320 \text{ m} = -1.844 \text{ MPa}$$

InSituSt.fis

* Calculate in stress stress gradient

* and in situ stress at the repository

* level from mass density for UDEC input

def param

rho=2210.0

grav=9.81

```

rdepth=320.0
poisson=0.21
end
param
set rho=2210.0 grav=9.81
set rdepth=320.0 poisson=0.21
*
def InStress
sigV_h=rho*grav/1000000.0
sigH_h=poisson/(1-poisson)*sigV_h
sigV=-sigV_h*rdepth
sigH=-sigH_h*rdepth
sigTop=sigV_h*270.0
end
*

```

Thermal Gradient in Rock (ambient condition)

Thermal Gradient (°C/m)	Depth (m)
0.020	0-150
0.018	150-400
0.030	400-541
0.030	541-700
0.008	700-911

At the repository level (320 m): 24.76°C
 At the base of the model (667 m): 34.2°C

iniTemp.fis

```

*****
* caculate initial temperature as
* a function of depth, using depth-
* dependent geothermal gradient
* Depth    Geothermal Grient
* (m)      (C/m)
* 0 - 150   0.020
* 150 - 400 0.018
* 400 - 541 0.030
* 541 - 700 0.030
* 700 - 911 0.008
*****
def setVarTemp

```

```

T_surf=18.7 ;fixed ground surface temperature
T_grad1=0.02 ;temperature gradient
T_grad2=0.018
T_grad3=0.030
y_surf=320.0 ;y-coord at ground surface
y_bottom=-350.0 ;y-coord at the bottom of the model
x_beg=-40.5
x_end=40.5
delt_y=5.0
end
*
def ini_Temp
  T150=T_surf+150.0*T_grad1
  T400=T150+(400-150)*T_grad2
  num_inc=(y_surf-y_bottom)/delt_y
  y_end=y_surf
  y_beg=y_end-delt_y
  loop ii (1,num_inc)
    yd_tem=y_surf-(0.5*(y_end+y_beg))
    if yd_tem<=400.0 then
      if yd_tem<=150
        item=T_surf+T_grad1*yd_tem
      else
        item=T150+T_grad2*(yd_tem-150)
      endif
    else
      item=T400+T_grad3*(yd_tem-400)
    endif
    command
      pr item yd_tem y_beg y_end
      initem item x_beg x_end y_beg y_end
    endcommand
    y_end=y_end-delt_y
    y_beg=y_beg-delt_y
  endloop
end
*
setVarTemp
set T_surf=18.7 T_grad1=0.02 T_grad2=0.018 T_grad3=0.030
set y_surf=320.0 y_bottom=-350.0
set x_beg=-40.5 x_end=40.5
set delt_y=5.0
*
```

APPENDIX C Thermal Loading Calculations

EDA II (shedding in pillar design)

- drive diameter = 5.5 m
- areal mass loading = 60 MTU/acre
- drive spacing = 81 meters
- total (mass) MTU = 70,011
- total (heat output) kw = 71,458

$$\text{Average KW per MTU: } \frac{71,499}{70,011} = 1.021 \text{ kw/MTU} \quad (\text{See table v-1 from thermal report})$$

Total area in acres per unit drift length (1 meter):

$$81 \text{ meters} * 1 \text{ meter} = 0.020015 \text{ acre}$$

Total mass loading (MTU) in a unit drift length:

$$60 \text{ MTU/acre} * 0.020015 \text{ acre} = 1.201 \text{ MTU}$$

Total kw per unit drift length:

$$\begin{aligned} &1.201 \text{ MTU} * 1.021 \text{ kw/MTU} \\ &= 1.226 \text{ kw} \end{aligned}$$

Heat flux along drift wall: $1.226 \text{ kw}/(\pi d)$

$$= 1.226 \text{ kw}/(3.14 * 5.5 \text{ m}) = 70.96 \text{ w/m}$$

APPENDIX D Seismic Wave Conversion

Converting from velocity to stress history:

$$\sigma_n = 2(\rho C_p) V_n = \text{norm-str} \cdot V_n \quad \text{-----} \quad (1)$$

$$\sigma_s = 2(\rho C_s) V_s = \text{norm-str} \cdot V_s \quad \text{-----} \quad (1)$$

 σ_n = applied normal stress σ_s = applied shear stress ρ = mass density C_p = p wave velocity C_s = s wave velocity V_n = normal velocity input V_s = shear velocity input

$$\rho = 0.002297$$

$$k = 18740$$

$$G = 13480$$

$$f = 10$$

$$a = 0.4 \text{ g}$$

$$C_p = \sqrt{\frac{k + 4\frac{G}{3}}{\rho}} = \sqrt{\frac{18740 + \frac{1}{3} \times 13480}{0.002297}} = 3924.627 \quad \text{-----} \quad (2)$$

$$C_s = \sqrt{\frac{G}{\rho}} = \sqrt{\frac{13480}{0.002297}} = 2422.504 \quad \text{-----} \quad (2)$$

$$\text{norm-str} = 2(\rho C_p) = 2 \times 0.002297 \times 3924.627 = 18.0297 \quad \text{-----} \quad (3)$$

$$\text{shear-str} = 2(\rho C_s) = 2 \times 0.002297 \times 2422.504 = 11.129 \quad \text{-----} \quad (3)$$

$$V_n = \frac{a \cdot 9.81}{2 \cdot \pi \cdot 10} = \frac{0.4 \times 9.81}{2 \cdot \pi \cdot 10} = 0.0625 \quad \text{-----} \quad (4)$$

From Eq (1):

$$\sigma_n = \text{norm-str} \cdot V_n = 18.029 \times 0.0625 = 1.127$$

For RMQ5, Frequency of 10 Hz

$$\rho = 0.00221 \times 10^6 \text{ kg/m}^3$$

$$k = 18740 \text{ MPa}$$

$$G = 13480 \text{ MPa}$$

$$f = 10$$

$$a = 0.4$$

$$C_p = \sqrt{\frac{k + 4\frac{G}{3}}{\rho}} = \left(\frac{(18740 + \frac{4}{3} \times 13480) \text{ MPa}}{0.00221 \text{ kg/m}^3} \right)^{\frac{1}{2}} = 4075.83$$

$$C_s = \sqrt{\frac{G}{\rho}} = \left(\frac{13480 \text{ MPa}}{0.00221 \times 10^6} \right)^{\frac{1}{2}} = 2469.73$$

$$\text{norm-str} = 2(\rho C_p) = 2 \times 0.00221 \times 4075.83 = 18.02$$

$$\text{shear-str} = 2(\rho C_s) = 2 \times 0.00221 \times 2469.73 = 10.92$$

$$\sigma_n = \text{norm-str} \cdot V_n = 18.02 \times 0.0625 = 1.1259$$

$$\sigma_s = \text{norm-str} \cdot V_s = 10.92 \times 0.0625 = 0.6285$$

For RMQ1 Frequency of 10 Hz

$$\rho = 0.00221 \times 10^6 \text{ kg/m}^3$$

$$k = 4460 \text{ MPa}$$

$$G = 3210 \text{ MPa}$$

$$f = 10$$

$$a = 0.4$$

$$C_p = \sqrt{\frac{k + 4\frac{G}{3}}{\rho}} = \left(\frac{4460 + \frac{4}{3} \times 3210}{0.00221} \right)^{\frac{1}{2}} = 1988.656$$

$$C_s = \sqrt{\frac{G}{\rho}} = \left(\frac{3210}{0.00221} \right)^{\frac{1}{2}} = 1205.19$$

$$\text{norm-str} = 2(\rho C_p) = 2 \times 0.00221 \times 1988.656 = 8.79$$

$$\text{shear-str} = 2(\rho C_s) = 2 \times 0.00221 \times 1205.19 = 5.327$$

$$\sigma_n = \text{norm-str} \cdot V_n = 8.79 \times 0.0625 = 0.55$$

$$\sigma_s = \text{norm-str} \cdot V_s = 5.32 \times 0.0625 = 0.333$$

For frequency of 5 hz, a=0.04g

$$V_n = V_s = 0.125$$

For RMQ5:

$$\sigma_n = 18.02 \times 0.125 = 2.25$$

$$\sigma_s = 10.92 \times 0.125 = 1.365$$

For RMQ1:

$$\sigma_n = 8.79 \times 0.125 = 1.099$$

$$\sigma_s = 5.327 \times 0.125 = 0.666$$

For frequency of 1 hz, a=0.04g

$$V_n = V_s = 0.625$$

For RMQ5:

$$\sigma_n = 18.02 \times 0.625 = 11.26$$

$$\sigma_s = 10.92 \times 0.625 = 6.825$$

For RMQ1:

$$\sigma_n = 8.79 \times 0.625 = 5.49$$

$$\sigma_s = 5.327 \times 0.625 = 3.33$$

dRMQ1F1.fis

```

* -----
* define properties for calculating wave velocities
* m_dens = mass density
* b_mod = bulk modulus (K)
* s_mod = shear modulus (G)
* -----
def properties
  m_dens=0.00221
  b_mod=4460.0
  s_mod=3210.0
end
properties
* -----
* convert velocity history to stress history to
* apply to a quiet boundary
* c_p = compressive wave velocity
* c_s = shear wave velocity

```

```

* norm_str = factor to convert velocity to stress
* shear_str = factor to convert velocity to stress
* -----
def conver
  c_p=sqrt((b_mod+(4.0*s_mod/3.0))/m_dens)
  c_s=sqrt(s_mod/m_dens)
  norm_str=-2.0*m_dens*c_p
  shear_str=-2.0*m_dens*c_s
end
conver
* -----
* calculate boundary velocity history
* Where:
*   env_time: duration
*   ampl: velocity amplitude
*   freq: frequency
*   accel: acceleration level in g
* -----
def blvel
  ampl=9.81*accel/(2*pi*freq)
  whilestepping
  if time > env_time
    wave=0.0
  else
    wave=ampl*sin(2.0*pi*freq*time)
  endif
  h_ns=norm_str*wave
  h_ss=shear_str*wave
end
set freq=1.0 accel=0.40 env_time=5.0
blvel
* set freq=10.0 ampl=0.0625 env_time=2.0

```

dRMQ1F10.fis

```

* -----
* define properties for calculating wave velocities
* m_dens = mass density
* b_mod = bulk modulus (K)
* s_mod = shear modulus (G)
* -----
def properties
  m_dens=0.00221
  b_mod=4460.0
  s_mod=3210.0

```

```

end
properties
* -----
* convert velocity history to stress history to
* apply to a quiet boundary
*   c_p = compressive wave velocity
*   c_s = shear wave velocity
* norm_str = factor to convert velocity to stress
* shear_str = factor to convert velocity to stress
* -----
def conver
  c_p=sqrt((b_mod+(4.0*s_mod/3.0))/m_dens)
  c_s=sqrt(s_mod/m_dens)
  norm_str=-2.0*m_dens*c_p
  shear_str=-2.0*m_dens*c_s
end
conver
* -----
* calculate boundary velocity history
* Where:
*   env_time: duration
*   ampl: velocity amplitude
*   freq: frequency
*   accel: acceleration level in g
* -----
def blvel
  ampl=9.81*accel/(2*pi*freq)
  whilestepping
  if time > env_time
    wave=0.0
  else
    wave=ampl*sin(2.0*pi*freq*time)
  endif
  h_ns=norm_str*wave
  h_ss=shear_str*wave
end
set freq=10.0 accel=0.40 env_time=1.0
blvel
* set freq=10.0 ampl=0.0625 env_time=2.0

```

dRMQ1F5.fis

```

* -----
* define properties for calculating wave velocities
* m_dens = mass density

```

```

* b_mod = bulk modulus (K)
* s_mod = shear modulus (G)
* -----
def properties
  m_dens=0.00221
  b_mod=4460.0
  s_mod=3210.0
end
properties
* -----
* convert velocity history to stress history to
* apply to a quiet boundary
*   c_p = compressive wave velocity
*   c_s = shear wave velocity
* norm_str = factor to convert velocity to stress
* shear_str = factor to convert velocity to stress
* -----
def conver
  c_p=sqrt((b_mod+(4.0*s_mod/3.0))/m_dens)
  c_s=sqrt(s_mod/m_dens)
  norm_str=-2.0*m_dens*c_p
  shear_str=-2.0*m_dens*c_s
end
conver
* -----
* calculate boundary velocity history
* Where:
*   env_time: duration
*   ampl: velocity amplitude
*   freq: frequency
*   accel: acceleration level in g
* -----
def blvel
  ampl=9.81*accel/(2*pi*freq)
  whilestepping
  if time > env_time
    wave=0.0
  else
    wave=ampl*sin(2.0*pi*freq*time)
  endif
  h_ns=norm_str*wave
  h_ss=shear_str*wave
end
set freq=5.0 accel=0.40 env_time=1.0
blvel

```

```
* set freq=10.0 ampl=0.0625 env_time=2.0
```

dRMQ5f1.fis

```
* -----
* define properties for calculating wave velocities
* m_dens = mass density
* b_mod = bulk modulus (K)
* s_mod = shear modulus (G)
* -----
def properties
  m_dens=0.00221
  b_mod=18740.0
  s_mod=13480.0
end
properties
* -----
* convert velocity history to stress history to
* apply to a quiet boundary
*   c_p = compressive wave velocity
*   c_s = shear wave velocity
* norm_str = factor to convert velocity to stress
* shear_str = factor to convert velocity to stress
* -----
def conver
  c_p=sqrt((b_mod+(4.0*s_mod/3.0))/m_dens)
  c_s=sqrt(s_mod/m_dens)
  norm_str=-2.0*m_dens*c_p
  shear_str=-2.0*m_dens*c_s
end
conver
* -----
* calculate boundary velocity history
* Where:
*   env_time: duration
*   ampl: velocity amplitude
*   freq: frequency
*   accel: acceleration level in g
* -----
def blvel
  ampl=9.81*accel/(2*pi*freq)
  whilestepping
  if time > env_time
    wave=0.0
  else
    wave=ampl*sin(2.0*pi*freq*time)
```

```

endif
h_ns=norm_str*wave
h_ss=shear_str*wave
end
set freq=1.0 accel=0.40 env_time=5.0
blvel
* set freq=10.0 ampl=0.0625 env_time=2.0

```

dRMQ5F10.fis

```

* -----
* define properties for calculating wave velocities
* m_dens = mass density
* b_mod = bulk modulus (K)
* s_mod = shear modulus (G)
* -----
def properties
  m_dens=0.00221
  b_mod=18740.0
  s_mod=13480.0
end
properties
* -----
* convert velocity history to stress history to
* apply to a quiet boundary
*   c_p = compressive wave velocity
*   c_s = shear wave velocity
*   norm_str = factor to convert velocity to stress
*   shear_str = factor to convert velocity to stress
* -----
def conver
  c_p=sqrt((b_mod+(4.0*s_mod/3.0))/m_dens)
  c_s=sqrt(s_mod/m_dens)
  norm_str=-2.0*m_dens*c_p
  shear_str=-2.0*m_dens*c_s
end
conver
* -----
* calculate boundary velocity history
* Where:
*   env_time: duration
*   ampl: velocity amplitude
*   freq: frequency
*   accel: acceleration level in g
* -----

```

```

def blvel
  ampl=9.81*accel/(2*pi*freq)
  whilestepping
  if time > env_time
    wave=0.0
  else
    wave=ampl*sin(2.0*pi*freq*time)
  endif
  h_ns=norm_str*wave
  h_ss=shear_str*wave
end
set freq=10.0 accel=0.40 env_time=1.0
blvel
* set freq=10.0 ampl=0.0625 env_time=2.0

```

dRMQ5F5.fis

```

* -----
* define properties for calculating wave velocities
* m_dens = mass density
* b_mod = bulk modulus (K)
* s_mod = shear modulus (G)
* -----
def properties
  m_dens=0.00221
  b_mod=18740.0
  s_mod=13480.0
end
properties
* -----
* convert velocity history to stress history to
* apply to a quiet boundary
*   c_p = compressive wave velocity
*   c_s = shear wave velocity
* norm_str = factor to convert velocity to stress
* shear_str = factor to convert velocity to stress
* -----
def conver
  c_p=sqrt((b_mod+(4.0*s_mod/3.0))/m_dens)
  c_s=sqrt(s_mod/m_dens)
  norm_str=-2.0*m_dens*c_p
  shear_str=-2.0*m_dens*c_s
end
conver
* -----

```

```

* calculate boundary velocity history
* Where:
*   env_time: duration
*   ampl: velocity amplitude
*   freq: frequency
*   accel: acceleration level in g
* -----
def blvel
  ampl=9.81*accel/(2*pi*freq)
  whilestepping
  if time > env_time
    wave=0.0
  else
    wave=ampl*sin(2.0*pi*freq*time)
  endif
  h_ns=norm_str*wave
  h_ss=shear_str*wave
end
set freq=5.0 accel=0.40 env_time=1.0
blvel
* set freq=10.0 ampl=0.0625 env_time=2.0

```

dRMQ5F5_b.fis

```

* -----
* define properties for calculating wave velocities
* m_dens = mass density
* b_mod = bulk modulus (K)
* s_mod = shear modulus (G)
* -----
def properties
  m_dens=0.00221
  b_mod=18740.0
  s_mod=13480.0
end
properties
* -----
* convert velocity history to stress history to
* apply to a quiet boundary
*   c_p = compressive wave velocity
*   c_s = shear wave velocity
* norm_str = factor to convert velocity to stress
* shear_str = factor to convert velocity to stress
* -----
def conver

```

```

c_p=sqrt((b_mod+(4.0*s_mod/3.0))/m_dens)
c_s=sqrt(s_mod/m_dens)
norm_str=-2.0*m_dens*c_p
shear_str=-2.0*m_dens*c_s
end
conver
* -----
* calculate boundary velocity history
* Where:
*   env_time: duration
*   ampl: velocity amplitude
*   freq: frequency
*   accel: acceleration level in g
* -----
def blvel
  ampl=9.81*accel/(2*pi*freq)
  whilestepping
    if time > env_time
      wave=0.0
    else
      wave=ampl*sin(2.0*pi*freq*time)
    endif
    h_ns=norm_str*wave
    h_ss=shear_str*wave
  end
set freq=5.0 accel=0.80 env_time=1.0
blvel
* set freq=10.0 ampl=0.0625 env_time=2.0

```

dRMQ5F5_c.fis

```

* -----
* define properties for calculating wave velocities
* m_dens = mass density
* b_mod = bulk modulus (K)
* s_mod = shear modulus (G)
* -----
def properties
  m_dens=0.00221
  b_mod=18740.0
  s_mod=13480.0
end
properties
* -----
* convert velocity history to stress history to

```

```

* apply to a quiet boundary
*   c_p = compressive wave velocity
*   c_s = shear wave velocity
* norm_str = factor to convert velocity to stress
* shear_str = factor to convert velocity to stress
* -----
def conver
  c_p=sqrt((b_mod+(4.0*s_mod/3.0))/m_dens)
  c_s=sqrt(s_mod/m_dens)
  norm_str=-2.0*m_dens*c_p
  shear_str=-2.0*m_dens*c_s
end
conver
* -----
* calculate boundary velocity history
* Where:
*   env_time: duration
*   ampl: velocity amplitude
*   freq: frequency
*   accel: acceleration level in g
* -----
def blvel
  ampl=9.81*accel/(2*pi*freq)
  whilestepping
  if time > env_time
    wave=0.0
  else
    wave=ampl*sin(2.0*pi*freq*time)
  endif
  h_ns=norm_str*wave
  h_ss=shear_str*wave
end
set freq=5.0 accel=0.80 env_time=4.0
blvel
* set freq=10.0 ampl=0.0625 env_time=2.0

```

dRMQ5F5_d.fis

```

* -----
* define properties for calculating wave velocities
* m_dens = mass density
* b_mod = bulk modulus (K)
* s_mod = shear modulus (G)
* -----
def properties
  m_dens=0.00221
  b_mod=18740.0
  s_mod=13480.0
end
properties
* -----
* convert velocity history to stress history to
* apply to a quiet boundary
*   c_p = compressive wave velocity
*   c_s = shear wave velocity
* norm_str = factor to convert velocity to stress
* shear_str = factor to convert velocity to stress
* -----
def conver
  c_p=sqrt((b_mod+(4.0*s_mod/3.0))/m_dens)
  c_s=sqrt(s_mod/m_dens)
  norm_str=-2.0*m_dens*c_p
  shear_str=-2.0*m_dens*c_s
end
conver
table 1 read Reposi_V.tab
table 2 read Reposi_H.tab

```

*** dRMQ5F5_e.fis**

```

* -----
* calculate boundary velocity history
* Where:
*   env_time: duration
*   ampl: velocity amplitude
*   freq: frequency
*   accel: acceleration level in g
* -----
def blvel2
  env_time2=3.75
  whilestepping
  if time > env_time2
    wave2=0.0

```

```
else
  wave2=ampl*sin(2.0*pi*freq*time)
endif
end
set env_time2=3.75
blvel2
```

ARC

APPENDIX E Example Input Files

PatternE2.dat

- * Model setup is based on EAD #2. Drift spacing is 81 m. Mass density
- * is 60 MTU/acre, drift diameter is 5.5 m.
- *
- * Model extended vertical region to ground surface and ground water
- * level for thermal analyses prior to dynamics analyses. Dynamic
- * analyses then uses a sub model that extend 50 m above and below the
- * drift.
- *
- * Includes fish functions for automatically converting
- * g level to v and then to boundary stresses.
- *
- * Base.dat is with very few fractures, almost equivalent to a
- * continuum model. Base1.dat subject to cos p-wave, Base2.dat
- * subject to cos s-wave, Base3.dat subject to both s- and p-wave.
- * Base4.dat subject to both s- and p-waves with design ground motions.
- *
- * Base5.dat is the same as Base4.dat, except some history points are
- * added for monitoring the results
- *
- * PatternA6.dat is the same as Base5.dat, except rock mass friction angle * is reduced to 28 from 46
- *
- * In PatternA9.dat, parameters are changed to that of RMQ5, in-situ temperature
- * changes with depth depend on geothermal gradient and thermal decay
- * curve is fitting better with multiple exponential segments, also
- * material properties are check against Ground Support Design for VA
- * properties
- *
- * PatternA14.dat is the run with new RMQ5 properties and scaled initial thermal
- * strength.
- * PatternA16.dat is the same as PatternA14.dat, except thermal expansion
- * coefficient is increased to 7.5×10^{-6} instead of 6×10^{-6} .
- * PatternE1.dat: irregular joint pattern, RMQ5, alpha $7.5e-6$
- * PatternE2.dat: irregular joint pattern throughout the model

*

* Part I: Mechanical

```
set log PatternE2.log
set plot ps co
set plot wind
```



start

*

* -----

* Title

* -----

head

Thermal-Dynamic Analysis (EDA#2)/PatternE2.dat

*

* Rock Mass Elastic Properties (RMQ5) (RMQ1) VA_RMQ5 VA_RMQ1

* Mass density (kg/m³): 2210 2210 2235 2235

* Young's modulus (GPa): 32.61 7.76 32.61 7.76

* Poisson's ratio 0.21 0.21 0.21 0.21

* Bulk modulus (GPa): 18.74 4.46 18.74 4.46

* Shear modulus (GPa): 13.48 3.21 13.48 3.21

*

* Rock Mass Strength Properties (RMQ5) (RMQ1) VA_RMQ5 VA_RMQ1

* Cohesion (MPa): 5.08 2.82 5.2 1.5

* Friction angle (degrees): 34.42 27.50 46.0 43.0

* Unconf comp strength (MPa): 19.28 9.29 26.09 7.08

* Dilation angle: 17.21 13.75 0.0 0.0

* Tensile strength (MPa): 5.35 4.42 4.21 1.32

*

* Thermal properties

* Conductivity (W/m-K): 2.13

* Specific heat (J/kg-K): 968.96

* Thermal expansion (/C) 1.0E-5

*

* Joint Properties DOE_VA

* Cohesion (MPa): 0.07 0.07

* Friction angle (degrees): 35 56

* Dilation angle (degrees): 17.5 0.0

* Tensile strength (MPa): 0.0

* Normal stiffness (GPa/m): 500 (50?) 500

* Shear stiffness (GPa/m): 500 (50?) 500

*

* Size of problem domain is -40.5<x<40.5 -350<y<320

* - Vertical boundaries are located along symmetry lines assuming

* 81 m drift spacings

* - Upper and lower horizontal boundaries set near ground surface

* and water table, respectively, where thermal front is near zero

*

round 0.02

set ovtol 1.0

config thermal

block -40.5 -350 -40.5 320 40.5 320 40.5 -350

```

*
*****
* create jointing
*****
* -----
* splits needed for isolating the submodel
* -----
split -40.5 50 40.5 50
split -40.5 -50 40.5 -50
*
* split -40.5 -19.25 40.5 -19.25
* split -40.5 19.25 40.5 19.25
*split -19.25 -19.25 -19.25 19.25
*split 19.25 -19.25 19.25 19.25
*
* -----
* inner problem domain
* -----
* angle,length,gap,spacing
*jregion -19.25 -19.25 -19.25 19.25 -13.75 19.25 -13.75 -19.25
jregion -40.5 -19.25 -40.5 19.25 -13.75 19.25 -13.75 -19.25
jset 85.0 10.0 40.0 5.0 0.0 0.0 1.5 0.2 0 0
jset 110.0 10.0 17.0 4.0 -0.3 0.1 5 0.5 0 0
*
*jregion -19.25 -19.25 -19.25 19.25 -12.75 19.25 -12.75 -19.25
jregion -40.5 -19.25 -40.5 19.25 -13.75 19.25 -13.75 -19.25
jset 20.0 5.0 20.0 2.5 0.0 0.0 3.0 0.2 0 0
*
*jregion 13.75 -19.25 13.75 19.25 19.25 19.25 19.25 -19.25
jregion 13.75 -19.25 13.75 19.25 40.5 19.25 40.5 -19.25
jset 85.0 10.0 40.0 5.0 0.0 0.0 1.5 0.2 1 1
jset 110.0 10.0 17.0 4.0 -0.3 0.1 5 0.5 1 1
*
* jregion 12.75 -19.25 12.75 19.25 19.25 19.25 19.25 -19.25
jregion 12.75 -19.25 12.75 19.25 40.5 19.25 40.5 -19.25
jset 20.0 5.0 20.0 2.5 0.0 0.0 3.0 0.2 0 0
*
jregion -13.75 -19.25 -13.75 -12.75 13.75 -12.75 13.75 -19.25
jset 85.0 10.0 40.0 5.0 0.0 0.0 1.5 0.2
jset 110.0 10.0 17.0 4.0 -0.3 0.1 5 0.5
*
jregion -13.75 -19.25 -13.75 -13.75 13.75 -13.75 13.75 -19.25
jset 20.0 5.0 20.0 2.5 0.0 0.0 3.0 0.2
*
jregion -13.75 12.75 -13.75 19.25 13.75 19.25 13.75 12.75

```

```

jset 85.0 10.0 40.0 5.0 0.0 0.0 1.5 0.2
jset 110.0 10.0 17.0 4.0 -0.3 0.1 5 0.5
*
jregion -13.75 13.75 -13.75 19.25 13.75 19.25 13.75 13.75
jset 20.0 5.0 20.0 2.5 0.0 0.0 3.0 0.2
*
* -----
* More detailed inner problem domain
* -----
* angle,length,gap,spacing
*
jregion -13.75 -13.75 -13.75 13.75 -6 13.75 -6 -13.75
jset 85.0 10.0 17.5 1.0 -0.2 0.0 1.0 0.3
jset 110.0 10.0 17.0 4.0 -0.3 0.1 3.6 0.5
*
jregion -13.75 -13.75 -13.75 13.75 -4.5 13.75 -4.5 -13.75
jset 20.0 5.0 15.0 1.0 -0.2 0.0 1.5 0.3
*
jregion 6 -13.75 6 13.75 13.75 13.75 13.75 -13.75
jset 85.0 15.0 17.5 1.0 -0.2 0.0 1.0 0.3
jset 110.0 10.0 17.0 4.0 -0.3 0.1 3.6 0.5
*
jregion 4.5 -13.75 4.5 13.75 13.75 13.75 13.75 -13.75
jset 20.0 5.0 15.0 1.0 -0.2 0.0 1.5 0.3
*
jregion -6 -13.75 -6 -5 6 -5 6 -13.75
jset 85.0 15.0 17.5 1.0 -0.2 0.0 1.0 0.3
jset 110.0 10.0 17.0 4.0 -0.3 0.1 3.6 0.5
*
jregion -5 -13.75 -5 -6 5 -6 5 -13.75
jset 20.0 5.0 15.0 1.0 -0.2 0.0 1.5 0.3
*
jregion -6 5 -6 13.75 6 13.75 6 5
jset 85.0 15.0 17.5 1.0 -0.2 0.0 1.0 0.3
jset 110.0 10.0 17.0 4.0 -0.3 0.1 3.6 0.5
*
jregion -5 6 -5 13.75 5 13.75 5 6
jset 20.0 5.0 15.0 1.0 -0.2 0.0 1.5 0.3
*
* -----
* Detailed joint spacing around the tunnel
* -----
* angle,length,gap,spacing
*
jregion -6 -6 -6 6 6 6 6 -6

```

```

jset 85.0 10.0 7.5 1.0 -0.2 0.0 0.4 0.1
jset 20.0 5.0 5.0 1.0 -0.2 0.0 0.75 0.1 -1 -1
jset 110.0 10.0 12.0 4.0 -0.3 0.1 1.8 0.5 -1 0
*
* -----
* outer domain
* -----
* angle,length,gap,spacing
jregion -40.5 -50 -40.5 -16.25 40.5 -16.25 40.5 -50
jset 85.0 10.0 50.0 1.0 0.0 0.0 3.0 0.3
jset 110.0 10.0 25.0 4.0 -0.3 0.1 8.0 0.5
*
jregion -40.5 -50 -40.5 -19.25 40.5 -19.25 40.5 -50
jset 20.0 5.0 25.0 1.0 0.0 0.0 5.0 0.3
*
jregion -40.5 16.25 -40.5 50 40.5 50 40.5 16.25
jset 85.0 10.0 50.0 1.0 0.0 0.0 3.0 0.3
jset 110.0 10.0 25.0 4.0 -0.3 0.1 8.0 0.5
*
jregion -40.5 19.25 -40.5 50 40.5 50 40.5 19.25
jset 20.0 5.0 25.0 1.0 0.0 0.0 5.0 0.3
*
* -----
* out domain for the whole model
* -----
* angle,length,gap,spacing
jregion -40.5 -350 -40.5 -50 40.5 -50 40.5 -350
jset 85.0 0.0 70.0 15.0 -0.5 0.0 10.0 0.05 10 10
jset 20.0 0.0 25.0 3.0 -0.5 0.0 25.0 0.8 10 10
*
jregion -40.5 50 -40.5 320 40.5 320 40.5 50
jset 85.0 0.0 70.0 15.0 -0.5 0.0 10.0 0.05 10 10
jset 20.0 0.0 25.0 3.0 -0.5 0.0 25.0 0.8 10 10
*
tunnel 0 0 2.75 36
del area 1.5e-2
jd
*
* *****
* auto generation of zones
* *****
gen region -6 -6 -6 6 6 6 -6 edge 3.5
* gen region -7 -7 -7 7 7 7 -7 edge 0.7
* gen region -40.5 -19.5 -40.5 19.5 40.5 19.5 40.5 -19.5 edge 3.0
gen region -40.5 -21 -40.5 21 40.5 21 40.5 -21 edge 3.0

```

```

gen region -40.5 -25 -40.5 25 40.5 25 40.5 -25 edge 8
gen region -40.5 -28 -40.5 28 40.5 28 40.5 -28 edge 4
gen region -40.5 -35 -40.5 35 40.5 35 40.5 -35 edge 6
gen region -40.5 -40 -40.5 40 40.5 40 40.5 -40 edge 5
gen region -40.5 -50 -40.5 50 40.5 50 40.5 -50 edge 8
*
gen region -40.5 -350 -40.5 320 40.5 320 40.5 -350 edge 14
pr max
*
damp auto
*
*****
* apply mechanical boundary conditions (units, MPa)
*****
call InSituSt.fis
InStress
*
grav 0.0 -9.81
insitu stress sigH 0.0 sigV ygrad sigH_h 0.0 sigV_h szz sigH &
zgrad 0.0 sigH_h
bound -42 42 315 325 stress sigH 0.0 sigV ygrad sigH_h 0.0 sigV_h
bound -42 42 -355 -345 yvel=0.0
bound -42 -39 -351 321 xvel=0.0
bound 39 42 -351 321 xvel=0.0
*
*****
* define mechanical and thermal material properties for joints/intact blocks
*****
*
* material 1 = rock
*
change -42 42 -350 320 jcons=5
**
prop mat=1 k=18.74e3 g=13.48e3 d=0.00221
** !! would like to use: prop mat=1 cond=2.13 thexp=1.0e-05 spec=9.6896e08
prop mat=1 cond=2.13 thexp=7.5e-06 spec=9.6896e08
prop jmat=1 jks=5.0e5 jkn=5.0e5 jdil=0 jc=0.07 jfric=35.0 jtens=0.0 &
kn=5.0e4 ks=5.0e4
** !! try to used orginal properties
*** %%% prop mat=1 cond=2.06 thexp=6.0e-06 spec=9.58e08
*** %%% prop jmat=1 jks=5.0e5 jkn=5.0e5 jdil=0 jc=0.07 jfric=56.0 jtens=0.0 &
*** %%% kn=5.0e5 ks=5.0e5
*
set jcondf 5
*
```

```

* mohr-coulomb failure parameters
*
prop mat=1 coh=5.08 fric=34.42 tens=5.35 dil=17.21
*** %%% change this back prop mat=1 coh=5.2 fric=28 tens=4.21 dil=0.0
*
*****
* history records
*****
hist nycyc=10 unbal damp type 4
hist ydis 0 0 yvel 0 0 ydis 0 320 ydis 0 -350
hist sxx 0.0 0.0 syy 0.0 0.0
*
*****
* initial cycling equilibrium
*****
cycle 4000
save E2_ini.sav
*
*****
* remove tunnel blocks
*****
*
del ann 0 0 0 2.75
*
*** call Set_bolts
* -----
* Calculate room closures
* -----
call closure.fis
Closure
*
* reset displacements after applying in situ loading conditions
*
reset damp time hist dis rot
hist unbal damp
hist ydis 0.0 2.75 ydis 0 -2.75
hist xdis -2.75 0.0 xdis 2.75 0.0
hist ydis 0.0 320 ydis -40.5 320 ydis 40.5 320
hist sdis 2.75,10 sdis -2.75,10 sdis 2.75 -10 sdis -2.75,-10
his ClosureV
his ClosureH
*
*
* change material property to Mohr-Coulomb
change cons=3 mat=1

```

```

*
cycle 4000
*
sav E2_exc.sav
*
*****
* Part II: Thermal
*****
*
*****
* set thermal boundary and histories
*****
*
* set up thermal boundaries (default thermal b.c. are adiabatic)
*
** tfix 18.7 range (-42 42) (316 318)
** tfix 34.2 range (-42 42) (-351 -349)
*
* Call FISH FUNCTION to cal initem according to geothermal gradient
call iniTemp.fis
ini_Temp
*
** initem 29.0 -42 42 -350 320
*
thist ntcyc=10 tem 0 2.75 tem 0 5 tem 0 10 tem 0 25 tem 0 50 tem 0 100
thist tem 0 150 tem 0 200 tem 0 250 tem 0 320
this tem 2.75 0 tem 5 0 tem 10 0
thist tem 15 0 tem 20 0 tem 30 0 tem 40.5 0
*
*****
* apply heat flux to tunnel wall
*****
* run initial thermal time by explicit scheme for 100 steps
*
** thapp ann 0.0 0.0 2.71 2.79 flux 71.0152 -7.5e-10
** thapp ann 0.0 0.0 2.71 2.79 flux 71.0152 -3.5e-10
* scaled initial strength (71.0152*196.3/225)
thapp ann 0.0 0.0 2.71 2.79 flux 61.95 -3.5e-10
run age=3600 step=1000000 tol=0.05
reset damp
cycle 4000
pr max
*
* run thermal time to 3 months
*

```

```
run age=7.776e6 delt=3600.0 temp=10000 step=1000000 tol=0.05 impl
reset damp
cycle 4000
pr max
*
* run thermal time to 1 year
*
run age=3.1536e7 delt=7200.0 temp=10000 step=1000000 tol=0.05 impl
reset damp
cycle 4000
pr max
*
* run thermal time to 18 months
*
run age=4.7304e7 delt=7200.0 temp=10000 step=1000000 tol=0.05 impl
reset damp
cycle 4000
pr max
*
* run thermal time to 2 years
*
run age=6.3072e7 delt=7200.0 temp=10000 step=1000000 tol=0.05 impl
reset damp
cycle 4000
pr max
* sav E2_2y.sav
*
* run thermal time to 3 years
*
run age=9.4608e7 delt=7200.0 temp=10000 step=1000000 tol=0.05 impl
reset damp
cycle 4000
* sav E2_3y.sav
pr max
*
* run thermal time to 4 years
*
run age=1.26144e8 delt=7200.0 temp=10000 step=1000000 tol=0.05 impl
reset damp
cycle 4000
pr max
* sav E2_4y.sav
*
* run thermal time to 5 years
*
```

```
run age=1.5768e8 delt=7200.0 temp=10000 step=1000000 tol=0.05 impl
reset damp
cycle 4000
pr max
sav E2_5y.sav
*
* run thermal time to 7.5 years
*
** thapp ann 0.0 0.0 2.71 2.79 flux -71.0152 -7.5e-10
** thapp ann 0.0 0.0 2.71 2.79 flux 69.2 -6e-10
run age=2.3652e8 delt=7200.0 temp=10000 step=1000000 tol=0.05 impl
reset damp
cycle 4000
pr max
*
* run thermal time to 10 years
*
run age=3.1536e8 delt=7200.0 temp=10000 step=1000000 tol=0.05 impl
reset damp
cycle 4000
pr max
sav E2_10y.sav
*
* run thermal time to 20 years
*
** thapp ann 0.0 0.0 2.71 2.79 flux -69.2 -6e-10
** thapp ann 0.0 0.0 2.71 2.79 flux 66.2 -5e-10
run age=6.3072e8 delt=7200.0 temp=10000 step=1000000 tol=0.05 impl
reset damp
cycle 4000
pr max
* save E2_20y.sav
*
* run thermal time to 30 years
*
** thapp ann 0.0 0.0 2.71 2.79 flux -66.2 -5e-10
** thapp ann 0.0 0.0 2.71 2.79 flux 66.0 -5e-10
run age=9.4608e8 delt=7200.0 temp=10000 step=1000000 tol=0.05 impl
reset damp
cycle 4000
pr max
* sav E2_30y.sav
*
* run thermal time to 40 years
*
```

```

** thapp ann 0.0 0.0 2.71 2.79 flux -66.0 -5e-10
** thapp ann 0.0 0.0 2.71 2.79 flux 59.3 -4e-10
run age=12.6144e8 delt=7200.0 temp=10000 step=1000000 tol=0.05 impl
reset damp
cycle 4000
pr max
* sav E2_40y.sav
*
* run thermal time to 50 years
*
** thapp ann 0.0 0.0 2.71 2.79 flux -59.3 -4e-10
** thapp ann 0.0 0.0 2.71 2.79 flux 58.9 -4e-10
run age=1.5768e9 delt=7200.0 temp=10000 step=1000000 tol=0.05 impl
reset damp
cycle 4000
pr max
sav E2_50y.sav
*
res E2_50y.sav
* run thermal time to 60 years
** thapp ann 0.0 0.0 2.71 2.79 flux -58.9 -4e-10
** thapp ann 0.0 0.0 2.71 2.79 flux 59.0 -4e-10
run age=1.89216e9 delt=7200.0 temp=10000 step=1000000 tol=0.05 impl
reset damp
cycle 4000
pr max
sav E2_60y.sav
*
* run thermal time to 70 years
*
** thapp ann 0.0 0.0 2.71 2.79 flux -59.0 -4e-10
** thapp ann 0.0 0.0 2.71 2.79 flux 59.7 -4e-10
run age=2.20752e9 delt=7200.0 temp=10000 step=1000000 tol=0.05 impl
reset damp
cycle 5000
pr max
sav E2_70y.sav
*
* run thermal time to 80 years
*
** thapp ann 0.0 0.0 2.71 2.79 flux -59.7 -4e-10
** thapp ann 0.0 0.0 2.71 2.79 flux 47.4 -3e-10
run age=2.52288e9 delt=7200.0 temp=10000 step=1000000 tol=0.05 impl
reset damp
cycle 4000

```

```

pr max
sav E2_80y.sav
*
*
* run thermal time to 90 years
*
res E2_80y.sav
** thapp ann 0.0 0.0 2.71 2.79 flux -47.4 -3e-10
** thapp ann 0.0 0.0 2.71 2.79 flux 47.7 -3e-10
run age=2.83824e9 delt=7200.0 temp=10000 step=1000000 tol=0.05 impl
reset damp
cycle 4000
pr max
sav E2_90y.sav
*
* run thermal time to 100 years
*
** thapp ann 0.0 0.0 2.71 2.79 flux -47.7 -3e-10
** thapp ann 0.0 0.0 2.71 2.79 flux 48.4 -3e-10
run age=3.1536e9 delt=7200.0 temp=10000 step=1000000 tol=0.05 impl
reset damp
cycle 4000
pr max
sav E2_100y.sav
*
* run thermal time to 150 years
*
** thapp ann 0.0 0.0 2.71 2.79 flux -48.4 -3e-10
** thapp ann 0.0 0.0 2.71 2.79 flux 35.7 -2e-10
run age=4.7304e9 delt=7200.0 temp=10000 step=1000000 tol=0.05 impl
reset damp
cycle 8000
pr max
sav E2_150y.sav
*
return

```

PatternE4.dat

```

*****
* Model setup is based on EAD #2. Drift spacing is 81 m. Mass density
* is 60 MTU/acre, drift diameter is 5.5 m.
*
* Model extended vertical region to ground surface and ground water

```

```

* level for thermal analyses prior to dynamics analyses. Dynamic
* analyses then uses a sub model that extend 50 m above and below the
* drift.
*
* Includes fish functions for automatically converting
* g level to v and then to boundary stresses.
*
* Base.dat is with very few fractures, almost equivalent to a
* continuum model. Base1.dat subject to cos p-wave, Base2.dat
* subject to cos s-wave, Base3.dat subject to both s- and p-wave.
* Base4.dat subject to both s- and p-waves with design ground motions.
*
* Base5.dat is the same as Base4.dat, except some histry points are
* added for monitoring the results
*
* PatternA6.dat is the same as Base5.dat, except rock mass friction angle * is reduced to 28 from 46
*
* In PatternA9.dat, parameters are changed to that of RMQ5, in-situ temperature
* changes with depth depend on geothermal gradient and thermal decay
* curve is fitting better with multiple exponential segments, also
* material properties are check against Ground Support Design for VA
* properties
*
* PatternA14.dat is the run with new RMQ5 properties and scaled initial thermal
* strength.
* PatternA16.dat is the same as PatternA14.dat, except thermal expansion
* coeficient is increased to 7.5x10-6 instead of 6x10-6.
* PatternE1.dat: irregular joint pattern, RMQ5, alpha 7.5e-6
* PatternE2.dat: irregular joint pattern throughout the model
* PatternE3.dat: similar to PatternE2, RMQ1, alpha 7.5e-6
*****
*
*****
* Part I: Mechanial
*****
set log PatternE4.log
set plot ps co
start
*
* -----
* Title
* -----
head
Thermal-Dynamic Analysis (EDA#2)/PatternE4.dat
*

```

```
* Rock Mass Elastic Properties (RMQ5) (RMQ1) VA_RMQ5 VA_RMQ1
* Mass density (kg/m^3):      2210  2210  2235  2235
* Young's modulus (GPa):     32.61  7.76  32.61  7.76
* Poisson's ratio           0.21   0.21  0.21   0.21
* Bulk modulus (GPa):       18.74  4.46  18.74  4.46
* Shear modulus (GPa):      13.48  3.21  13.48  3.21
```

```
* Rock Mass Strength Properties (RMQ5) (RMQ1) VA_RMQ5 VA_RMQ1
* Cohesion (MPa):           5.08   2.82   5.2    1.5
* Friction angle (degrees): 34.42 27.50 46.0   43.0
* Unconf comp strength (MPa): 19.28 9.29  26.09  7.08
* Dilation angle:           17.21 13.75 0.0    0.0
* Tensile strength (MPa):    5.35  4.42  4.21   1.32
```

```
* Thermal properties
* Conductivity (W/m-K):      2.13
* Specific heat (J/kg-K):    968.96
* Thermal expansion (/C)     1.0E-5
```

```
* Joint Properties          DOE_VA
* Cohesion (MPa):           0.07   0.07
* Friction angle (degrees): 35      56
* Dilation angle (degrees): 17.5     0.0
* Tensile strength (MPa):   0.0
* Normal stiffness (GPa/m): 500 (50?) 500
* Shear stiffness (GPa/m): 500 (50?) 500
```

```
* Size of problem domain is -40.5<x<40.5 -350<y<320
* - Vertical boundaries are located along symmetry lines assuming
*   81 m drift spacings
* - Upper and lower horizontal boundaries set near ground surface
*   and water table, respectively, where thermal front is near zero
```

```
round 0.02
set ovtol 1.0
config thermal
block -40.5 -350 -40.5 320 40.5 320 40.5 -350
```

```
* create jointing
```

```
* -----
* splits needed for isolating the submodel
```

* -----

```
split -40.5 50 40.5 50
```

```

split -40.5 -50 40.5 -50
*
* split -40.5 -19.25 40.5 -19.25
* split -40.5 19.25 40.5 19.25
*split -19.25 -19.25 -19.25 19.25
*split 19.25 -19.25 19.25 19.25
*
* -----
* inner problem domain
* -----
* angle,length,gap,spacing
*jregion -19.25 -19.25 -19.25 19.25 -13.75 19.25 -13.75 -19.25
jregion -40.5 -19.25 -40.5 19.25 -13.75 19.25 -13.75 -19.25
jset 85.0 10.0 40.0 5.0 0.0 0.0 1.5 0.2 0 0
jset 110.0 10.0 17.0 4.0 -0.3 0.1 5 0.5 0 0
*
*jregion -19.25 -19.25 -19.25 19.25 -12.75 19.25 -12.75 -19.25
jregion -40.5 -19.25 -40.5 19.25 -13.75 19.25 -13.75 -19.25
jset 20.0 5.0 20.0 2.5 0.0 0.0 3.0 0.2 0 0
*
*jregion 13.75 -19.25 13.75 19.25 19.25 19.25 19.25 -19.25
jregion 13.75 -19.25 13.75 19.25 40.5 19.25 40.5 -19.25
jset 85.0 10.0 40.0 5.0 0.0 0.0 1.5 0.2 1 1
jset 110.0 10.0 17.0 4.0 -0.3 0.1 5 0.5 1 1
*
* jregion 12.75 -19.25 12.75 19.25 19.25 19.25 19.25 -19.25
jregion 12.75 -19.25 12.75 19.25 40.5 19.25 40.5 -19.25
jset 20.0 5.0 20.0 2.5 0.0 0.0 3.0 0.2 0 0
*
jregion -13.75 -19.25 -13.75 -12.75 13.75 -12.75 13.75 -19.25
jset 85.0 10.0 40.0 5.0 0.0 0.0 1.5 0.2
jset 110.0 10.0 17.0 4.0 -0.3 0.1 5 0.5
*
jregion -13.75 -19.25 -13.75 -13.75 13.75 -13.75 13.75 -19.25
jset 20.0 5.0 20.0 2.5 0.0 0.0 3.0 0.2
*
jregion -13.75 12.75 -13.75 19.25 13.75 19.25 13.75 12.75
jset 85.0 10.0 40.0 5.0 0.0 0.0 1.5 0.2
jset 110.0 10.0 17.0 4.0 -0.3 0.1 5 0.5
*
jregion -13.75 13.75 -13.75 19.25 13.75 19.25 13.75 13.75
jset 20.0 5.0 20.0 2.5 0.0 0.0 3.0 0.2
*
* -----
* More detailed inner problem domain

```

```

* -----
* angle,length,gap,spacing
*
jregion -13.75 -13.75 -13.75 13.75 -6 13.75 -6 -13.75
jset 85.0 10.0 17.5 1.0 -0.2 0.0 1.0 0.3
jset 110.0 10.0 17.0 4.0 -0.3 0.1 3.6 0.5
*
jregion -13.75 -13.75 -13.75 13.75 -4.5 13.75 -4.5 -13.75
jset 20.0 5.0 15.0 1.0 -0.2 0.0 1.5 0.3
*
jregion 6 -13.75 6 13.75 13.75 13.75 -13.75
jset 85.0 15.0 17.5 1.0 -0.2 0.0 1.0 0.3
jset 110.0 10.0 17.0 4.0 -0.3 0.1 3.6 0.5
*
jregion 4.5 -13.75 4.5 13.75 13.75 13.75 -13.75
jset 20.0 5.0 15.0 1.0 -0.2 0.0 1.5 0.3
*
jregion -6 -13.75 -6 -5 6 -5 6 -13.75
jset 85.0 15.0 17.5 1.0 -0.2 0.0 1.0 0.3
jset 110.0 10.0 17.0 4.0 -0.3 0.1 3.6 0.5
*
jregion -5 -13.75 -5 -6 5 -6 5 -13.75
jset 20.0 5.0 15.0 1.0 -0.2 0.0 1.5 0.3
*
jregion -6 5 -6 13.75 6 13.75 6 5
jset 85.0 15.0 17.5 1.0 -0.2 0.0 1.0 0.3
jset 110.0 10.0 17.0 4.0 -0.3 0.1 3.6 0.5
*
jregion -5 6 -5 13.75 5 13.75 5 6
jset 20.0 5.0 15.0 1.0 -0.2 0.0 1.5 0.3
*
* -----
* Detailed joint spacing around the tunnel
* -----
* angle,length,gap,spacing
*
jregion -6 -6 -6 6 6 6 6 -6
jset 85.0 10.0 7.5 1.0 -0.2 0.0 0.4 0.1
jset 20.0 5.0 5.0 1.0 -0.2 0.0 0.75 0.1 -1 -1
jset 110.0 10.0 12.0 4.0 -0.3 0.1 1.8 0.5 -1 0
*
* -----
* outer domain
* -----
* angle,length,gap,spacing

```

```

jregion -40.5 -50 -40.5 -16.25 40.5 -16.25 40.5 -50
jset 85.0 10.0 50.0 1.0 0.0 0.0 3.0 0.3
jset 110.0 10.0 25.0 4.0 -0.3 0.1 8.0 0.5
*
jregion -40.5 -50 -40.5 -19.25 40.5 -19.25 40.5 -50
jset 20.0 5.0 25.0 1.0 0.0 0.0 5.0 0.3
*
jregion -40.5 16.25 -40.5 50 40.5 50 40.5 16.25
jset 85.0 10.0 50.0 1.0 0.0 0.0 3.0 0.3
jset 110.0 10.0 25.0 4.0 -0.3 0.1 8.0 0.5
*
jregion -40.5 19.25 -40.5 50 40.5 50 40.5 19.25
jset 20.0 5.0 25.0 1.0 0.0 0.0 5.0 0.3
*
* -----
* out domain for the whole model
* -----
* angle,length,gap,spacing
jregion -40.5 -350 -40.5 -50 40.5 -50 40.5 -350
jset 85.0 0.0 70.0 15.0 -0.5 0.0 10.0 0.05 10 10
jset 20.0 0.0 25.0 3.0 -0.5 0.0 25.0 0.8 10 10
*
jregion -40.5 50 -40.5 320 40.5 320 40.5 50
jset 85.0 0.0 70.0 15.0 -0.5 0.0 10.0 0.05 10 10
jset 20.0 0.0 25.0 3.0 -0.5 0.0 25.0 0.8 10 10
*
tunnel 0 0 2.75 36
del area 1.5e-2
jd
*
* *****
* auto generation of zones
* *****
gen region -6 -6 -6 6 6 6 -6 edge 3.5
* gen region -7 -7 -7 7 7 7 -7 edge 0.7
* gen region -40.5 -19.5 -40.5 19.5 40.5 19.5 40.5 -19.5 edge 3.0
gen region -40.5 -21 -40.5 21 40.5 21 40.5 -21 edge 3.0
gen region -40.5 -25 -40.5 25 40.5 25 40.5 -25 edge 8
gen region -40.5 -28 -40.5 28 40.5 28 40.5 -28 edge 4
gen region -40.5 -35 -40.5 35 40.5 35 40.5 -35 edge 6
gen region -40.5 -40 -40.5 40 40.5 40 40.5 -40 edge 5
gen region -40.5 -50 -40.5 50 40.5 50 40.5 -50 edge 8
*
gen region -40.5 -350 -40.5 320 40.5 320 40.5 -350 edge 14
pr max

```

```

*
damp auto
*
*****
* apply mechanical boundary conditions (units, MPa)
*****
call InSituSt.fis
InStress
*
grav 0.0 -9.81
insitu stress sigH 0.0 sigV ygrad sigH_h 0.0 sigV_h szz sigH &
zgrad 0.0 sigH_h
bound -42 42 315 325 stress sigH 0.0 sigV ygrad sigH_h 0.0 sigV_h
bound -42 42 -355 -345 yvel=0.0
bound -42 -39 -351 321 xvel=0.0
bound 39 42 -351 321 xvel=0.0
*
*****
* define mechanical and thermal material properties for joints/intact blocks
*****
*
* material 1 = rock
*
change -42 42 -350 320 jcons=5
**
** prop mat=1 k=18.74e3 g=13.48e3 d=0.00221 *RMQ5
prop mat=1 k=4.46e3 g=3.21e3 d=0.00221 *RMQ1
** !! would like to use: prop mat=1 cond=2.13 thexp=1.0e-05 spec=9.6896e08
prop mat=1 cond=2.13 thexp=7.5e-06 spec=9.6896e08
prop jmat=1 jks=5.0e5 jkn=5.0e5 jdil=0 jc=0.07 jfric=35.0 jtens=0.0 &
kn=5.0e5 ks=5.0e5
** !! try to used orginal properties
*** %%% prop mat=1 cond=2.06 thexp=6.0e-06 spec=9.58e08
*** %%% prop jmat=1 jks=5.0e5 jkn=5.0e5 jdil=0 jc=0.07 jfric=56.0 jtens=0.0 &
*** %%% kn=5.0e5 ks=5.0e5
*
set jcondf 5
*
* mohr-coulomb failure parameters
*
** prop mat=1 coh=5.08 fric=34.42 tens=5.35 dil=17.21 *RMQ5
prop mat=1 coh=2.82 fric=27.5 tens=4.42 dil=13.75 *RMQ1
*** %%% change this back prop mat=1 coh=5.2 fric=28 tens=4.21 dil=0.0
*
*****

```

```

* history records
*****
hist nyc=10 unbal damp type 4
hist ydis 0 0 yvel 0 0 ydis 0 320 ydis 0 -350
hist sxx 0.0 0.0 syy 0.0 0.0
*
*****
* initial cycling equilibrium
*****
cycle 4000
save E4_ini.sav
*
*****
* remove tunnel blocks
*****
*
del ann 0 0 0 2.75
*
*** call Set_bolts
* -----
* Calculate room closures
* -----
call closure.fis
Closure
*
* reset displacements after applying in situ loading conditions
*
reset damp time hist dis rot
hist unbal damp
hist ydis 0.0 2.75 ydis 0 -2.75
hist xdis -2.75 0.0 xdis 2.75 0.0
hist ydis 0.0 320 ydis -40.5 320 ydis 40.5 320
hist sdis 2.75,10 sdis -2.75,10 sdis 2.75 -10 sdis -2.75,-10
his ClosureV
his ClosureH
*
*
* change material property to Mohr-Coulomb
change cons=3 mat=1
*
cycle 4000
*
sav E4_exc.sav
*
*****

```

* Part II: Thermal

*

* set thermal boundary and histories

*

* set up thermal boundaries (default thermal b.c. are adiabatic)

*

** tfix 18.7 range (-42 42) (316 318)

** tfix 34.2 range (-42 42) (-351 -349)

*

* Call FISH FUNCTION to cal initem according to geothermal gradient

call iniTemp.fis

ini_Temp

*

** initem 29.0 -42 42 -350 320

*

thist ntcyc=10 tem 0 2.75 tem 0 5 tem 0 10 tem 0 25 tem 0 50 tem 0 100

thist tem 0 150 tem 0 200 tem 0 250 tem 0 320

this tem 2.75 0 tem 5 0 tem 10 0

thist tem 15 0 tem 20 0 tem 30 0 tem 40.5 0

*

* apply heat flux to tunnel wall

* run initial thermal time by explicit scheme for 100 steps

*

** thapp ann 0.0 0.0 2.71 2.79 flux 71.0152 -7.5e-10

** thapp ann 0.0 0.0 2.71 2.79 flux 71.0152 -3.5e-10

* scaled initial strength (71.0152*196.3/225)

thapp ann 0.0 0.0 2.71 2.79 flux 61.95 -3.5e-10

run age=3600 step=1000000 tol=0.05

reset damp

cycle 4000

pr max

*

* run thermal time to 3 months

*

run age=7.776e6 delt=3600.0 temp=10000 step=1000000 tol=0.05 impl

reset damp

cycle 4000

pr max

*

* run thermal time to 1 year

```
*
run age=3.1536e7 delt=7200.0 temp=10000 step=1000000 tol=0.05 impl
reset damp
cycle 4000
pr max
*
* run thermal time to 18 months
*
run age=4.7304e7 delt=7200.0 temp=10000 step=1000000 tol=0.05 impl
reset damp
cycle 4000
pr max
*
* run thermal time to 2 years
*
run age=6.3072e7 delt=7200.0 temp=10000 step=1000000 tol=0.05 impl
reset damp
cycle 4000
pr max
* sav E4_2y.sav
*
* run thermal time to 3 years
*
run age=9.4608e7 delt=7200.0 temp=10000 step=1000000 tol=0.05 impl
reset damp
cycle 4000
* sav E4_3y.sav
pr max
*
* run thermal time to 4 years
*
run age=1.26144e8 delt=7200.0 temp=10000 step=1000000 tol=0.05 impl
reset damp
cycle 4000
pr max
* sav E4_4y.sav
*
* run thermal time to 5 years
*
run age=1.5768e8 delt=7200.0 temp=10000 step=1000000 tol=0.05 impl
reset damp
cycle 4000
pr max
sav E4_5y.sav
*
```

```

* run thermal time to 7.5 years
*
** thapp ann 0.0 0.0 2.71 2.79 flux -71.0152 -7.5e-10
** thapp ann 0.0 0.0 2.71 2.79 flux 69.2 -6e-10
run age=2.3652e8 delt=7200.0 temp=10000 step=1000000 tol=0.05 impl
reset damp
cycle 4000
pr max
*
* run thermal time to 10 years
*
run age=3.1536e8 delt=7200.0 temp=10000 step=1000000 tol=0.05 impl
reset damp
cycle 4000
pr max
sav E4_10y.sav
*
res E4_10y.sav
* run thermal time to 20 years
*
** thapp ann 0.0 0.0 2.71 2.79 flux -69.2 -6e-10
** thapp ann 0.0 0.0 2.71 2.79 flux 66.2 -5e-10
run age=6.3072e8 delt=7200.0 temp=10000 step=1000000 tol=0.05 impl
reset damp
cycle 4000
pr max
* save E4_20y.sav
*
* run thermal time to 30 years
*
** thapp ann 0.0 0.0 2.71 2.79 flux -66.2 -5e-10
** thapp ann 0.0 0.0 2.71 2.79 flux 66.0 -5e-10
run age=9.4608e8 delt=7200.0 temp=10000 step=1000000 tol=0.05 impl
reset damp
cycle 4000
pr max
* sav E4_30y.sav
*
* run thermal time to 40 years
*
** thapp ann 0.0 0.0 2.71 2.79 flux -66.0 -5e-10
** thapp ann 0.0 0.0 2.71 2.79 flux 59.3 -4e-10
run age=12.6144e8 delt=7200.0 temp=10000 step=1000000 tol=0.05 impl
reset damp
cycle 4000

```

```

pr max
* sav E4_40y.sav
*
* run thermal time to 50 years
*
** thapp ann 0.0 0.0 2.71 2.79 flux -59.3 -4e-10
** thapp ann 0.0 0.0 2.71 2.79 flux 58.9 -4e-10
run age=1.5768e9 delt=7200.0 temp=10000 step=1000000 tol=0.05 impl
reset damp
cycle 4000
pr max
sav E4_50y.sav
*
* run thermal time to 60 years
** thapp ann 0.0 0.0 2.71 2.79 flux -58.9 -4e-10
** thapp ann 0.0 0.0 2.71 2.79 flux 59.0 -4e-10
run age=1.89216e9 delt=7200.0 temp=10000 step=1000000 tol=0.05 impl
reset damp
cycle 4000
pr max
sav E4_60y.sav
*
* run thermal time to 70 years
*
** thapp ann 0.0 0.0 2.71 2.79 flux -59.0 -4e-10
** thapp ann 0.0 0.0 2.71 2.79 flux 59.7 -4e-10
run age=2.20752e9 delt=7200.0 temp=10000 step=1000000 tol=0.05 impl
reset damp
cycle 5000
pr max
sav E4_70y.sav
*
* run thermal time to 80 years
*
** thapp ann 0.0 0.0 2.71 2.79 flux -59.7 -4e-10
** thapp ann 0.0 0.0 2.71 2.79 flux 47.4 -3e-10
run age=2.52288e9 delt=7200.0 temp=10000 step=1000000 tol=0.05 impl
reset damp
cycle 4000
pr max
sav E4_80y.sav
*
*
* run thermal time to 90 years
*

```

```
res E4_80y.sav
** thapp ann 0.0 0.0 2.71 2.79 flux -47.4 -3e-10
** thapp ann 0.0 0.0 2.71 2.79 flux 47.7 -3e-10
run age=2.83824e9 delt=7200.0 temp=10000 step=1000000 tol=0.05 impl
reset damp
cycle 4000
pr max
sav E4_90y.sav
*
* run thermal time to 100 years
*
** thapp ann 0.0 0.0 2.71 2.79 flux -47.7 -3e-10
** thapp ann 0.0 0.0 2.71 2.79 flux 48.4 -3e-10
run age=3.1536e9 delt=7200.0 temp=10000 step=1000000 tol=0.05 impl
reset damp
cycle 4000
pr max
sav E4_100y.sav
*
* run thermal time to 150 years
*
** thapp ann 0.0 0.0 2.71 2.79 flux -48.4 -3e-10
** thapp ann 0.0 0.0 2.71 2.79 flux 35.7 -2e-10
run age=4.7304e9 delt=7200.0 temp=10000 step=1000000 tol=0.05 impl
reset damp
cycle 8000
pr max
sav E4_150y.sav
*
return
```

APPENDIX F Bolt Parameters**Bolt_RMQ1.fis**

* This is modified based on Example 1.13 of Fish manual (UDEC31)

*

* Create variables for later use

def setup

```
xCentre=0.0 ;x-coord of tunnel center
yCentre=0.0 ;y-coord of tunnel center
theta1=20.0 ;starting angle for bolts
theta2=160.0 ;ending angle for bolts
radius1=2.75 ;tunnel radius
radius2=5.5 ;ending radius for remote end of bolts
nCables=12 ;number of bolts
```

end

* Calculate x,y coords of cable end points

def place_cables

```
theta1=degrad*theta1
theta2=degrad*theta2
_angInc=(theta2-theta1)/float(nCables-1)
_ang=theta1
loop ii (1,nCables)
  _x1=radius1*cos(_ang)+xCentre
  _y1=radius1*sin(_ang)+yCentre
  _x2=radius2*cos(_ang)+xCentre
  _y2=radius2*sin(_ang)+yCentre
  Command
    cable _x1 _y1 _x2 _y2 20 8 2.85e-4 9
  endcommand
  _ang=_ang+_angInc
```

endloop

end

setup

```
set xCentre=0.0 yCentre=0.0
set theta1=20.0 theta2=160.0
set radius1=2.75 radius2=5.5
set nCables=12
```

place_cables

*

* (first set of bolt parameters, Mikko's)

** prop mat 8 cb_dens 0.007875 cb_y mod 2.0e5 cb_yield 0.1375 cb_ycomp 1.0e4

** prop mat 8 cb_thexp 7.5e-6

** prop mat 9 cb_kb 8.158e3 cb_sb 0.60

*

```

* (second set of bolt parameters, DOE Ground Support Analyses)
** prop mat 8 cb_dens 0.007875 cb_ymod 2.0e5 cb_yield 0.267 cb_ycomp 1.0e4
** prop mat 8 cb_thexp 7.5e-6
** prop mat 9 cb_kb 16.34e3 cb_sb 0.556
*
* (second set of bolt parameters, DOE Ground Support Analyses, increase cb_yield by 5 fold -
worked,
* but generated extremely high stress. Increase 3 fold instead)
* (3fold increase worked for E22, but not C27. Try 2 fold later!!)
prop mat 8 cb_dens 0.007875 cb_ymod 2.0e5 cb_yield 0.267 cb_ycomp 1.0e4
prop mat 8 cb_thexp 7.5e-6
prop mat 9 cb_kb 16.34e3 cb_sb 0.744

```

Bolt_RMQ5.fis

```

* This is modified based on Example 1.13 of Fish manual (UDEC31)
*
* Create variables for later use
def setup
  xCentre=0.0 ;x-coord of tunnel center
  yCentre=0.0 ;y-coord of tunnel center
  theta1=20.0 ;starting angle for bolts
  theta2=160.0 ;ending angle for bolts
  radius1=2.75 ;tunnel radius
  radius2=5.5 ;ending radius for remote end of bolts
  nCables=12 ;number of bolts
end
* Calculate x,y coords of cable end points
def place_cables
  theta1=degrad*theta1
  theta2=degrad*theta2
  _angInc=(theta2-theta1)/float(nCables-1)
  _ang=theta1
  loop ii (1,nCables)
    _x1=radius1*cos(_ang)+xCentre
    _y1=radius1*sin(_ang)+yCentre
    _x2=radius2*cos(_ang)+xCentre
    _y2=radius2*sin(_ang)+yCentre
    Command
      cable _x1 _y1 _x2 _y2 20 8 2.85e-4 9
    endcommand
    _ang=_ang+_angInc
  endloop
end

```

```

setup
set xCentre=0.0 yCentre=0.0
set theta1=20.0 theta2=160.0
set radius1=2.75 radius2=5.5
set nCables=12
place_cables
*
* (first set of bolt parameters, Mikko's)
** prop mat 8 cb_dens 0.007875 cb_ymod 2.0e5 cb_yield 0.1375 cb_ycomp 1.0e4
** prop mat 8 cb_thexp 7.5e-6
** prop mat 9 cb_kb 8.158e3 cb_sb 0.60
*
* (second set of bolt parameters, DOE Ground Support Analyses)
** prop mat 8 cb_dens 0.007875 cb_ymod 2.0e5 cb_yield 0.267 cb_ycomp 1.0e4
** prop mat 8 cb_thexp 7.5e-6
** prop mat 9 cb_kb 16.34e3 cb_sb 0.556
*
* (First set of parameters for RMQ5)
prop mat 8 cb_dens 0.007875 cb_ymod 2.0e5 cb_yield 0.267 cb_ycomp 1.0e4
prop mat 8 cb_thexp 7.5e-6
prop mat 9 cb_kb 16.34e3 cb_sb 1.513

```

Grout Maximum bond force (cb_sbond):

$$S_{\text{bond}} = \pi (D + 2t) \tau_{\text{peak}}$$

$$\tau_{\text{peak}} = \tau_i Q_B$$

$$Q_B = 1$$

τ_i = half of the compressive strength of rock or grout, whichever is smaller.

$$\text{For RMQ5: } q_u = 2c \tan \left(45 + \frac{\phi}{2} \right) \quad c = 5.08, \phi = 34.42$$

$$= 19.28 \text{ MPa}$$

$$\text{RMQ1: } q_u = 2c \tan \left(45 + \frac{\phi}{2} \right) \quad c = 2.82, \phi = 27.5$$

$$= 9.29 \text{ MPa}$$

Therefore,

$$\text{RMQ5: } S_{\text{bond}} = \pi (D + 2t) \tau_{\text{peak}}$$

$$= 1.513 \text{ MN/m}$$

$$\begin{aligned} \text{RMQ5: } S_{\text{bond}} &= \pi (D + 2t) \tau_{\text{peak}} \\ &= 0.744 \text{ MN/m} \end{aligned}$$

Design Parameters for Rock Bolts:

Bolt diameter (D)

Annual thickness of grout (hole diameter) (D + 2t)

Bolt Young's modules (E) (cb_ ymod)

Bolt tensile yield force (or ultimate tensile capacity) (cb_yield)

Bolt thermal expansion coefficient (cb_thexp)

Bolt density (cb_density)

Bolt extensional failure strain (optional can be unlimited) (cb_f strain)

Bolt Compressive yield force (cb_ycomp)

Grout shear modules (G)

Grout compressive strength

Estimate:

1. cb_Sbond (MN/m)

a. Maximum shear force (τ_{peak})

Method 1: $\tau_{\text{peak}} = \frac{1}{2} \times \text{Grout Compressive strength}$, If grout is weaker than surrounding rock

Method 2: pull out test (see p. 1-24 of UDEC for example)

b. If failure occurs at cable/ grout interface

$$S_{\text{bond}} = \pi D \tau_{\text{peak}}$$

2. cb-Kbond (MN/m / m-displacement)

$$K_{\text{bond}} = 2\pi G / [10 \ln(1+2t/D)]$$

3. 2D correction should be applied to: K_{bond} , S_{bond} , E, and bolt tensile yield force.

Final Input:

cb_Kbond (MN/m/m)

cb_Ycomp (MN)

cb_Sbond (MN/m)

cb_denisty

cb_Ymod (E) (MPa)

cb_f strain

cb_Yield (MN)

cb_thexp

Cable Element

Bolt cross sectional area
 Bolt density
 Bolt yield force resistance

Minimum extensional strain: optional (can be unlimited)

Grout shear stiffness: (cb_Kbond)

$$K_{\text{bond}} = 2\pi G / [10 \ln(1 + 2t/D)]$$

Where:

1. D = reinforcing diameter (bolt diameter)
2. t = annulus thickness
3. G = grout shear modulus

Grout shear strength: (cb_Sbond)

If failure occur at grout/rock

$$S_{\text{bond}} \approx \pi(D + 2t) \tau_{\text{peak}}$$

where: $\tau_{\text{peak}} = \tau_1 Q_B$ (Maximum shear force)

τ_1 = one-half of the uniaxial compressive strength of the weaker of rocks and grout

Q_B = quality of bond between the grout and rock ($Q_B = 1$ for perfect bond)

If failure occur at grout/reinforcing interface:

$$S_{\text{bond}} = \pi D \tau_{\text{peak}}$$

prop.dat

```
* Rock Mass Elastic Properties (RMQ5) (RMQ1) VA_RMQ5 VA_RMQ1
* Mass density (kg/m^3): 2210 2210 2235 2235
* Young's modulus (GPa): 32.61 7.76 32.61 7.76
* Poisson's ratio 0.21 0.21 0.21 0.21
* Bulk modulus (GPa): 18.74 4.46 18.74 4.46
* Shear modulus (GPa): 13.48 3.21 13.48 3.21
*
* Rock Mass Strength Properties (RMQ5) (RMQ1) VA_RMQ5 VA_RMQ1
* Cohesion (MPa): 5.08 2.82 5.2 1.5
* Friction angle (degrees): 34.42 27.50 46.0 43.0
* Unconf comp strength (MPa): 19.28 9.29 26.09 7.08
* Dilatation angle: 17.21 13.75 0.0 0.0
* Tensile strength (MPa): 5.35 4.42 4.21 1.32
*
* Thermal properties
* Conductivity (W/m-K): 2.13
* Specific heat (J/kg-K): 968.96
```

Rui Chen

SCIENTIFIC NOTEBOOK

INITIALS:

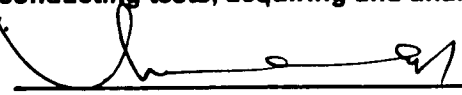
RC

- * Thermal expansion (/C) 1.0E-5
- *
- * Joint Properties DOE_VA
- * Cohesion (MPa): 0.07 0.07
- * Friction angle (degrees): 35 56
- * Dilation angle (degrees): 17.5 0.0
- * Tensile strength (MPa): 0.0
- * Normal stiffness (GPa/m): 500 (50?) 500
- * Shear stiffness (GPa/m): 500 (50?) 500

Entries into Scientific Notebook 274 for the period December 1999 to August 2000 have been made by Rui Chen/ Manager for Rui Chen 8/31/2000.

No original text entered into this Scientific Notebook has been removed. Manager for Rui Chen 8/31/2000

"I have reviewed this scientific notebook and find it in compliance with QAP-001. There is sufficient information regarding procedures used for conducting tests, acquiring and analyzing data so that another qualified individual could repeat the activity.

 8-31-2000

(Element Manager signature and date above line, Name of Element beneath line)" MGF